Radiação Térmica

Conteúdos:

- Introdução a Radiação.
- Propriedades Radiativas.
- Troca de Calor entre Superfícies.

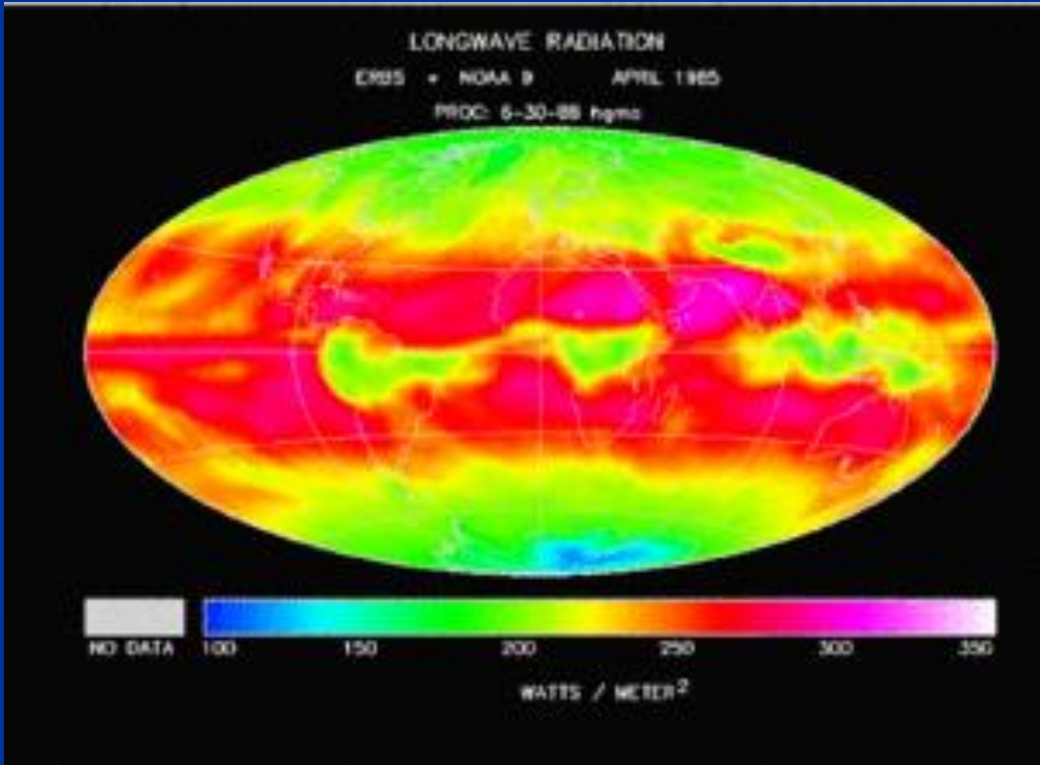

Efeito Estufa

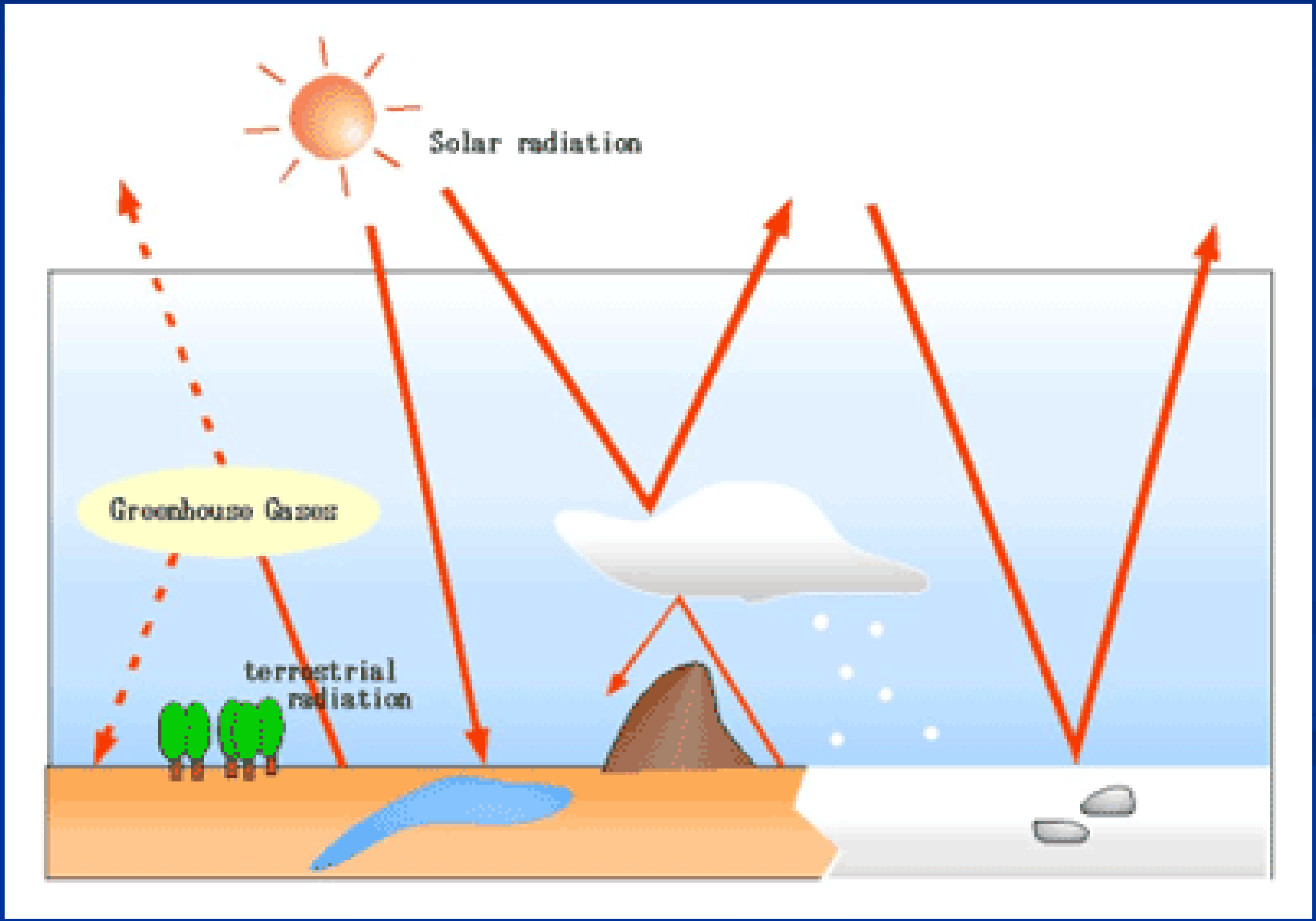

Aquecimento Solar

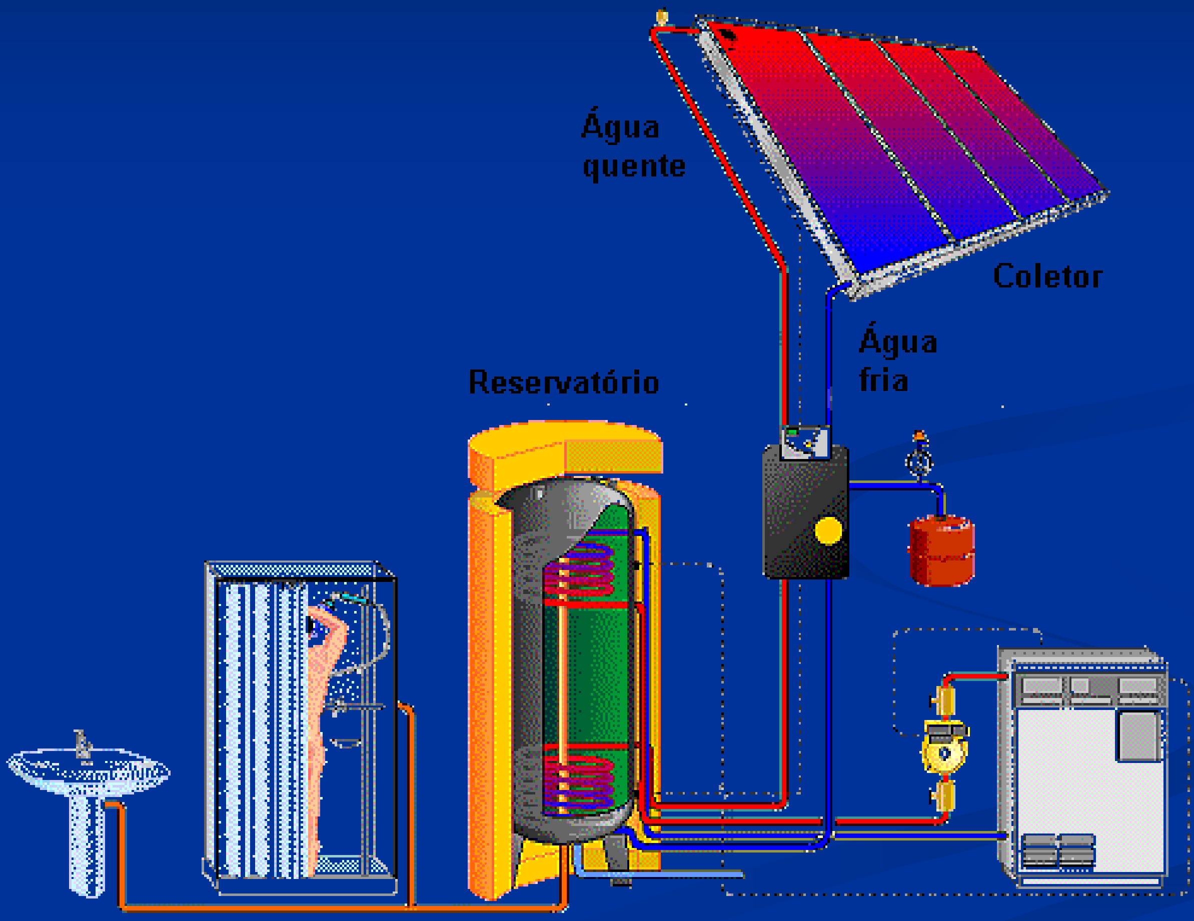

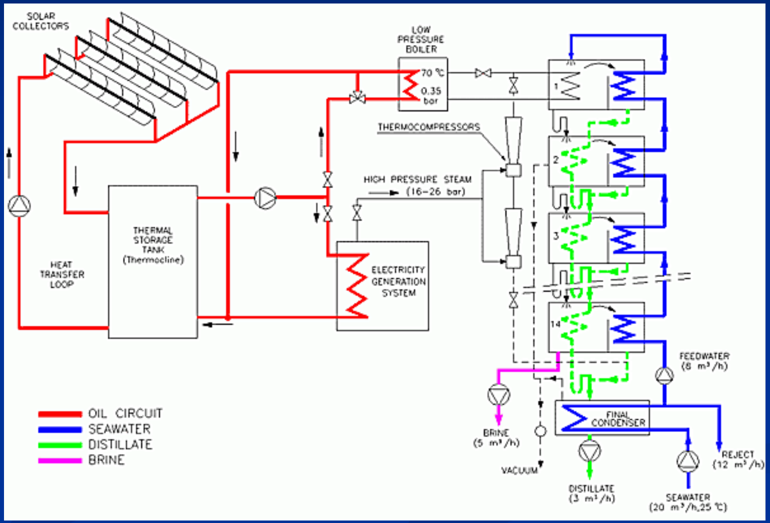

http://www.psa.es/

Nevada Solar Thermal Plant Breaks New Ground

350-acre solar power

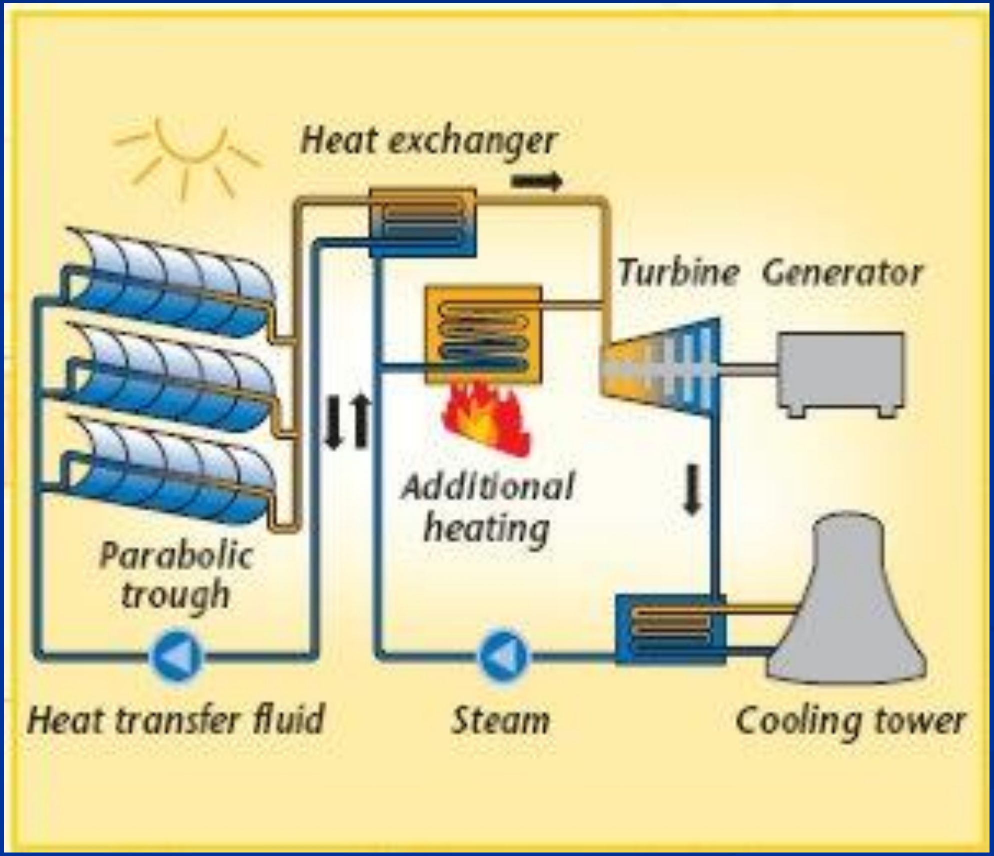

http://pesn.com/2006/02/12/9600234_Schott_solar_thermal_plant

Térmica de Edificações

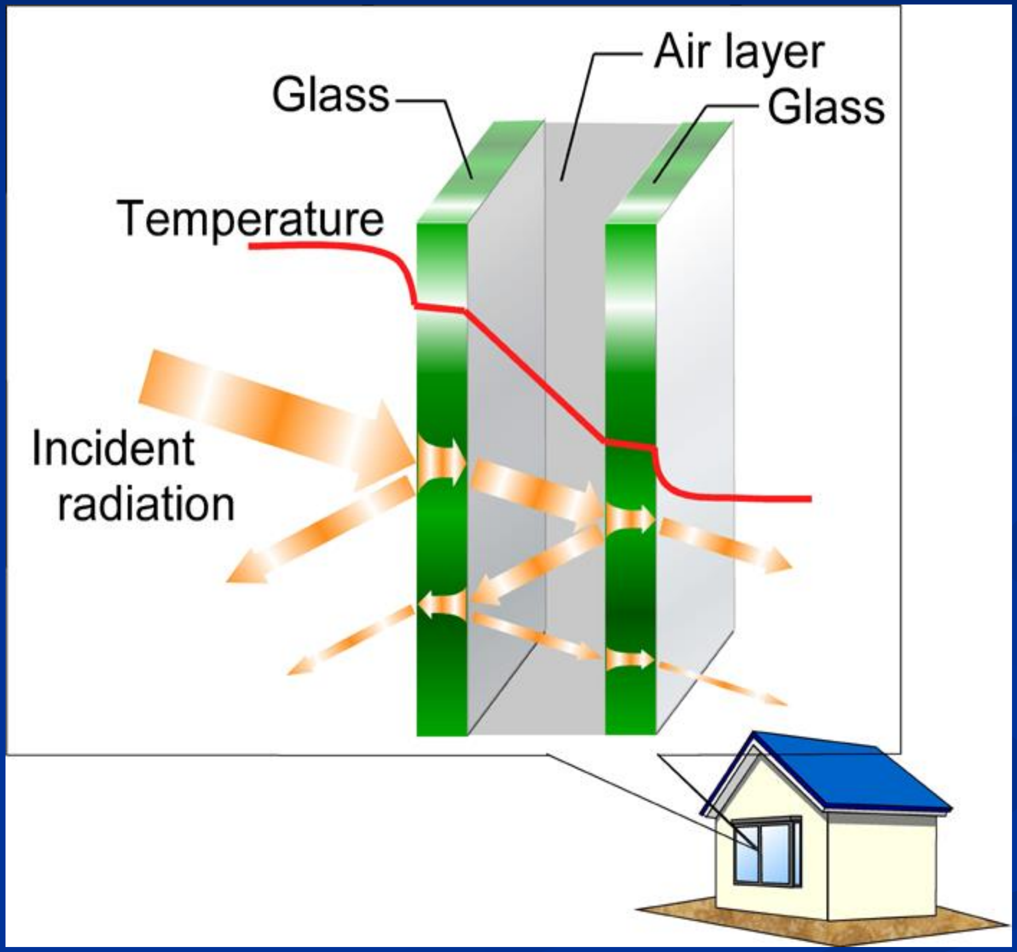

Térmica de Edificações

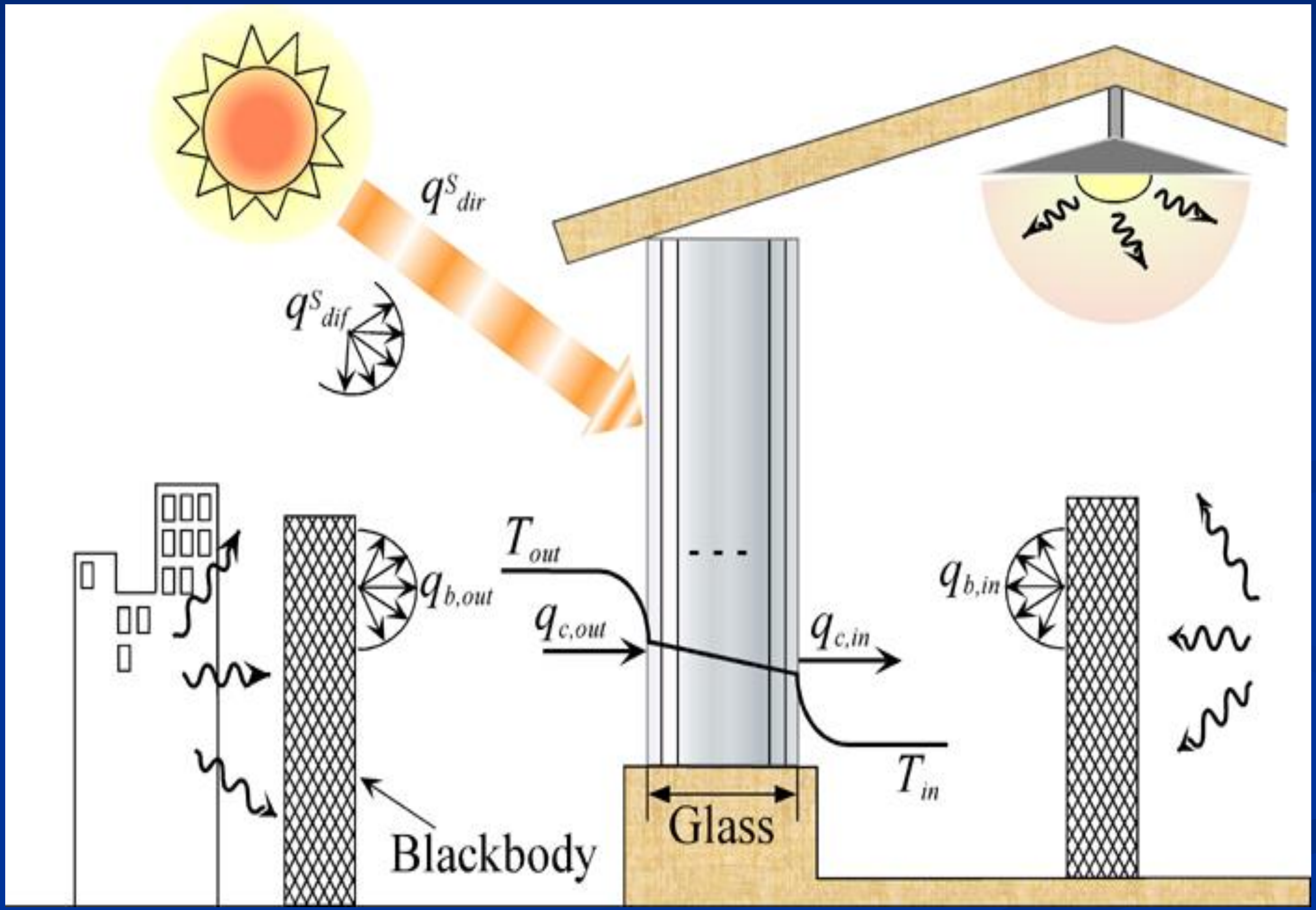

Aquecimento Solar

Odeillo, nos Pirineus franceses

http://www.solucar.es/

Vista Aérea da Plataforma Solar de Almería

http://www.psa.es/

http://peswiki.com/index.php/Directory:Solar_Tower

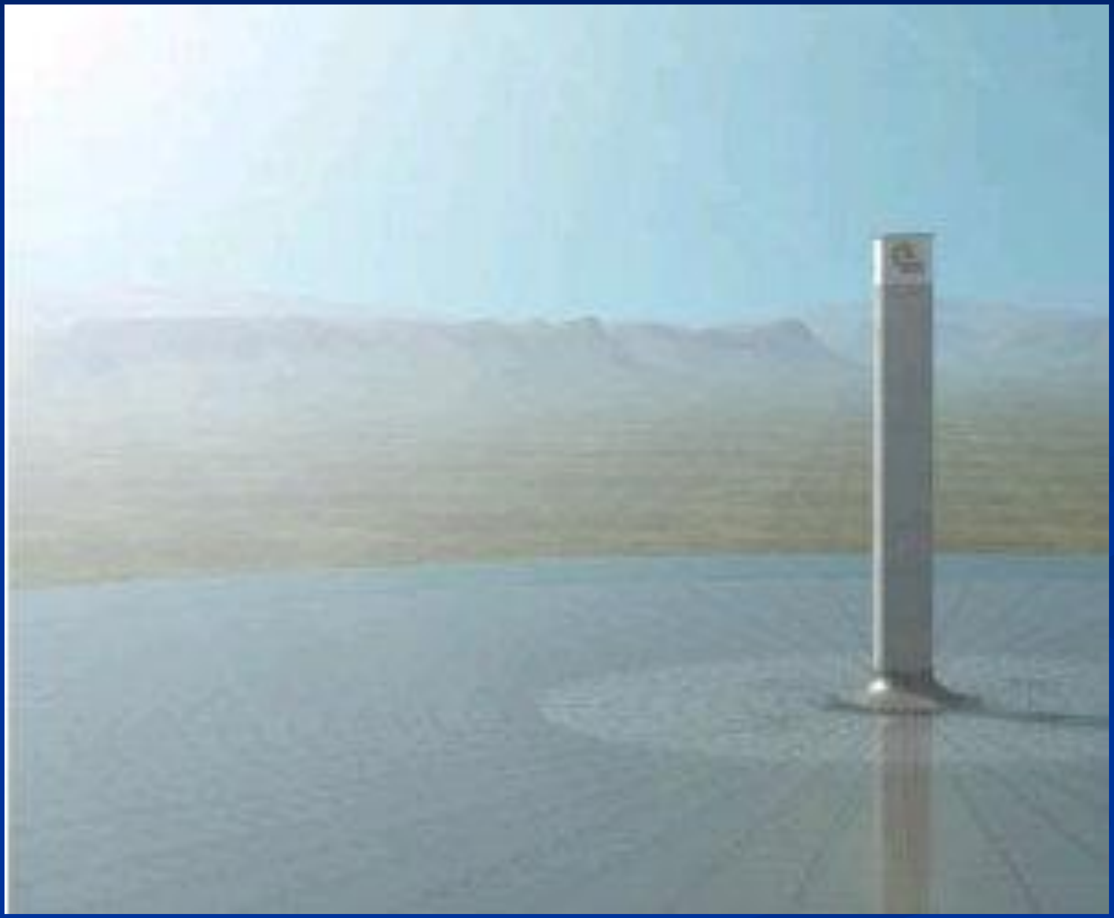

200 MW Solar Tower is planned to commence construction in Australia in 2006, at Burronga Station, in the Riverland area of New South Wales

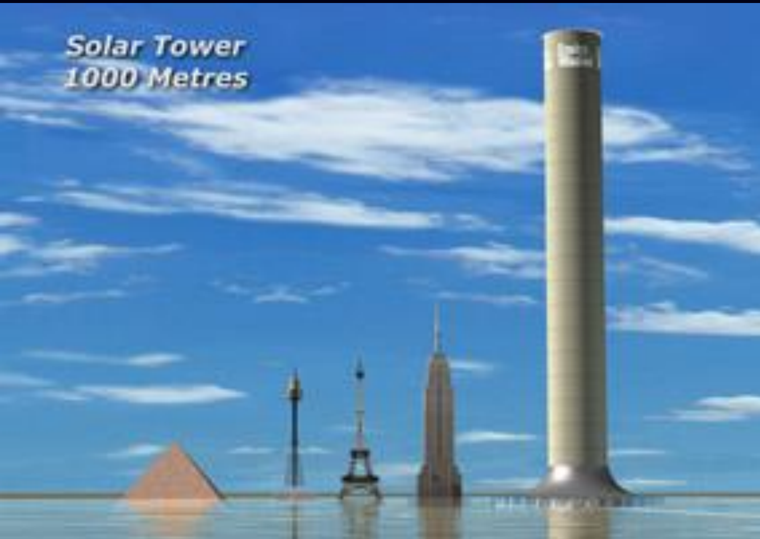

http://peswiki.com/index.php/Director

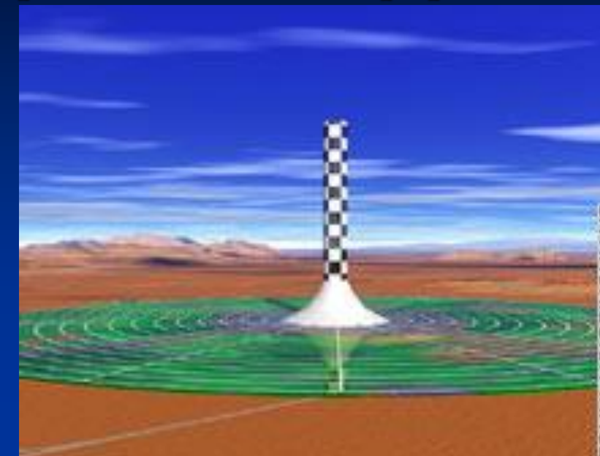

50kW prototype Solar Tower plant

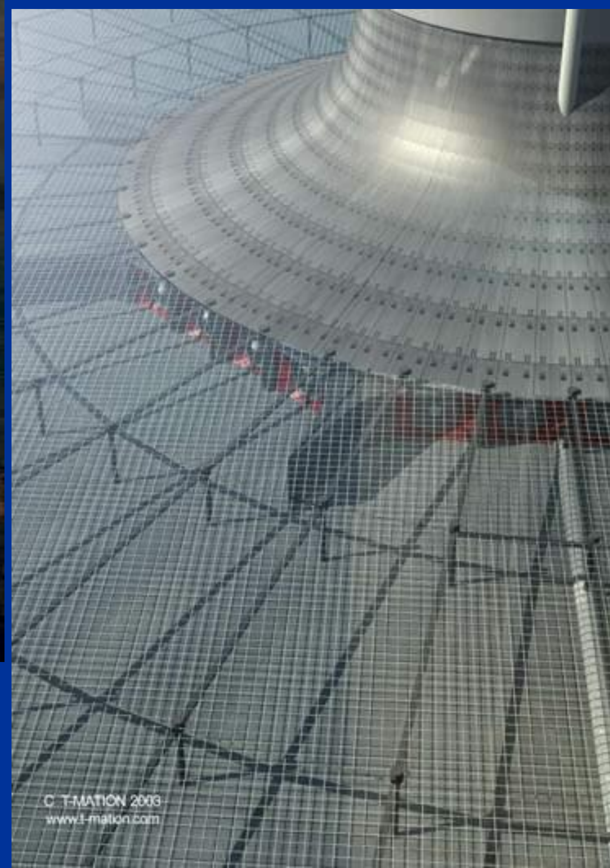

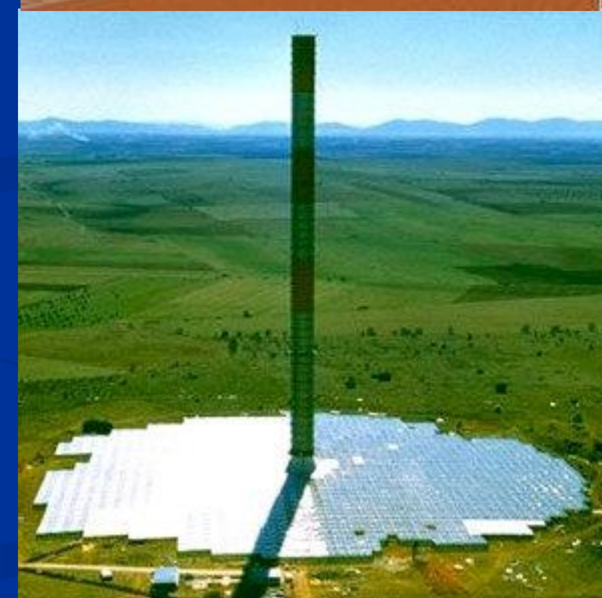

15-MW plant project

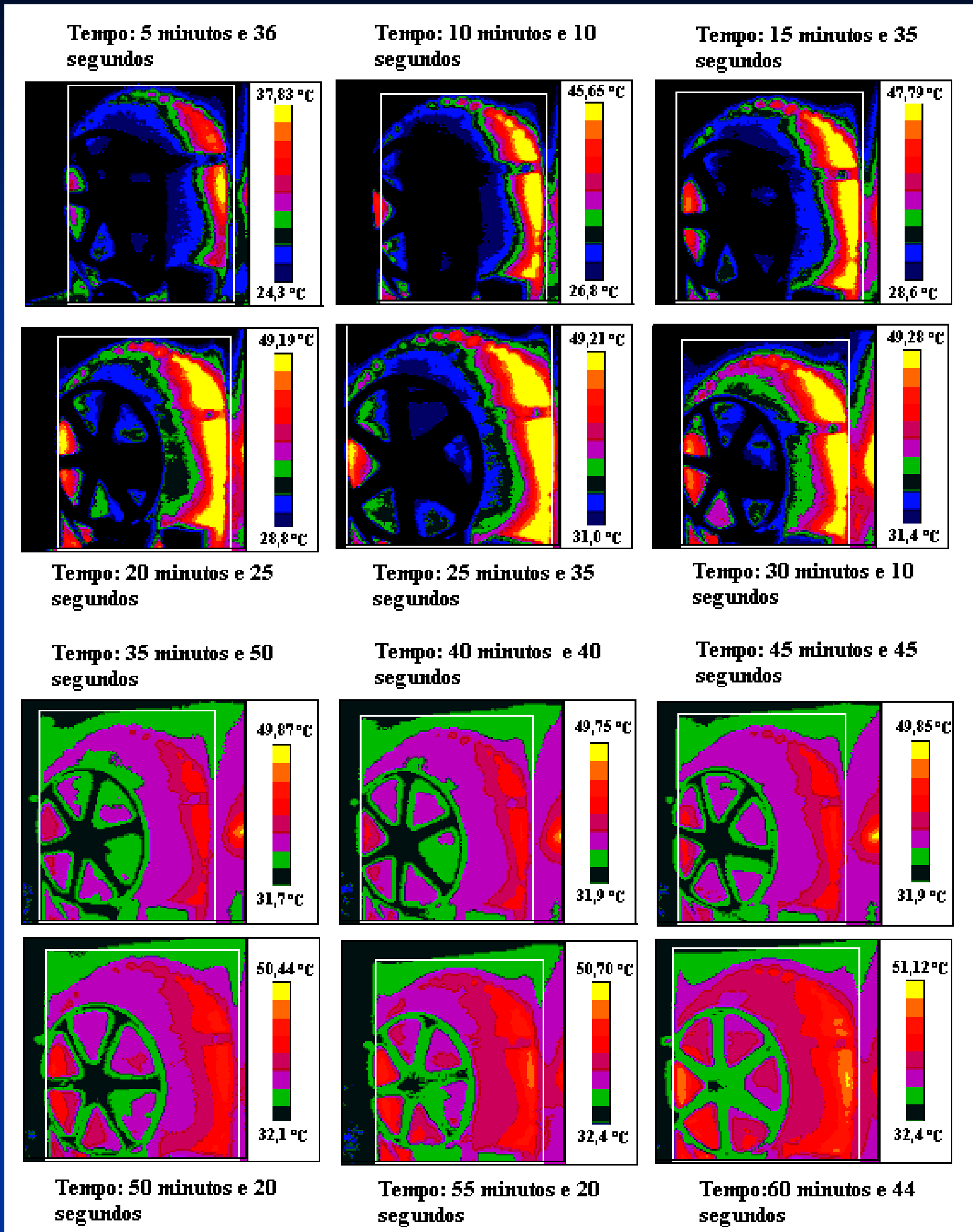
Tempo: 5 minutos e 36 segundos
37,83 °C
24,3 °C
Tempo: 10 minutos e 10 segundos
45,65 °C
26,8 °C
Tempo: 15 minutos e 35 segundos
47,79 °C
28,6 °C
49,19 °C
28,8 °C
Tempo: 20 minutos e 25 segundos
49,21 °C
31,0 °C
Tempo: 25 minutos e 35 segundos
49,28 °C
31,4 °C
Tempo: 30 minutos e 10 segundos
Tempo: 35 minutos e 50 segundos
49,87 °C
31,7 °C
Tempo: 40 minutos e 40 segundos
49,75 °C
31,9 °C
Tempo: 45 minutos e 45 segundos
49,85 °C
31,9 °C
50,44 °C
32,1 °C
Tempo: 50 minutos e 20 segundos
50,70 °C
32,4 °C
Tempo: 55 minutos e 20 segundos
51,12 °C
32,4 °C
Tempo:60 minutos e 44 segundos

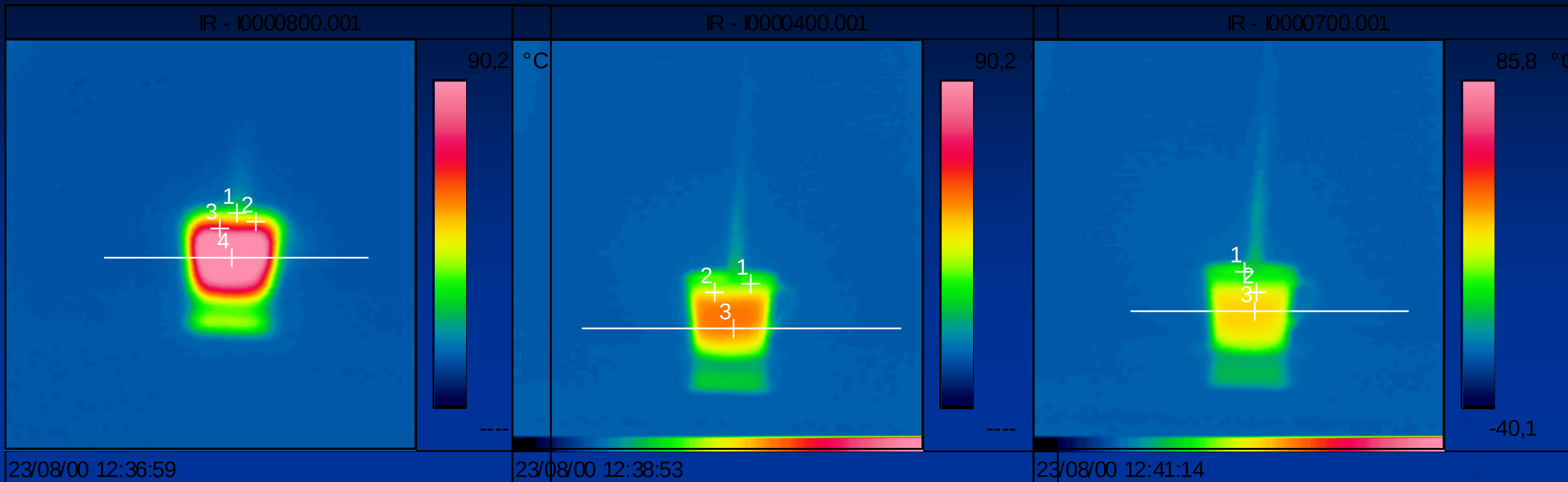
IR - I0000800.001
90,2 °C

23/08/00 12:36:59
IR - I0000400.001
90,2

23/08/00 12:38:53
IR - I0000700.001
85,8 °C
-40,1
23/08/00 12:41:14

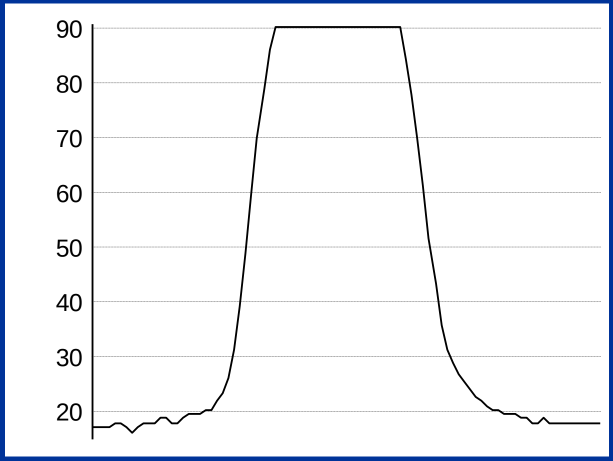
90
80
70
60
50
40
30
20

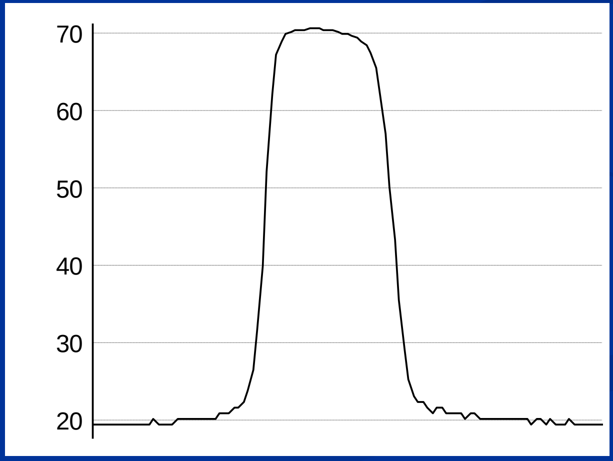
70
60
50
40
30
20

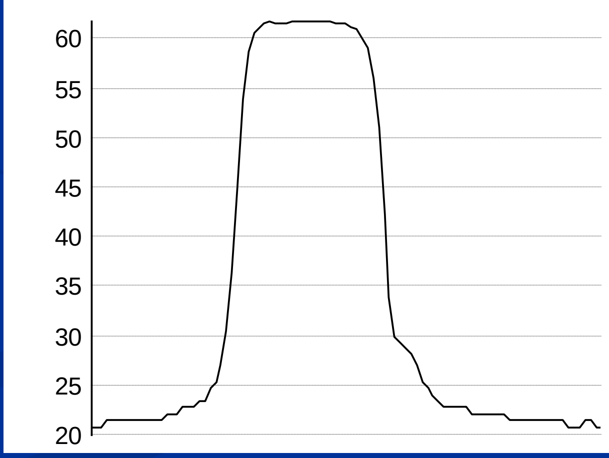
60
55
50
45
40
35
30
25
20

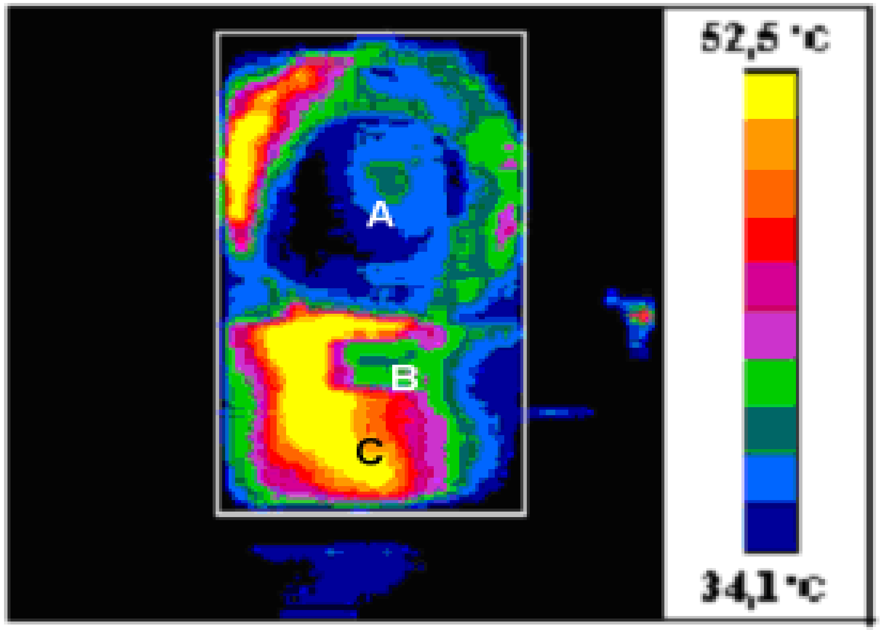

A= Tambor de secagem
B= Caixa Coletora de Fiapos
C= Saída do ar proveniente do tambor de secagem

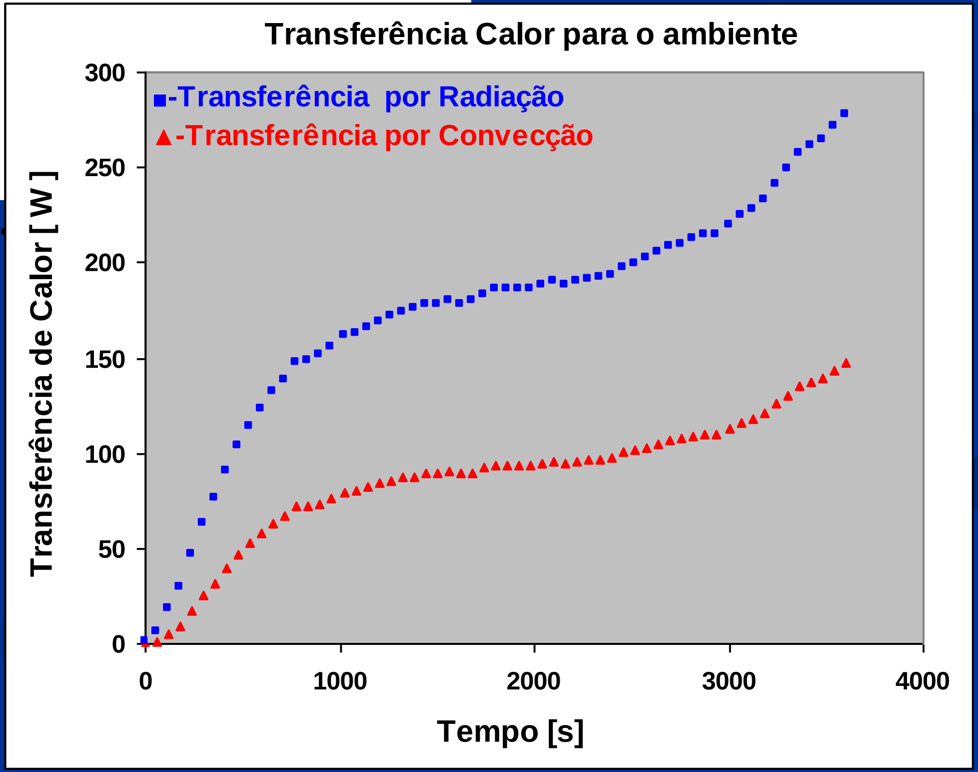

Sir William Crookes (1832-1919)

- Professor Crooks' principle lectures and papers on the fourth state of matter, that is to say, plasma. The material was presented in 1878 & 1879 before the Royal Society of London and British Association for the Advancement of Science.

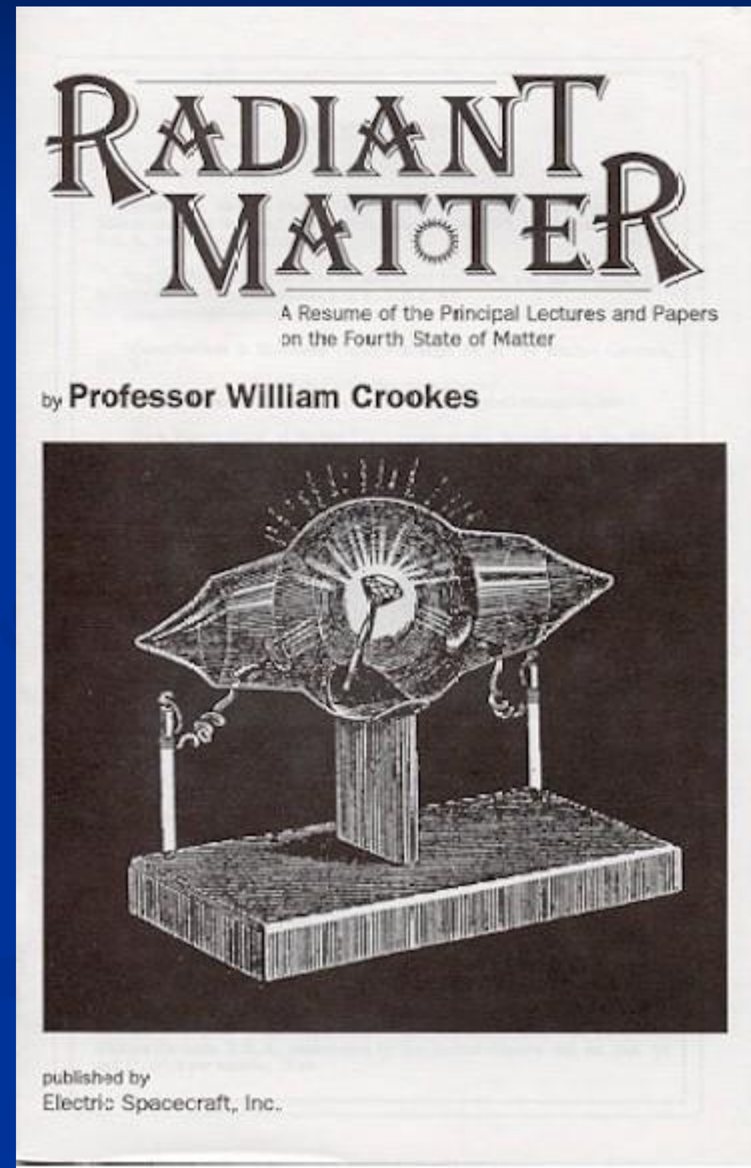

Crookes Radiometer and Otheoscope

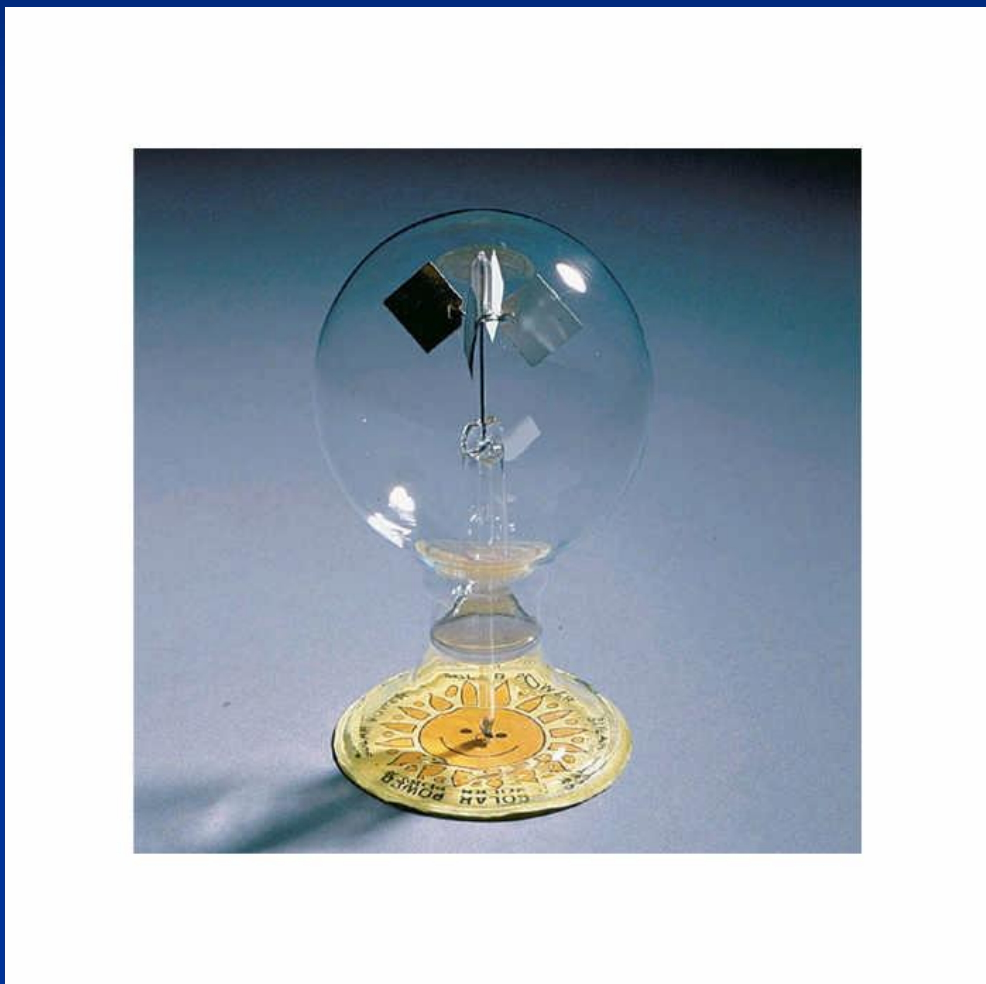

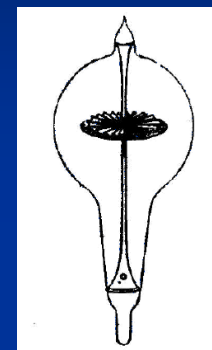

Figure 14

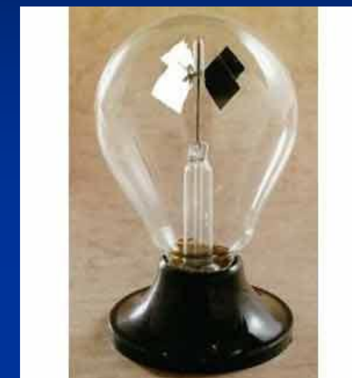

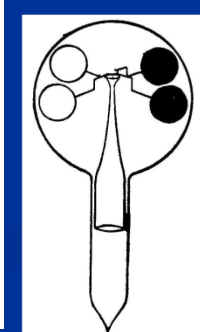

Figure 13

Considerações gerais

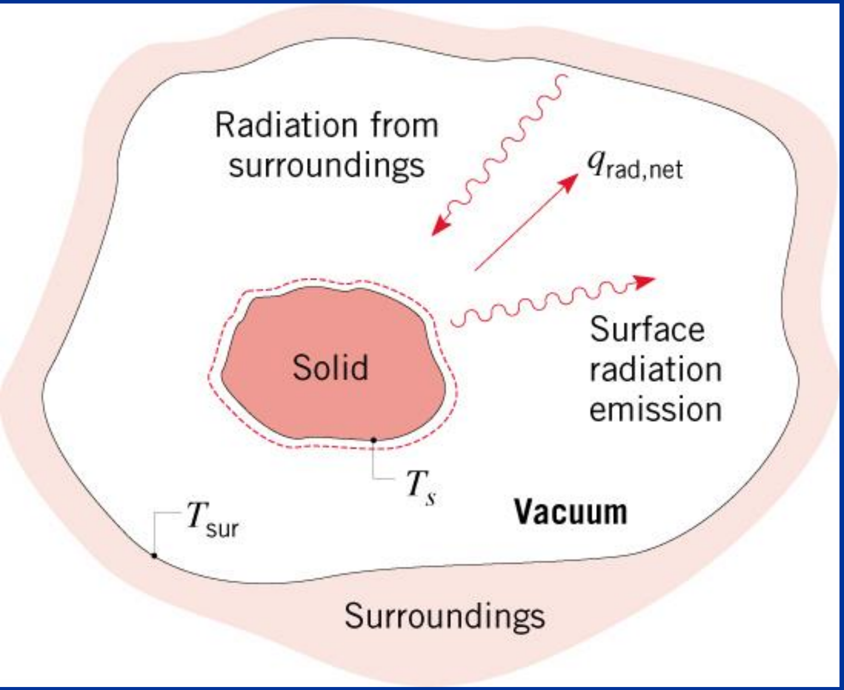

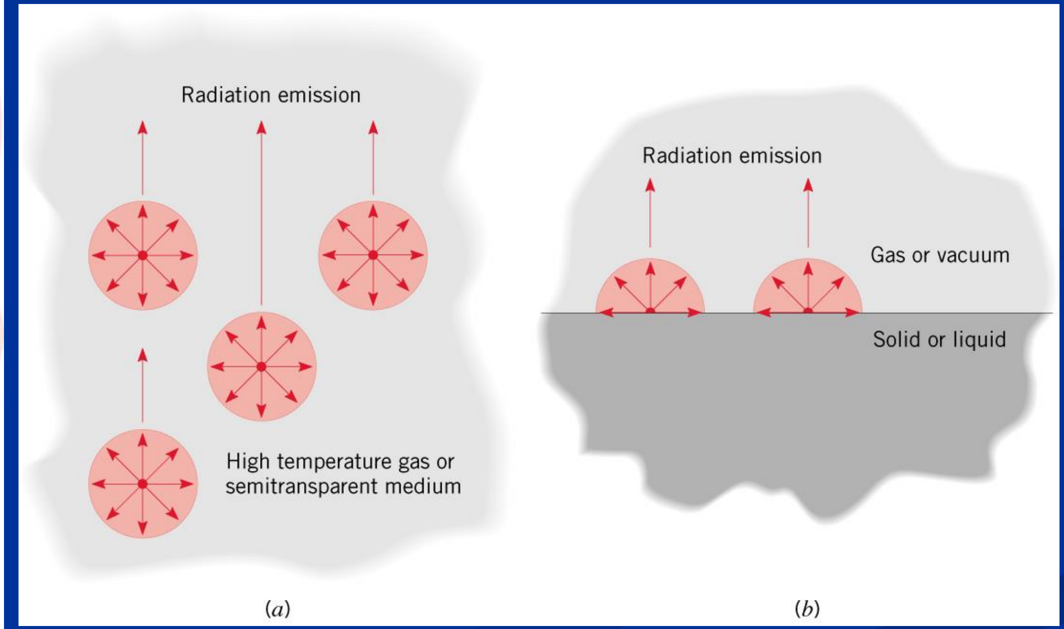

Transferência de Calor por Radiação

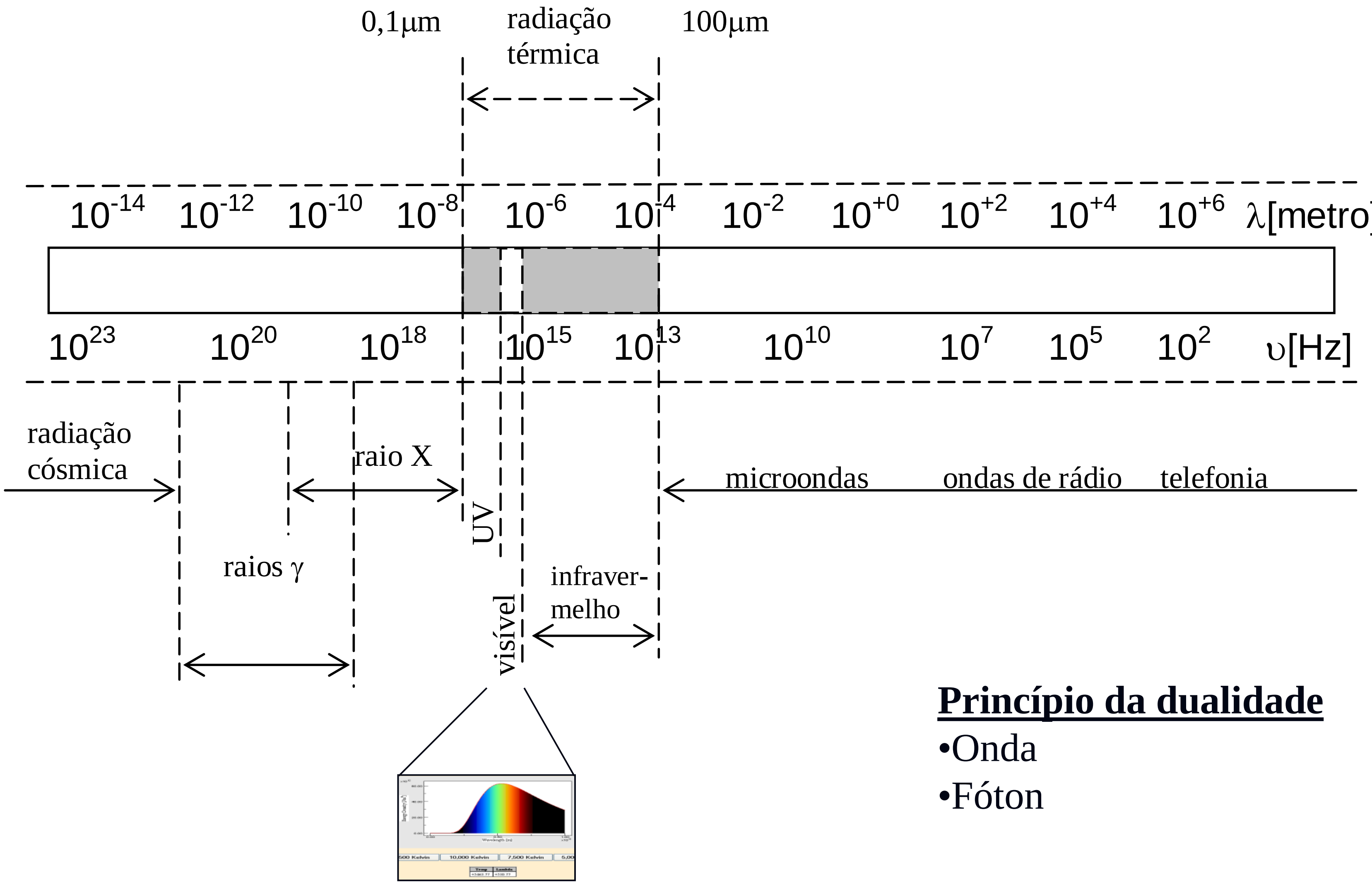

<u>Princípio da dualidade</u>

- Onda
- Fóton

http://guymcarthur.com/resources/java/applets/st/

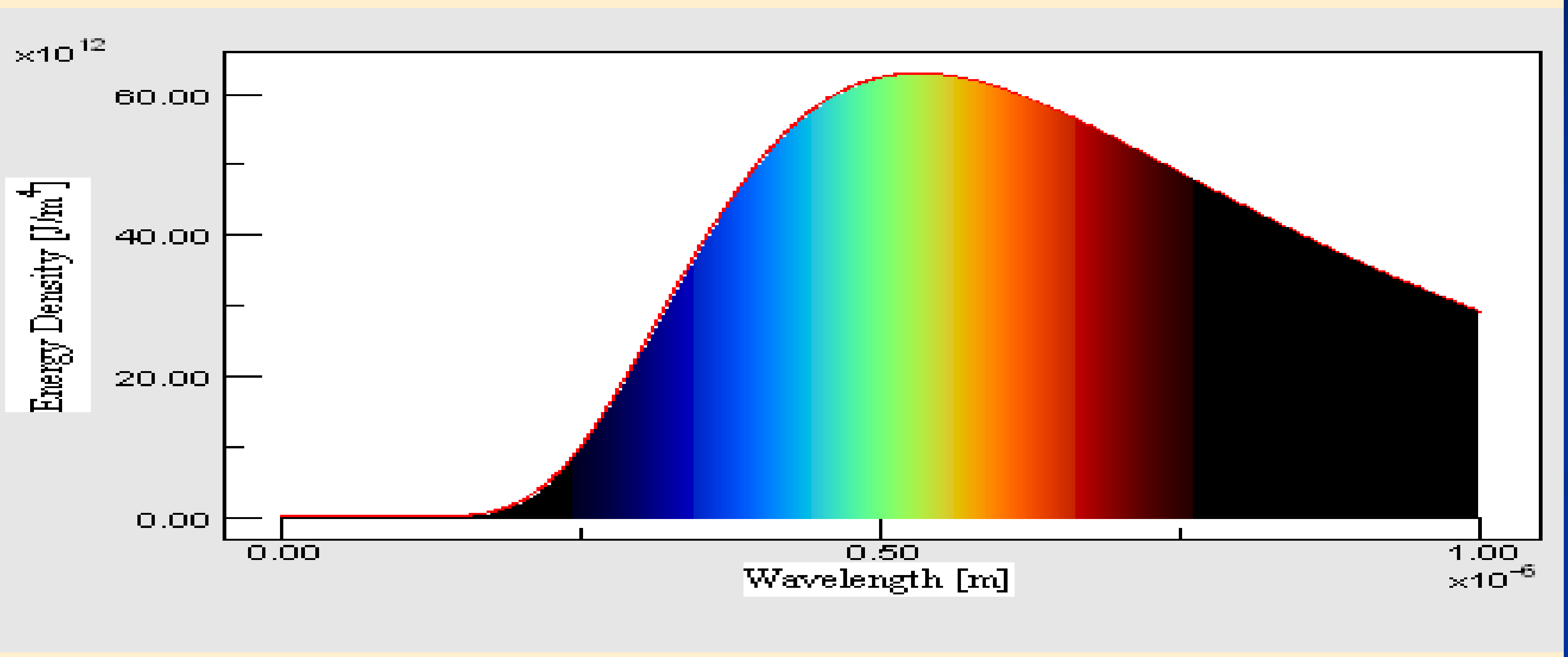

500 Kelvin | 10,000 Kelvin | 7,500 Kelvin | 5,00

Temp	Lambda
+5463.77	+530.77

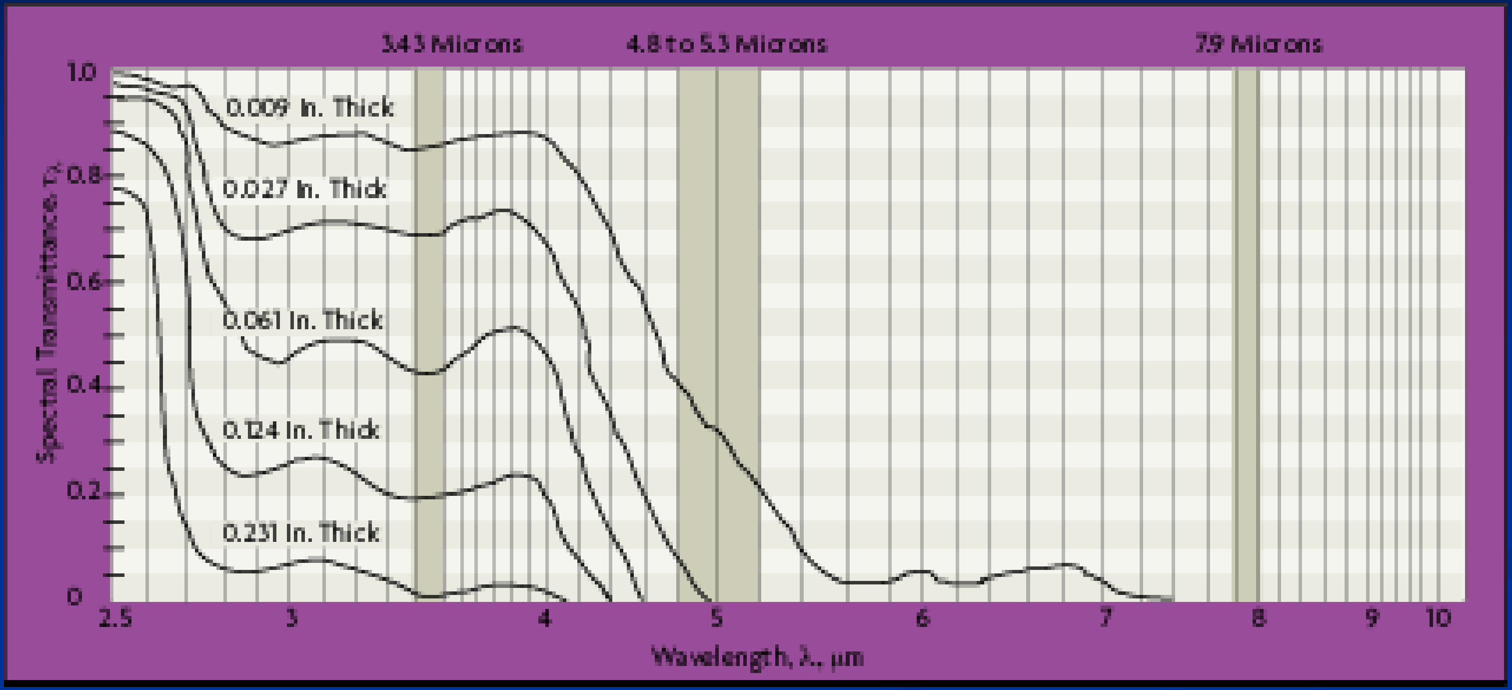

Figure 2-5: Soda-Lyme Glass Spectral Transmittance
http://www.omega.com/literature/transactions/volume1/theoretical3.html

– Comprimento de onda λ e frequência ν,

$$\lambda = \frac{c}{\nu}$$

vácuo,

$$c = c_o = 2.998 \;x\; 10^8 \text{ m/s}$$

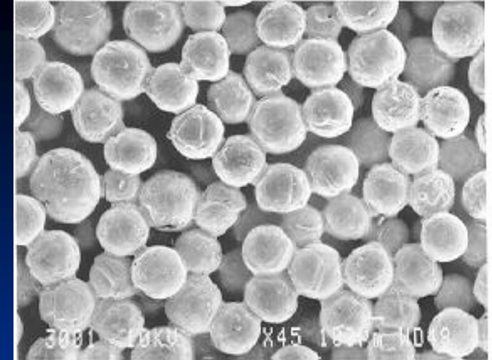

<u>Característica Espectral</u>

<u>Característica Direcional</u>

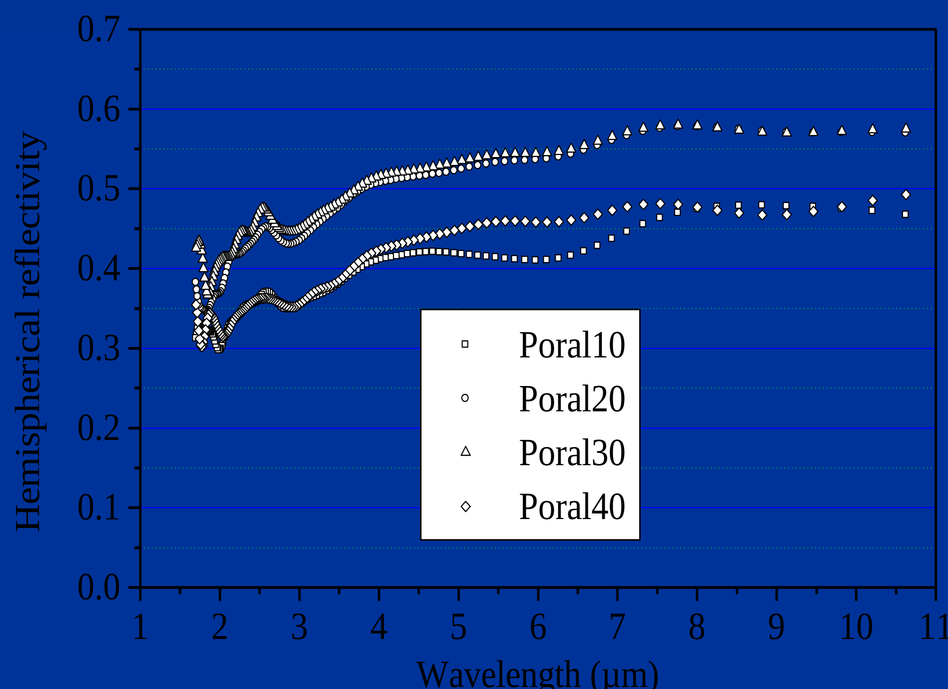

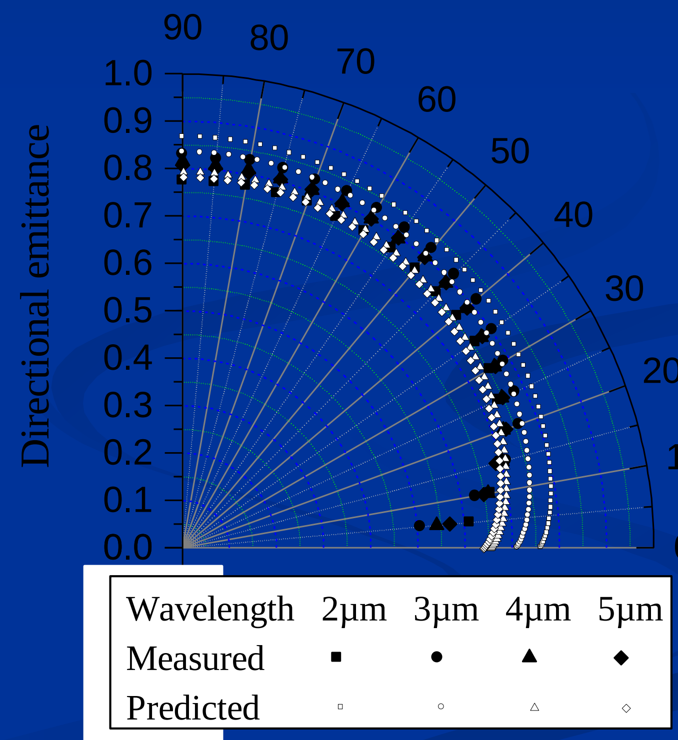

- Figure 6. Comparison of measured and predicted spectral directional emittance of Poral20 (*L*=2.93 mm, *fv*= 0.730, *d*= 200 µm, and *T*= 917 K).

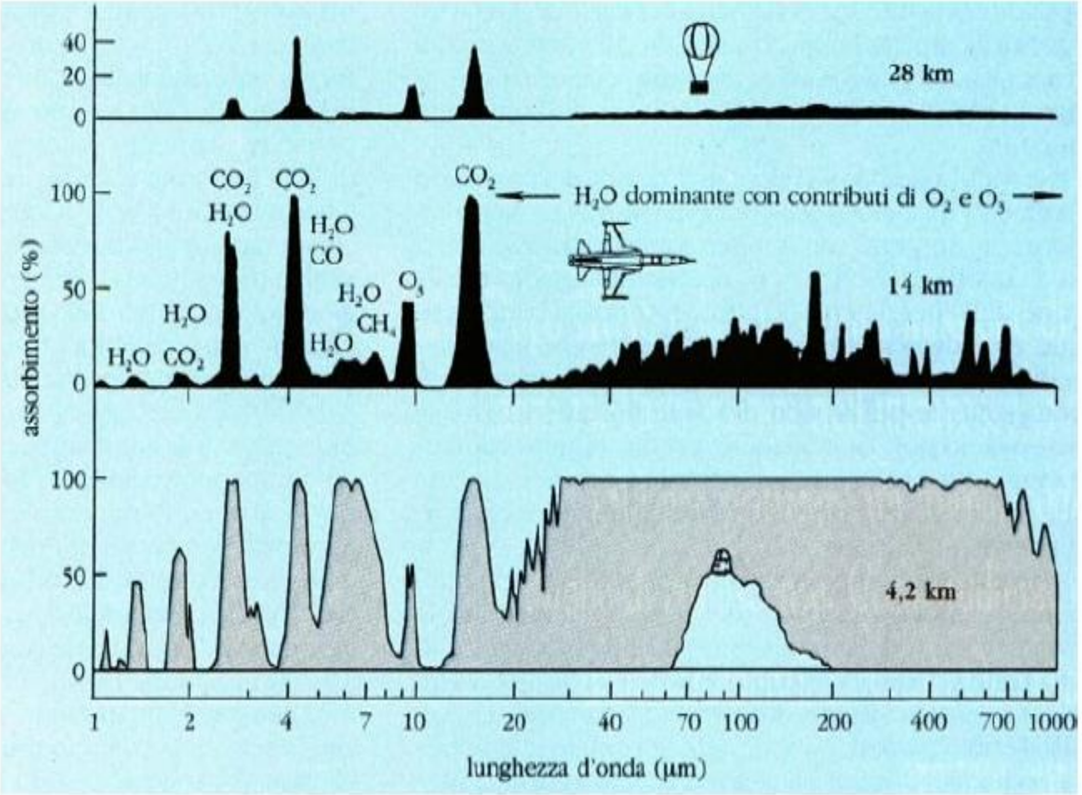

Fig. 1: Rappresentazione schematica della trasparenza atmosferica alla radiazione infrarossa cosmica in corrispondenza di varie altezze dal suolo.

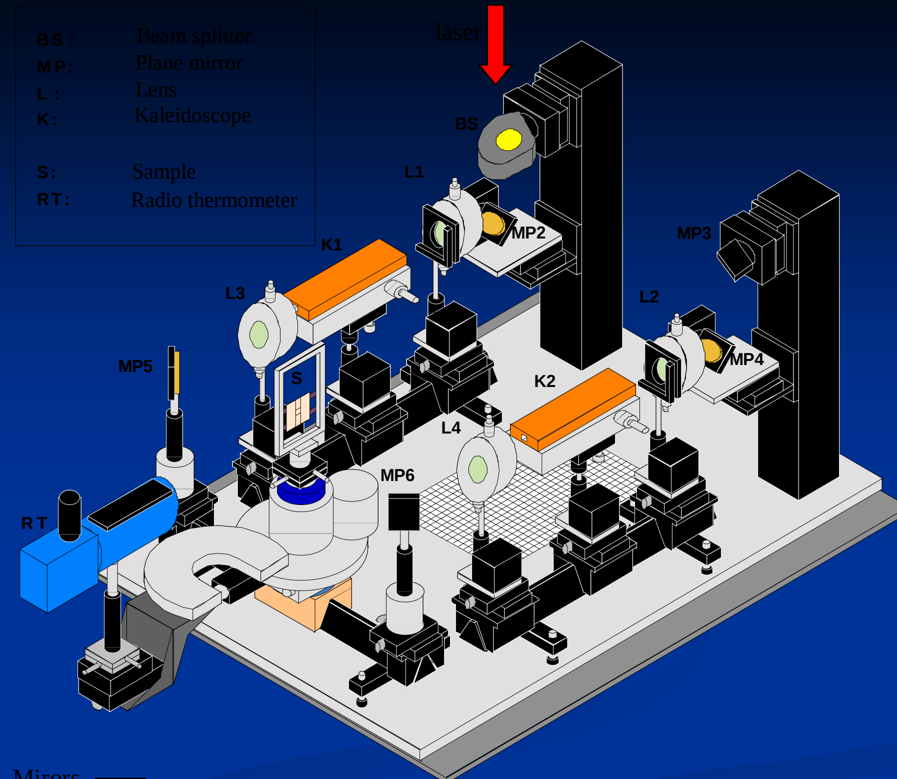
BS : Beam splitter
MP: Plane mirror
L : Lens
K: Kaleidoscope
S: Sample
RT: Radio thermometer
laser
BS
L1
MP2
MP3
K1
L3
L2
MP5
S
MP4
K2
L4
MP6
RT

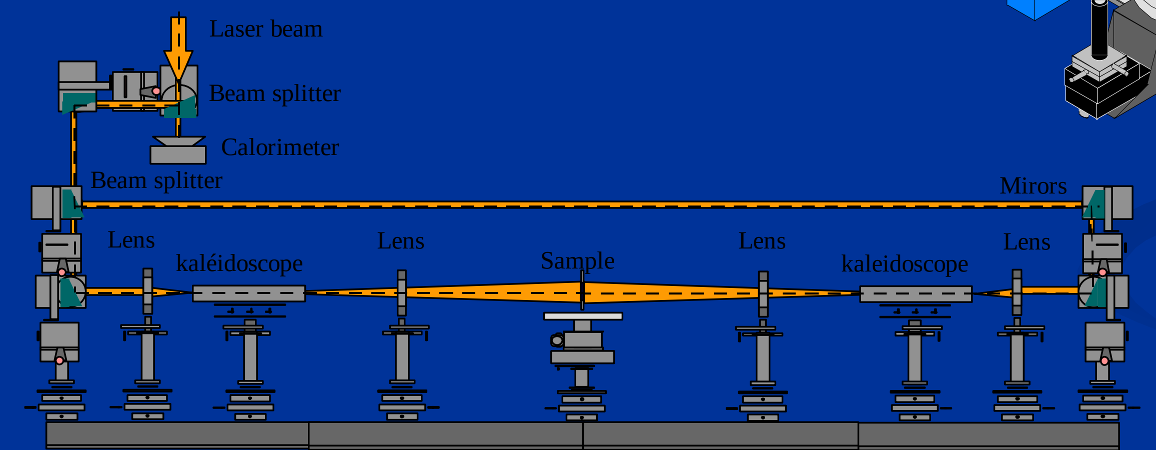
Laser beam
Beam splitter
Calorimeter
Beam splitter
Mirors
Lens
kaléidoscope
Lens
Sample
Lens
kaleidoscope
Lens

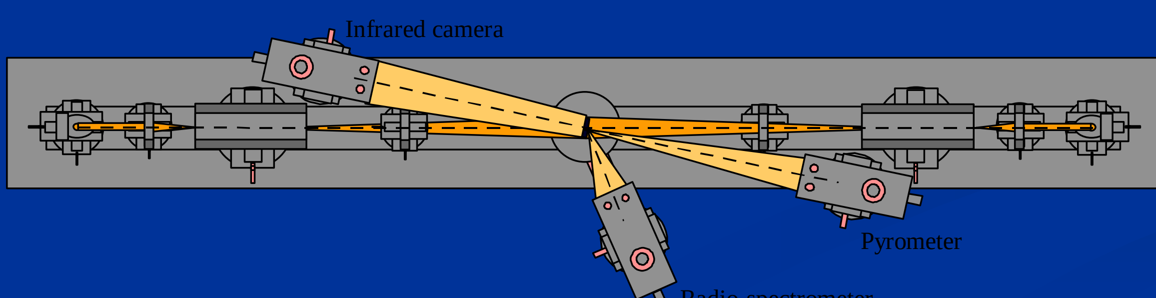
Infrared camera
Pyrometer
Radio-spectrometer

Ângulo Plano

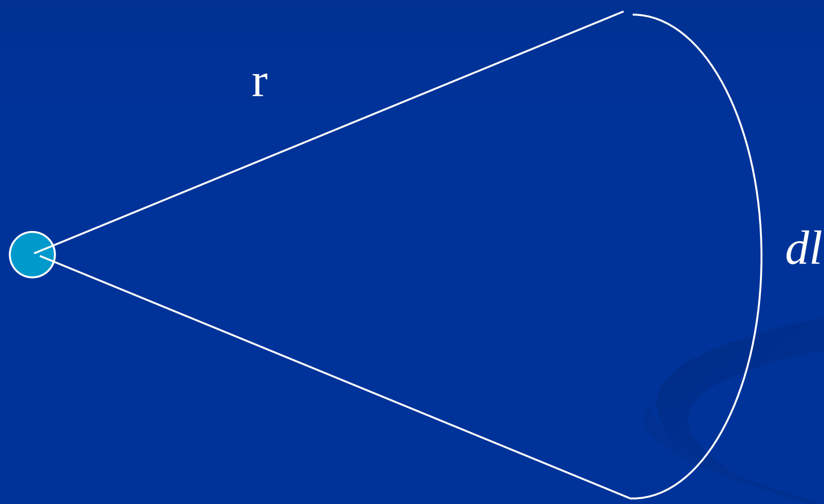

$$d\alpha = \frac{dl}{r}$$

Ângulo Sólido

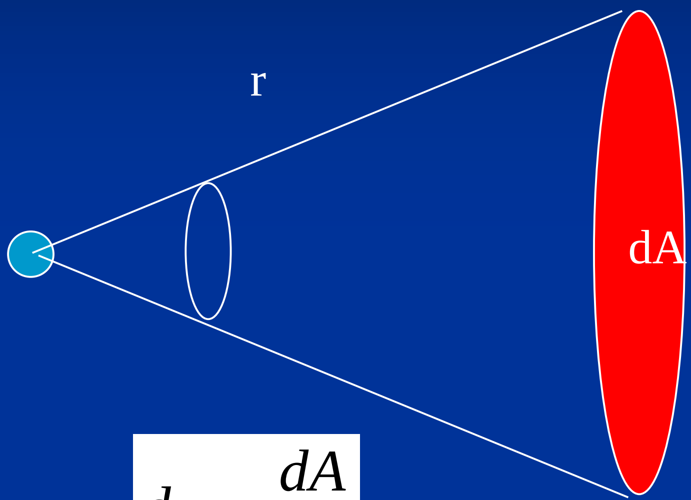

$$d\omega = \frac{dA}{r^2}$$

dω de um hemisfério = 2π
dω de uma esfera = 4π

– O ângulo sólido tem unidade esteradianos (sr).

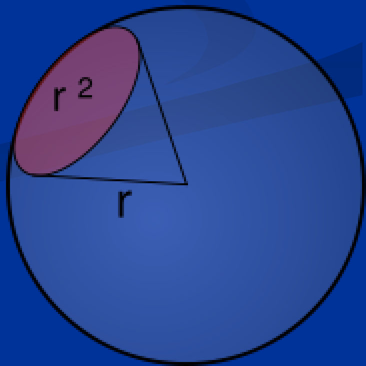

Considerações direcionais

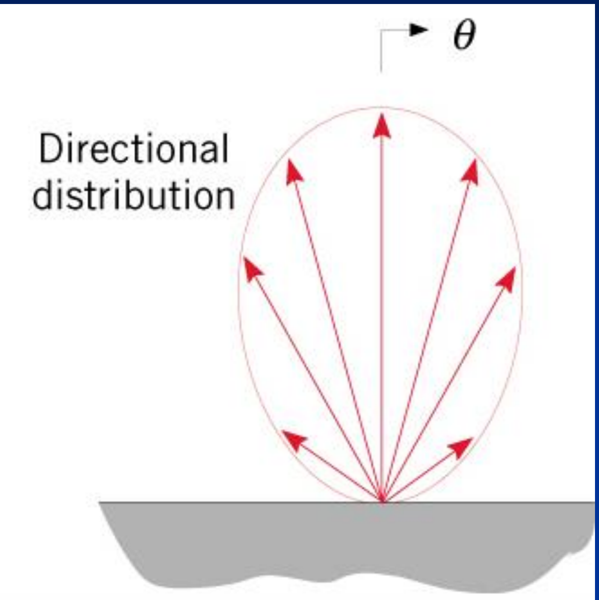

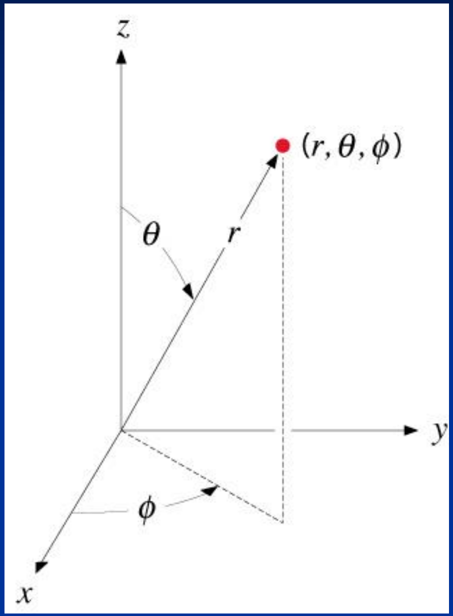

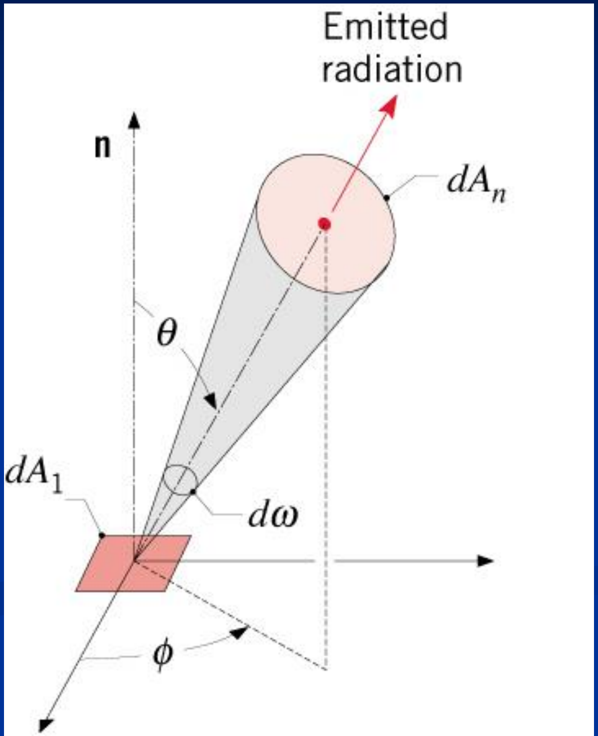

- Coordenadas esféricas: ângulo polar (zenite), θ, e ângulo de azimute, ϕ .

$$d\omega \equiv \frac{dA_n}{r^2}$$

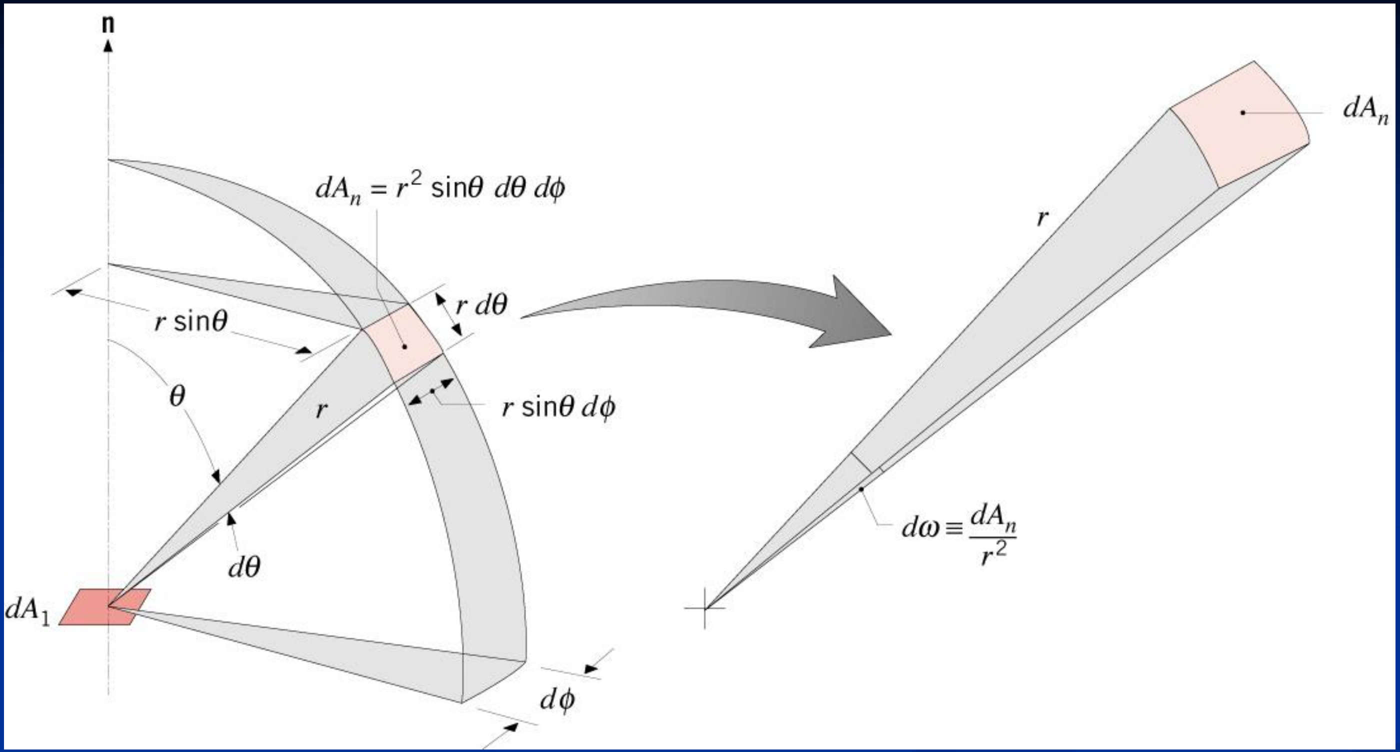

$$dA_n = r^2 \sin\theta d\theta d\phi$$

$$d\omega = \frac{dA_n}{r^2} = \sin\theta d\theta d\phi$$

– O ângulo sólido de um hemisfério completo é:

$$\omega_{hemi} = \int_0^{2\pi} \int_0^{\pi/2} \sin\theta d\theta d\phi = 2\pi \mathrm{sr}$$

Intensidade Espectral , $I_{\lambda,e}$

- A Intensidade espectral é a unidade utilizada para especificar fluxo radiativo (taxa transferida de energia radiativa por unidade de área normal) por unidade de ângulo sólido em um intervalo de comprimento de onda:

$$I_{\lambda,e}(\lambda,\theta,\phi) \equiv \frac{dq}{(dA_1 \cos\theta)\cdot d\omega \cdot d\lambda} \qquad \left(\mathrm{W/m^2 \cdot sr \cdot \mu m}\right).$$

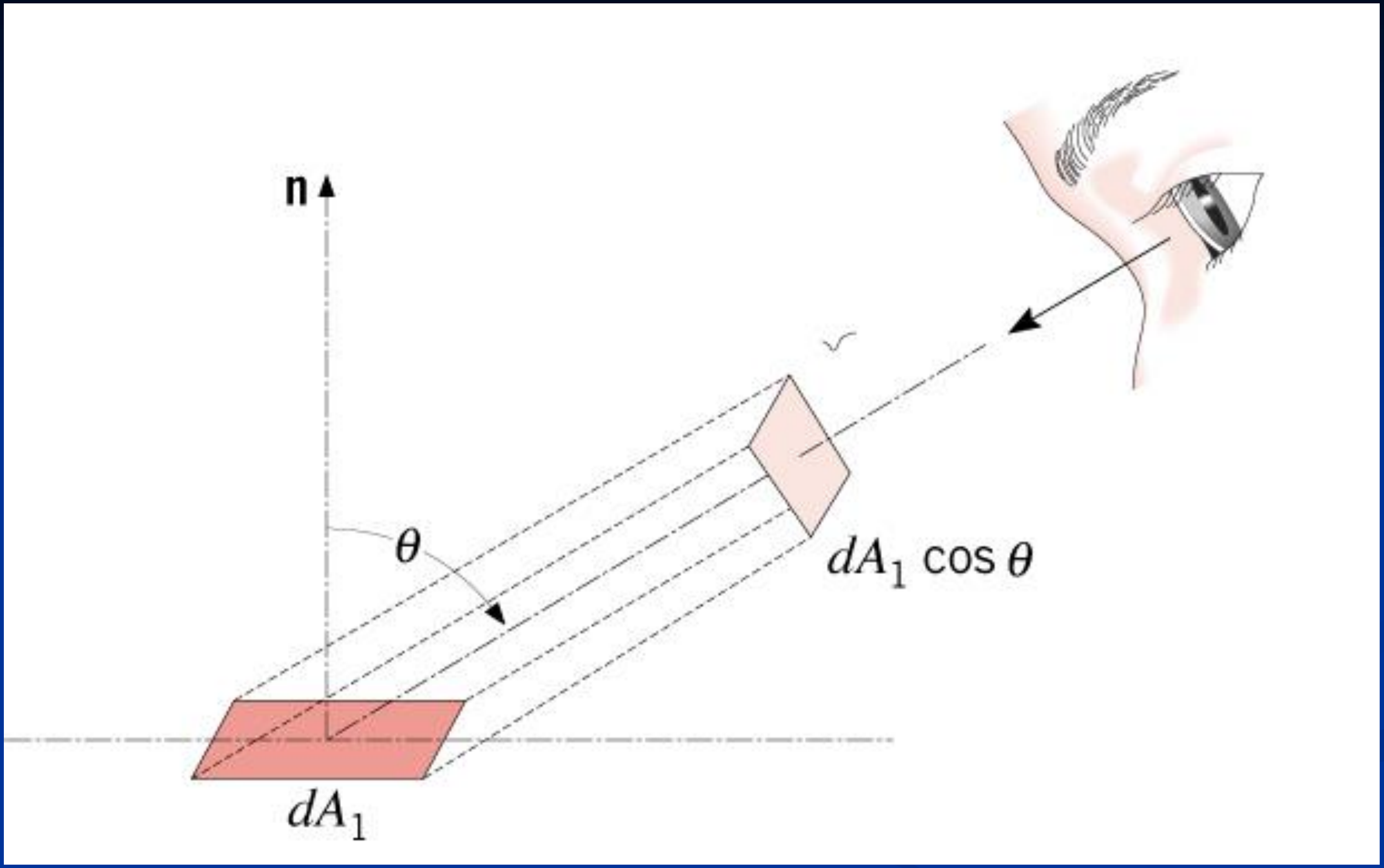

- A taxa radiativa e o fluxo radiativo associado com a emissão de uma superfície é, respectivamente:

$$dq_{\lambda} \equiv \frac{dq}{d\lambda} = I_{\lambda,e}\left(\lambda,\theta,\phi\right) dA_1 \cos\theta d\omega$$

$$dq''_{\lambda} = I_{\lambda,e}\left(\lambda,\theta,\phi\right)\cos\theta d\omega = I_{\lambda,e}\left(\lambda,\theta,\phi\right)\cos\theta \sin\theta d\theta d\phi$$

•poder emissivo espectral $\left(\mathrm{W/m^2 \cdot \mu m}\right)$

$$E_\lambda(\lambda) = \int_0^{2\pi} \int_0^{\pi/2} I_{\lambda,e}(\lambda,\theta,\phi) \cos\theta \sin\theta \, d\theta \, d\phi$$

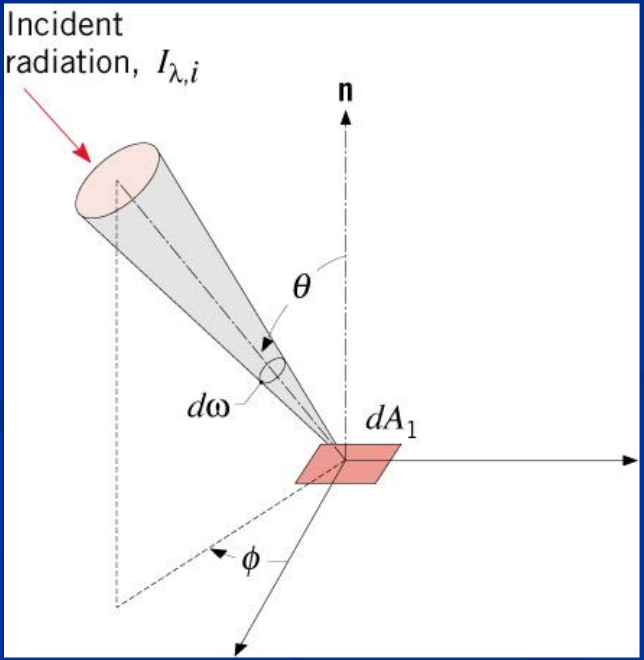

•poder emissivo total $\left(\mathrm{W/m^2}\right)$

$$E = \int_0^{\infty} E_\lambda(\lambda) \, d\lambda$$

•Para uma superfície difusa – emissão isotrópica

$$E_\lambda(\lambda) = \pi I_{\lambda,e}(\lambda) \qquad E = \pi I_e$$

• A irradiação espectral $\left(\mathrm{W/m^2} \cdot \mu\mathrm{m}\right)$

$$G_\lambda(\lambda) = \int_0^{2\pi} \int_0^{\pi/2} I_{\lambda,i}(\lambda,\theta,\phi)\cos\theta \sin\theta \, d\theta \, d\phi$$

irradiação total $\left(\mathrm{W/m^2}\right)$

$$G = \int_0^\infty G_\lambda(\lambda)\, d\lambda$$

• A radiosidade é reflection + emission.

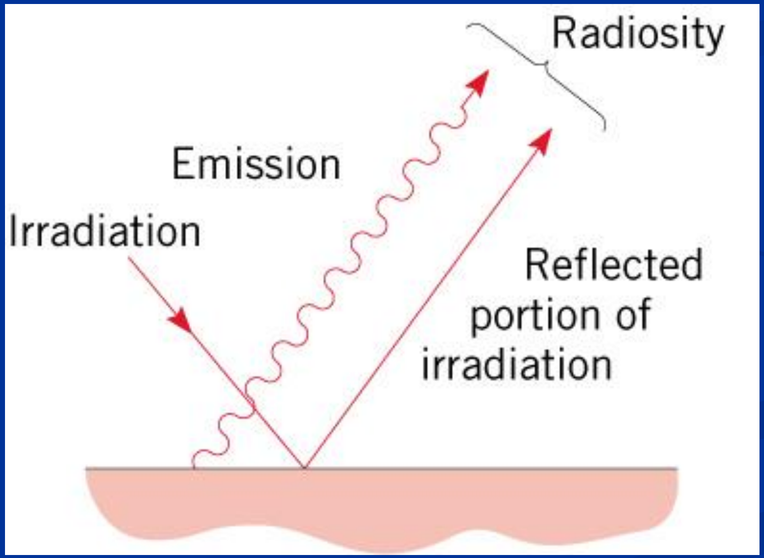

•Radiosidade espectral $\left(\mathrm{W/m^2 \cdot \mu m}\right)$

$$J_\lambda(\lambda) = \int_0^{2\pi}\int_0^{\pi/2} I_{\lambda,e+r}(\lambda,\theta,\phi)\cos\theta\sin\theta\, d\theta\, d\phi$$

radiosidade total $\left(\mathrm{W/m^2}\right)$

$$J = \int_0^\infty J_\lambda(\lambda)\, d\lambda$$

Corpo Negro - Blackbody Radiation

– Emissor ideal (difuso) em relação a sua temperatura.

– Absorvedor ideal.

- Cavidade Isotérmica (Hohlraum).

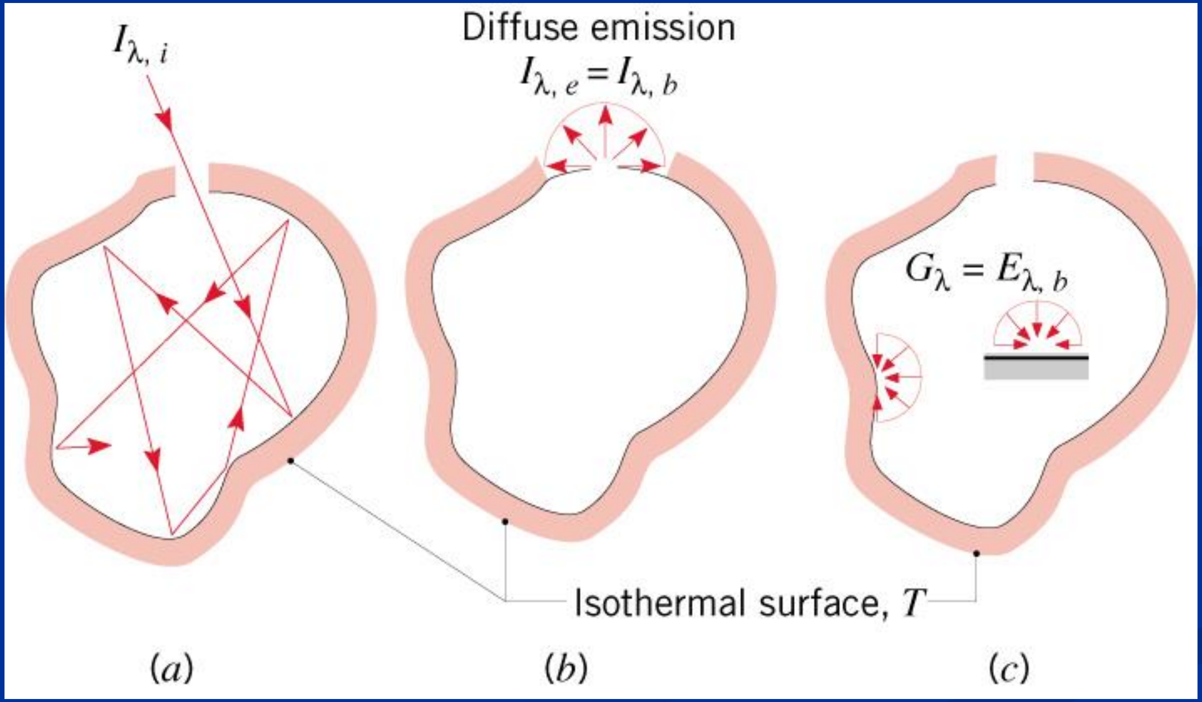

- Figure 7-2: cal Cavities

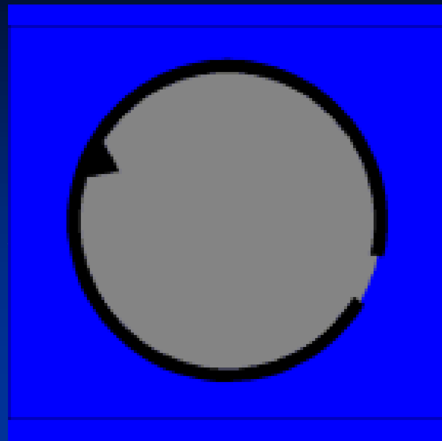

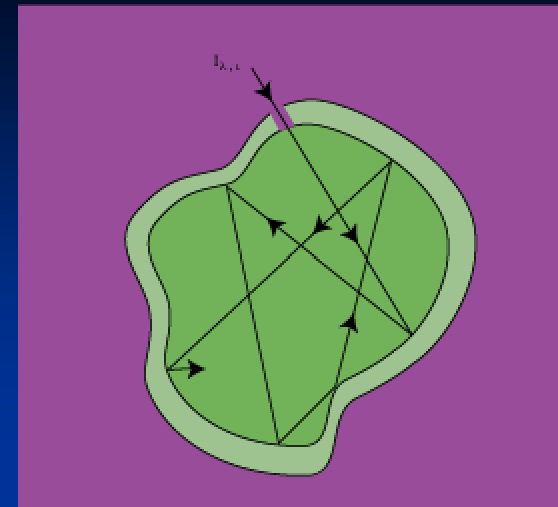

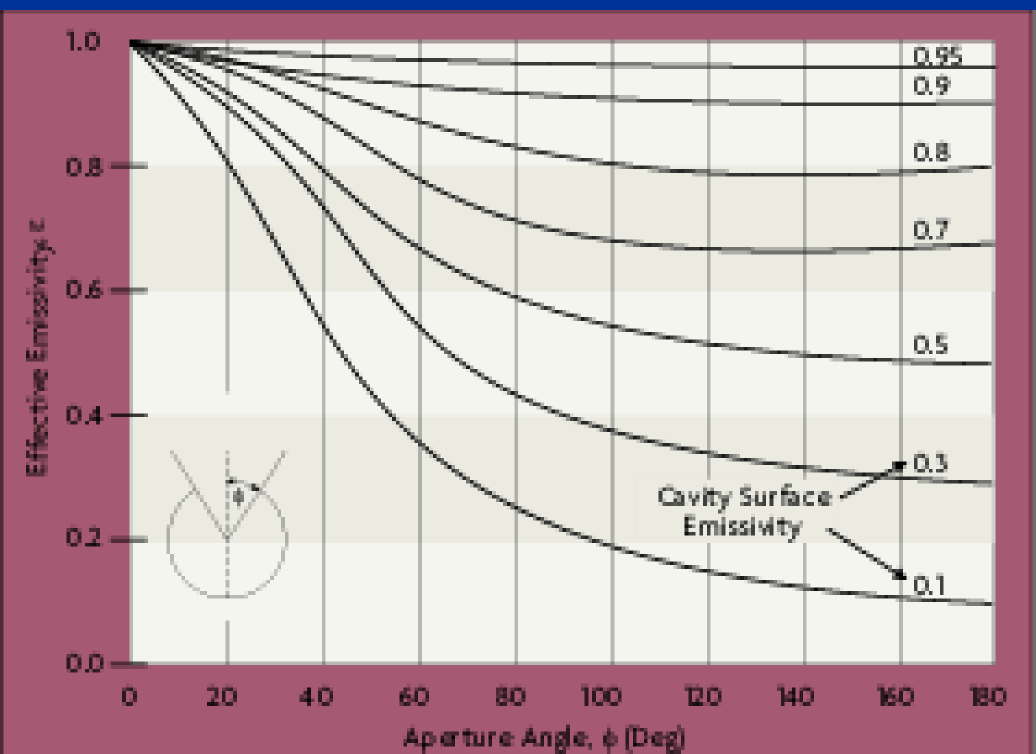

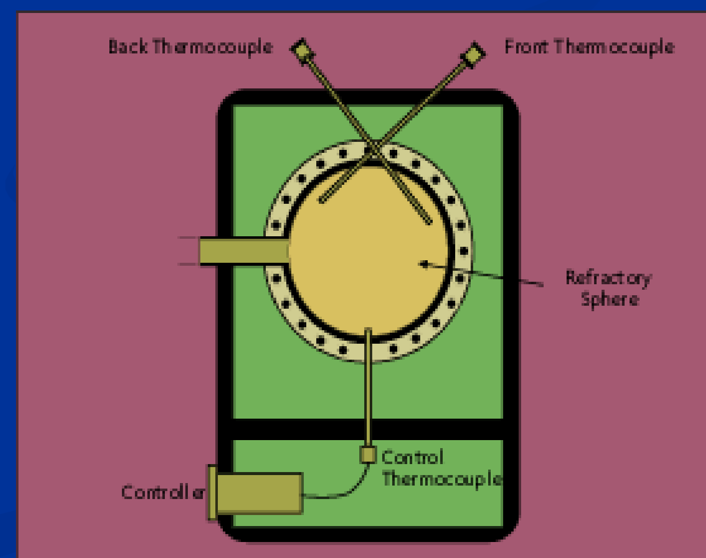

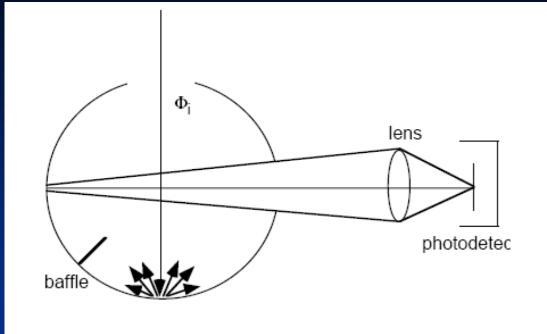

FIGURE 9

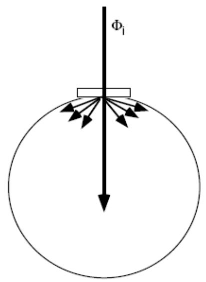

FIGURE 20

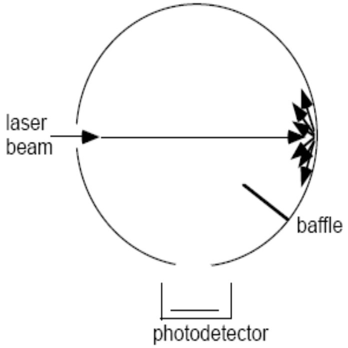

FIGURE 16

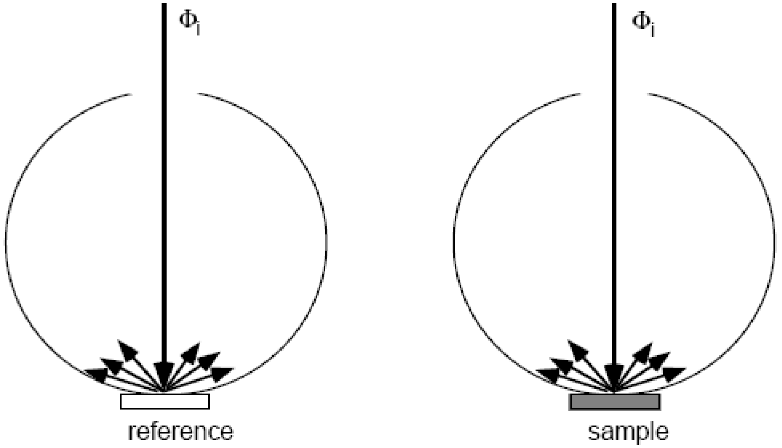

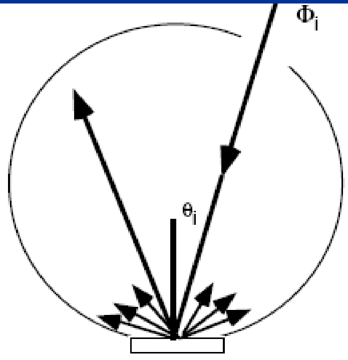

FIGURE 21


CAVITY TEMP
1000
SET TEMP
1000

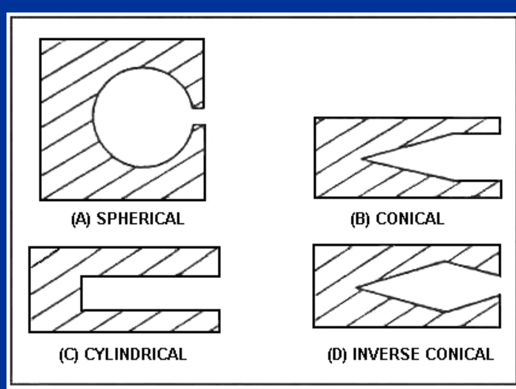
(A) SPHERICAL
(B) CONICAL
(C) CYLINDRICAL
(D) INVERSE CONICAL

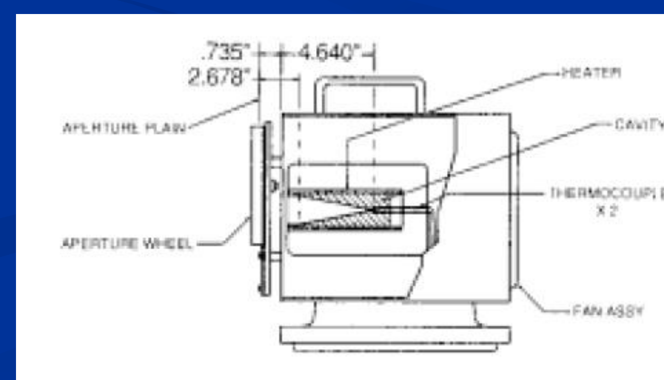
.735"
4.640"
2.678"
HEATER
APERTURE PLANE
CAVITY
THERMOCOUPLE X 2
APERTURE WHEEL
FAN ASSY

Operator calibrates a transfer standard (lower foreground)—an infrared thermometer with 0.1°C resolution—with a blackbody calibration source that provides temperatures from 600°C to 3000°C.

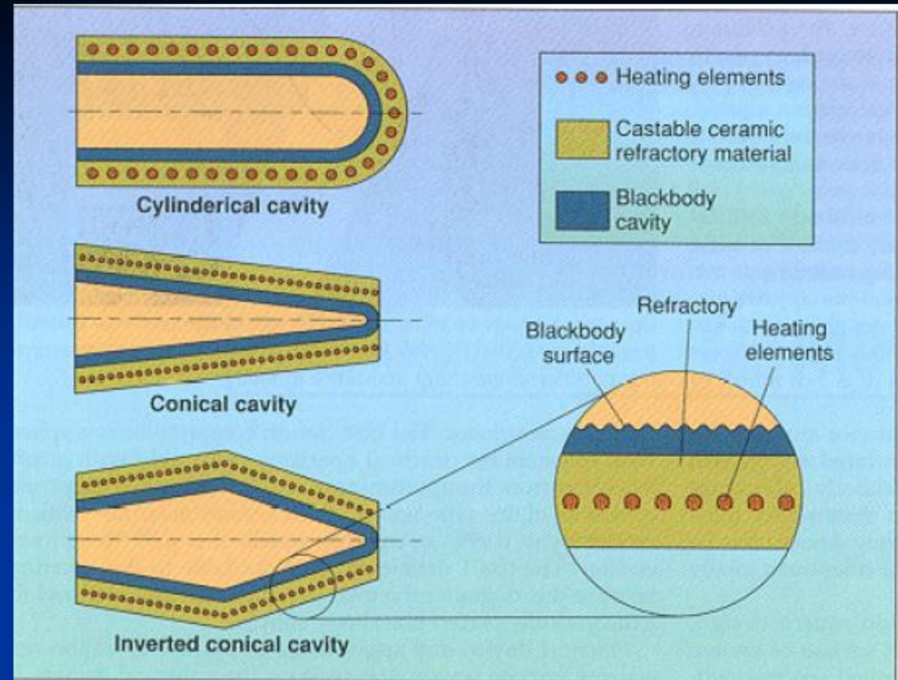

FIGURE 2. To address needs such as portability, small size, ruggedness, rapid and frequent source temperature change, and wide temperature range capabilities, blackbody calibration standards incorporate nonspherical cavity configurations.

MIKRON INSTRUMENT CO.

FIGURE 4. For calibrating thermal imaging systems or mapping and surveillance equipment, or for long-path spectrophotometers, a calibration source requires a large target area. Source (on the right) area is 305 mm square; the controller is on the left.

Distribuição espectral de Planck - Blackbody Radiation

$$E_{\lambda,b}(\lambda,T) = \pi I_{\lambda,b}(\lambda,T) = \frac{C_1}{\lambda^5\left[exp(C_2/\lambda T)-1\right]}$$

First radiation constant: $C_1 = 3.742\,x\,10^8\,\mathrm{W}\cdot\mu\mathrm{m}^4/\mathrm{m}^2$

Second radiation constant: $C_2 = 1.439\,x\,10^4\,\mu\mathrm{m}\cdot\mathrm{K}$

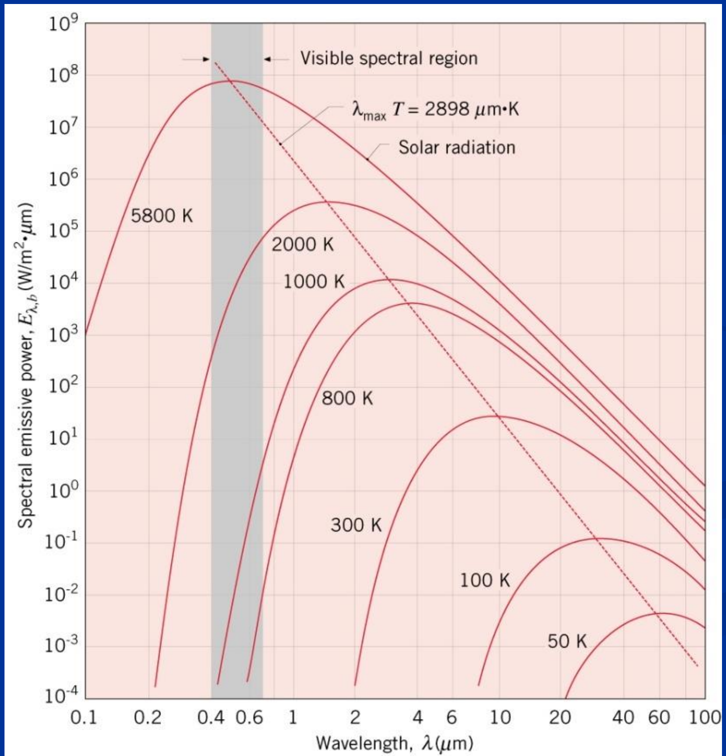

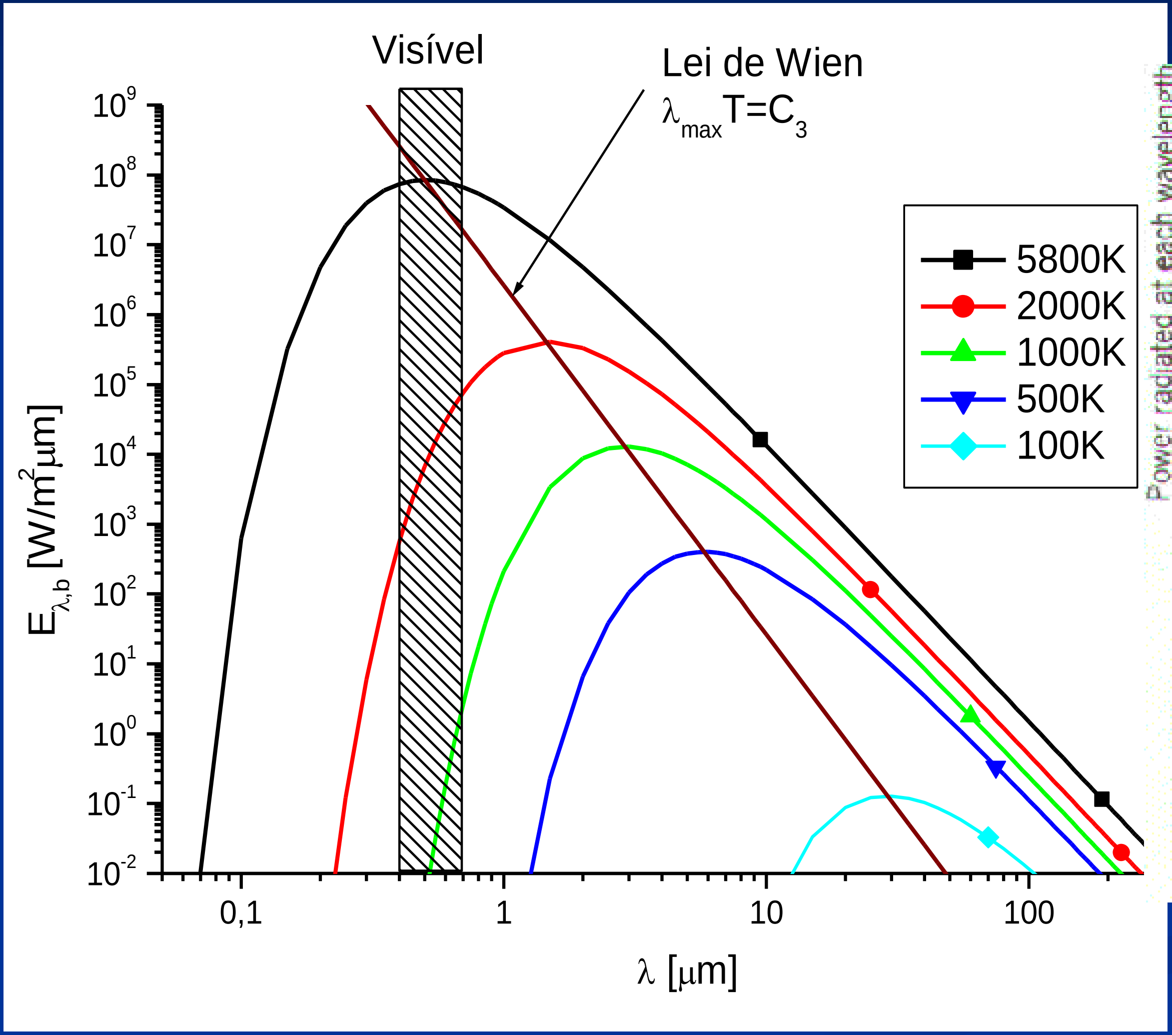

Visível
Lei de Wien
$\lambda_{max}T=C_3$
$E_{\lambda,b}$ [W/m^{2}μm]
10^9
10^8
10^7
10^6
10^5
10^4
10^3
10^2
10^1
10^0
10^{-1}
10^{-2}
0,1
1
10
100
λ [μm]
5800K
2000K
1000K
500K
100K

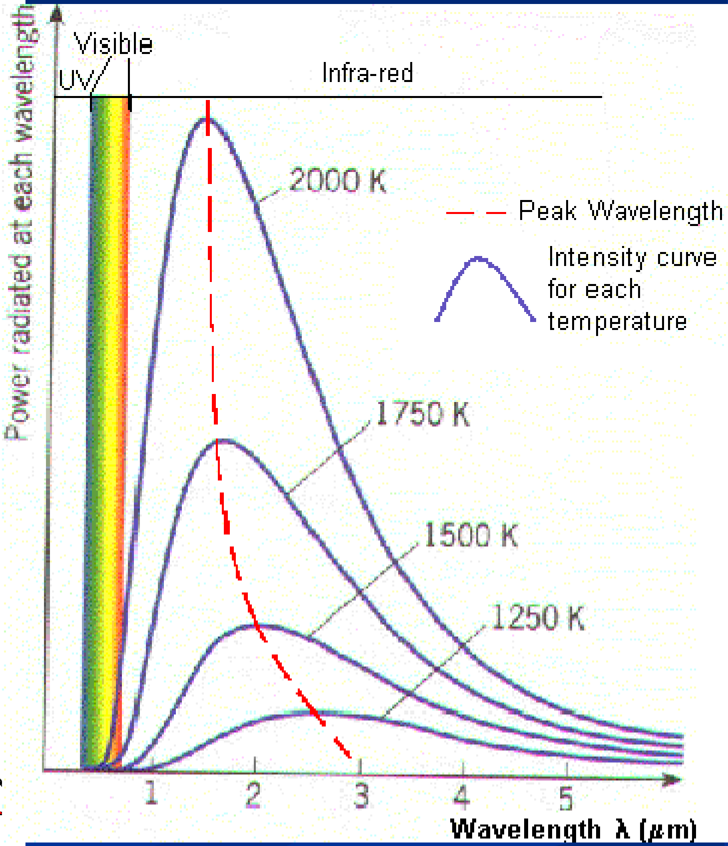

Power radiated at each wavelength
Visible
UV
Infra-red
2000 K
1750 K
1500 K
1250 K
Peak Wavelength
Intensity curve for each temperature
1
2
3
4
5
Wavelength λ (μm)

- Lei de Wien :

$$\lambda_{max} T = C_3 = 2898\ \mu\text{m} \cdot \text{K}$$

Lei de Stefan-Boltzmann

- Poder emissivo total:

$$E_b = \pi I_b = \int_0^{\infty} E_{\lambda,b} d\lambda = \sigma T^4$$

⟶ Lei de Stefan-Boltzmann law

$$\sigma = 5.670\, x 10^{-8}\ \mathrm{W/m^2 \cdot K^4} \rightarrow$$ the Stefan-Boltzmann constant

- Fração da emissão total de um corpo negro no intervalo $(\lambda_1 < \lambda < \lambda_2)$

$$F_{(\lambda_1 - \lambda_2)} = F_{(0-\lambda_2)} - F_{(0-\lambda_1)} = \frac{\int_0^{\lambda_2} E_{\lambda,b} d\lambda - \int_o^{\lambda_1} E_{\lambda,b} d\lambda}{\sigma T^4}$$

onde, em geral,

$$F_{(0-\lambda)} = \frac{\int_0^{\lambda} E_{\lambda,b} d\lambda}{\sigma T} = f(\lambda T)$$

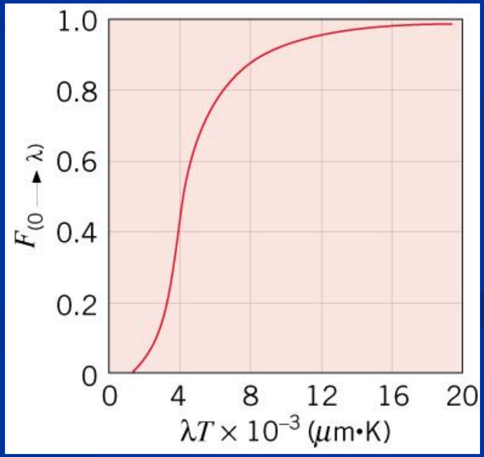

- Table 12.1

TABLE 12.1 Blackbody Radiation Functions

λT $(\mu m \cdot K)$	$F_{(0 \rightarrow \lambda)}$	$I_{\lambda,b}(\lambda, T)/\sigma T^5$ $(\mu m \cdot K \cdot sr)^{-1}$	$\frac{I_{\lambda,b}(\lambda, T)}{I_{\lambda,b}(\lambda_{max}, T)}$
200	0.000000	0.375034×10^{-27}	0.000000
400	0.000000	0.490335×10^{-13}	0.000000
600	0.000000	0.104046×10^{-8}	0.000014
800	0.000016	0.991126×10^{-7}	0.001372
1,000	0.000321	0.118505×10^{-5}	0.016406
1,200	0.002134	0.523927×10^{-5}	0.072534
1,400	0.007790	0.134411×10^{-4}	0.186082
1,600	0.019718	0.249130	0.344904
1,800	0.039341	0.375568	0.519949
2,000	0.066728	0.493432	0.683123
2,200	0.100888	0.589649×10^{-4}	0.816329
2,400	0.140256	0.658866	0.912155
2,600	0.183120	0.701292	0.970891
2,800	0.227897	0.720239	0.997123
2,898	0.250108	0.722318×10^{-4}	1.000000
3,000	0.273232	0.720254×10^{-4}	0.997143
3,200	0.318102	0.705974	0.977373
3,400	0.361735	0.681544	0.943551
3,600	0.403607	0.650396	0.900429
3,800	0.443382	0.615225×10^{-4}	0.851737
4,000	0.480877	0.578064	0.800291

Tabela 12.1 Funções da radiação do corpo negro[a]

λT (μm · K)	$F_{(0 \to \lambda)}$	$I_{\lambda,b}(\lambda, T)/\sigma T^5$ $(\mu\text{m} \cdot \text{K} \cdot \text{sr})^{-1}$	$\dfrac{I_{\lambda,b}(\lambda, T)}{I_{\lambda,b}(\lambda_{\text{máx}}, T)}$
200	0,000000	$0{,}375034 \times 10^{-27}$	0,000000
400	0,000000	$0{,}490335 \times 10^{-13}$	0,000000
600	0,000000	$0{,}104046 \times 10^{-8}$	0,000014
800	0,000016	$0{,}991126 \times 10^{-7}$	0,001372
1.000	0,000321	$0{,}118505 \times 10^{-5}$	0,016406
1.200	0,002134	$0{,}523927 \times 10^{-5}$	0,072534
1.400	0,007790	$0{,}134411 \times 10^{-4}$	0,186082
1.600	0,019718	0,249130	0,344904
1.800	0,039341	0,375568	0,519949
2.000	0,066728	0,493432	0,683123
2.200	0,100888	$0{,}589649 \times 10^{-4}$	0,816329
2.400	0,140256	0,658866	0,912155
2.600	0,183120	0,701292	0,970891
2.800	0,227897	0,720239	0,997123
2.898	0,250108	$0{,}722318 \times 10^{-4}$	1,000000
3.000	0,273232	$0{,}720254 \times 10^{-4}$	0,997143
3.200	0,318102	0,705974	0,977373
3.400	0,361735	0,681544	0,943551
3.600	0,403607	0,650396	0,900429
3.800	0,443382	0,615225	0,851737
4.000	0,480877	0,578064	0,800291
4.200	0,516014	$0{,}540394 \times 10^{-4}$	0,748139
4.400	0,548796	0,503253	0,696720
4.600	0,579280	0,467343	0,647004
4.800	0,607559	0,433109	0,599610
5.000	0,633747	0,400813	0,554898
5.200	0,658970	$0{,}370580 \times 10^{-4}$	0,513043
5.400	0,680360	0,342445	0,474092
5.600	0,701046	0,316376	0,438002
5.800	0,720158	0,292301	0,404671
6.000	0,737818	0,270121	0,373965
6.200	0,754140	$0{,}249723 \times 10^{-4}$	0,345724
6.400	0,769234	0,230985	0,319783
6.600	0,783199	0,213786	0,295973
6.800	0,796129	0,198008	0,274128
7.000	0,808109	0,183534	0,254090
7.200	0,819217	$0{,}170256 \times 10^{-4}$	0,235708
7.400	0,829527	0,158073	0,218842
7.600	0,839102	0,146891	0,203360
7.800	0,848005	0,136621	0,189143
8.000	0,856288	0,127185	0,176079
8.500	0,874608	$0{,}106772 \times 10^{-4}$	0,147819
9.000	0,890029	$0{,}901463 \times 10^{-5}$	0,124801
9.500	0,903085	0,765338	0,105956

Tabela 12.1 Funções da radiação do corpo negro[a] (cont.)

λT (μm · K)	$F_{(0 \to \lambda)}$	$I_{\lambda,b}(\lambda, T)/\sigma T^5$ $(\mu\text{m} \cdot \text{K} \cdot \text{sr})^{-1}$	$\dfrac{I_{\lambda,b}(\lambda, T)}{I_{\lambda,b}(\lambda_{\text{máx}}, T)}$
10.000	0,914199	0,653279	0,090442
10.500	0,923710	0,560522	0,077600
11.000	0,931890	$0{,}483321 \times 10^{-5}$	0,066913
11.500	0,939959	0,418725	0,057970
12.000	0,945098	0,364394	0,050448
13.000	0,955139	0,279457	0,038689
14.000	0,962898	0,217641	0,030131
15.000	0,969981	$0{,}171866 \times 10^{-5}$	0,023794
16.000	0,973814	0,137429	0,019026
18.000	0,980860	$0{,}908240 \times 10^{-6}$	0,012574
20.000	0,985602	0,623310	0,008629
25.000	0,992215	0,276474	0,003828
30.000	0,995340	$0{,}140469 \times 10^{-6}$	0,001945
40.000	0,997967	$0{,}473891 \times 10^{-7}$	0,000656
50.000	0,998953	0,201605	0,000279
75.000	0,999713	$0{,}418597 \times 10^{-8}$	0,000058
100.000	0,999905	0,135752	0,000019

[a] As constantes de radiação usadas para gerar estas funções do corpo negro foram

$C_1 = 3{,}7420 \times 10^8\ \text{W}\mu\text{m}^4/\text{m}^2$

$C_2 = 1{,}4388 \times 10^4\ \mu\text{m} \cdot \text{K}$

$\sigma = 5{,}670 \times 10^{-8}\ \text{W/m}^2 \cdot \text{K}^4$

Emissividade de uma superfície

- A emissividade espectral e direcional:

$$\varepsilon_{\lambda,\theta}\left(\lambda,\theta,\phi,T\right)\equiv\frac{I_{\lambda,e}\left(\lambda,\theta,\phi,T\right)}{I_{\lambda,b}\left(\lambda,T\right)}$$

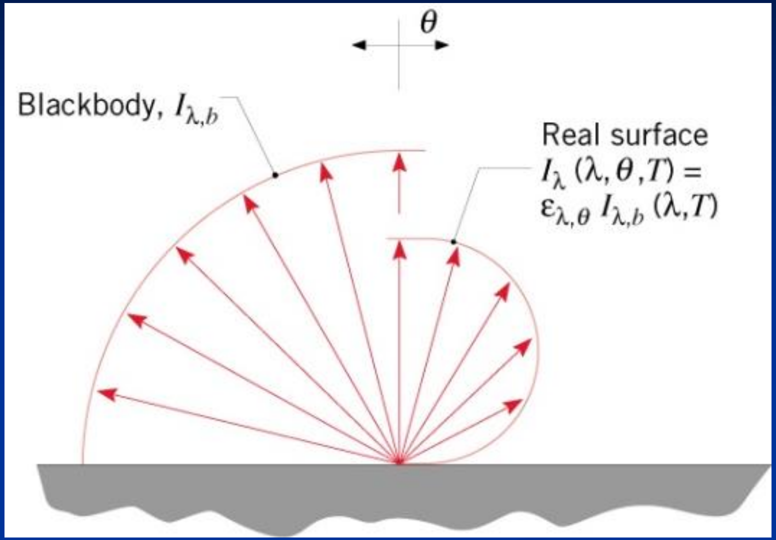

- A emissividade espectral e hemisférica:

$$\varepsilon_{\lambda}\left(\lambda,T\right)\equiv\frac{E_{\lambda}\left(\lambda,T\right)}{E_{\lambda,b}\left(\lambda,T\right)}=\frac{\int_0^{2\pi}\int_0^{\pi/2} I_{\lambda,e}\left(\lambda,\theta,\phi,T\right)\cos\theta\sin\theta\, d\theta\, d\phi}{\int_0^{2\pi}\int_0^{\pi/2} I_{\lambda,b}\left(\lambda,T\right)\cos\theta\sin\theta\, d\theta\, d\phi}$$

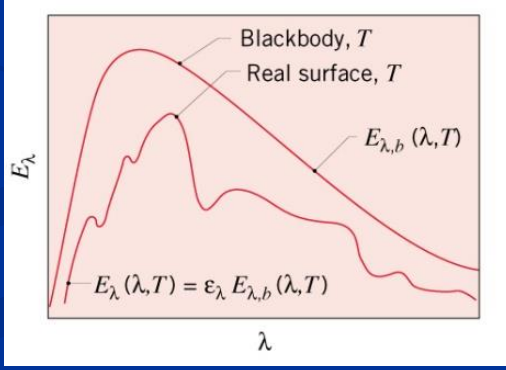

Emissivity (cont)

- A emissividade hemisférica total:

$$\varepsilon(T) \equiv \frac{E(T)}{E_b(T)} = \frac{\int_0^\infty \varepsilon_\lambda(\lambda,T)E_{\lambda,b}(\lambda,T)\,d,\lambda}{E_b(T)}$$

- De maneira aproximada

$$\varepsilon \approx \varepsilon_n$$

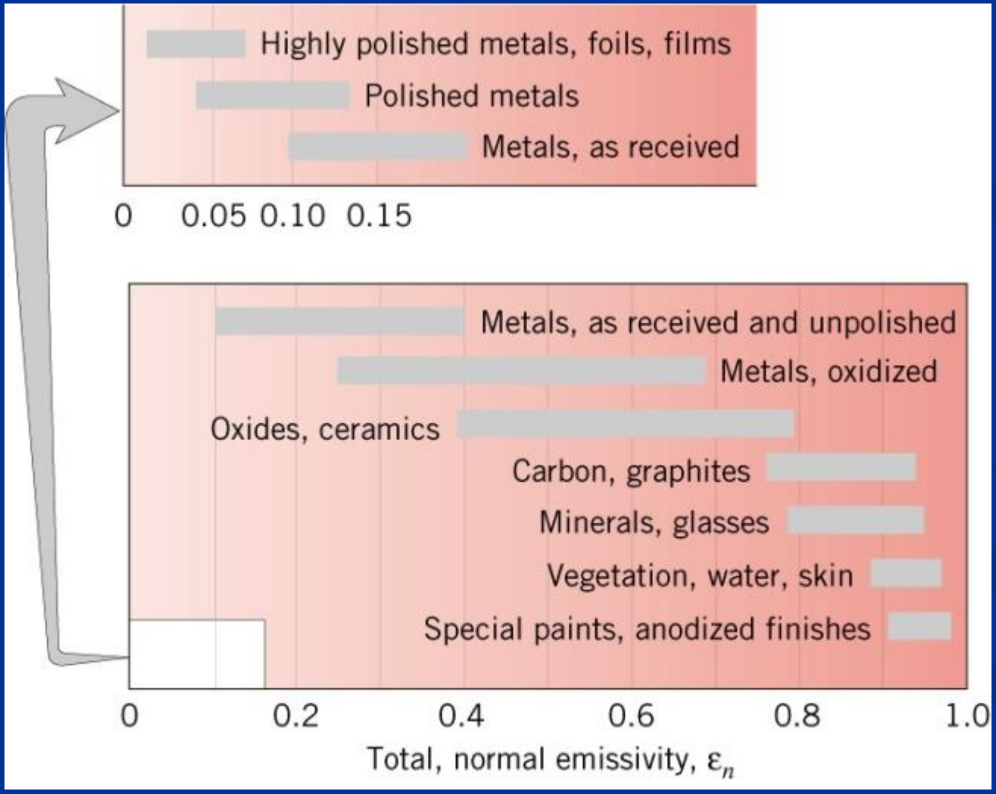

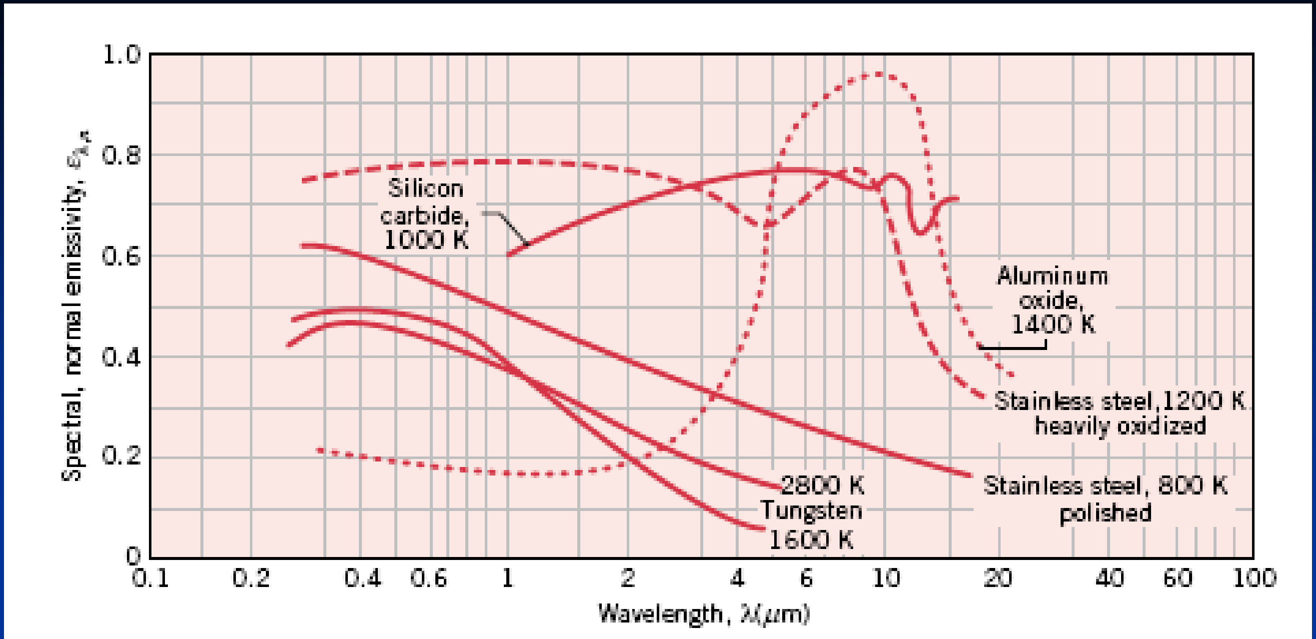

Spectral, normal emissivity, $\varepsilon_{\lambda,n}$
Wavelength, $\lambda(\mu m)$
Silicon carbide, 1000 K
Aluminum oxide, 1400 K
Stainless steel, 1200 K heavily oxidized
2800 K
Tungsten
1600 K
Stainless steel, 800 K polished

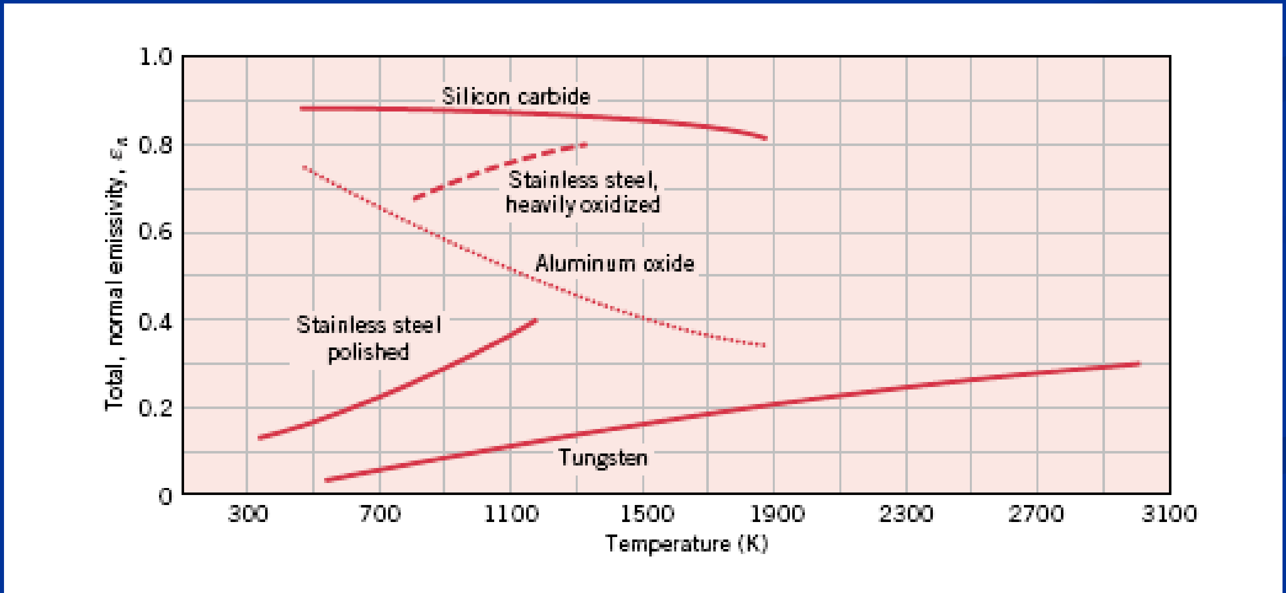

Total, normal emissivity, ε_n
Temperature (K)
Silicon carbide
Stainless steel, heavily oxidized
Aluminum oxide
Stainless steel polished
Tungsten

Absorção, Reflecção e Transmissão

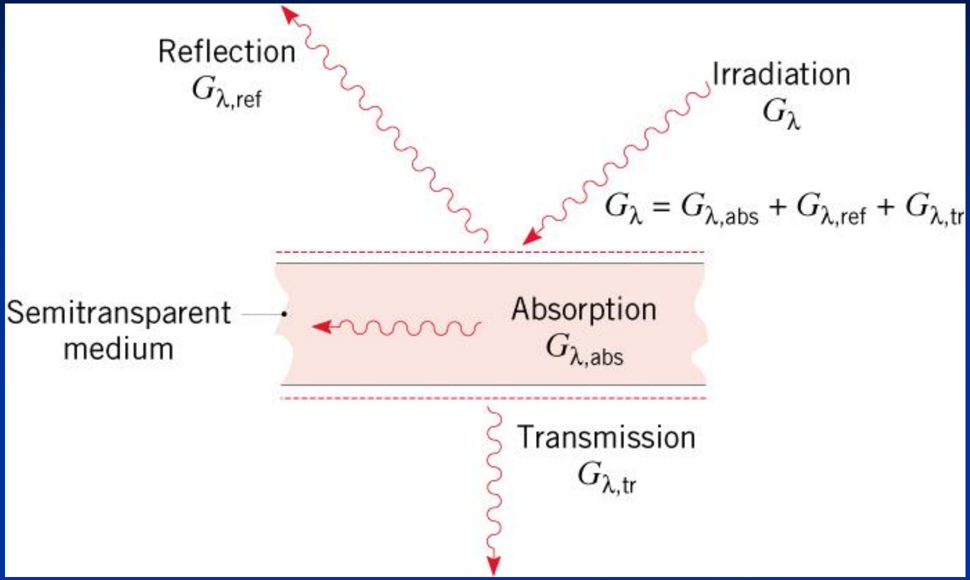

$$G_\lambda = G_{\lambda,ref} + G_{\lambda,abs} + G_{\lambda,tr}$$

- para materiais opacos $\quad G_{\lambda,tr} = 0.$

$$G_\lambda = G_{\lambda,ref} + G_{\lambda,tr}$$

Absorção de um material Opaco

- Absortividade direcional espectral:

$$\alpha_{\lambda,\theta}(\lambda,\theta,\phi) \equiv \frac{I_{\lambda,i,abs}(\lambda,\theta,\phi)}{I_{\lambda,i}(\lambda,\theta,\phi)}$$

- Absortividade hemisférica espectral:

$$\alpha_{\lambda}(\lambda) \equiv \frac{G_{\lambda,abs}(\lambda)}{G_{\lambda}(\lambda)} = \frac{\int_0^{2\pi}\int_0^{\pi/2} \alpha_{\lambda,\theta}(\lambda,\theta,\phi) I_{\lambda,i}(\lambda,\theta,\phi) \cos\theta \sin\theta d\theta d\phi}{\int_0^{2\pi}\int_0^{\pi/2} I_{\lambda,i}(\lambda,\theta,\phi) \cos\theta \sin\theta d\theta d\phi}$$

- Absortividade hemisférica total :

$$\alpha \equiv \frac{G_{abs}}{G} = \frac{\int_o^{\infty} \alpha_{\lambda}(\lambda) G_{\lambda}(\lambda) d\lambda}{\int_0^{\infty} G_{\lambda}(\lambda) d\lambda}$$

Reflexão de um material opaco

- Refletividade espectral e direcional :

$$\rho_{\lambda,\theta}(\lambda,\theta,\phi) \equiv \frac{I_{\lambda,i,ref}(\lambda,\theta,\phi)}{I_{\lambda,i}(\lambda,\theta,\phi)}$$

- Refletividade espectral e hemisférica:

$$\rho_{\lambda} \equiv \frac{G_{\lambda,ref}(\lambda)}{G_{\lambda}(\lambda)} = \frac{\int_0^{2\pi}\int_0^{\pi/2} \rho_{\lambda,\theta}(\lambda,\theta,\phi) I_{\lambda,i}(\lambda,\theta,\phi) \cos\theta \sin\theta d\theta d\phi}{I_{\lambda,i}(\lambda,\theta,\phi)}$$

- Refletividade hemisférica total :

$$\rho \equiv \frac{G_{ref}}{G} = \frac{\int_0^{\infty} \rho_{\lambda}(\lambda) G_{\lambda}(\lambda) d\lambda}{\int_0^{\infty} G_{\lambda}(\lambda) d\lambda}$$

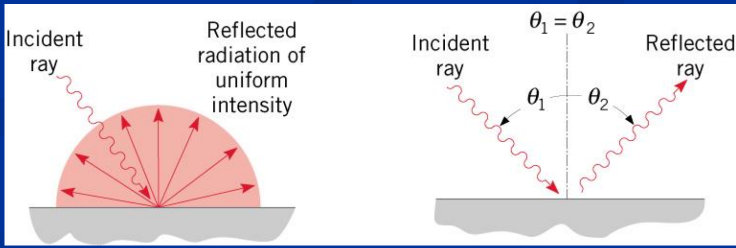

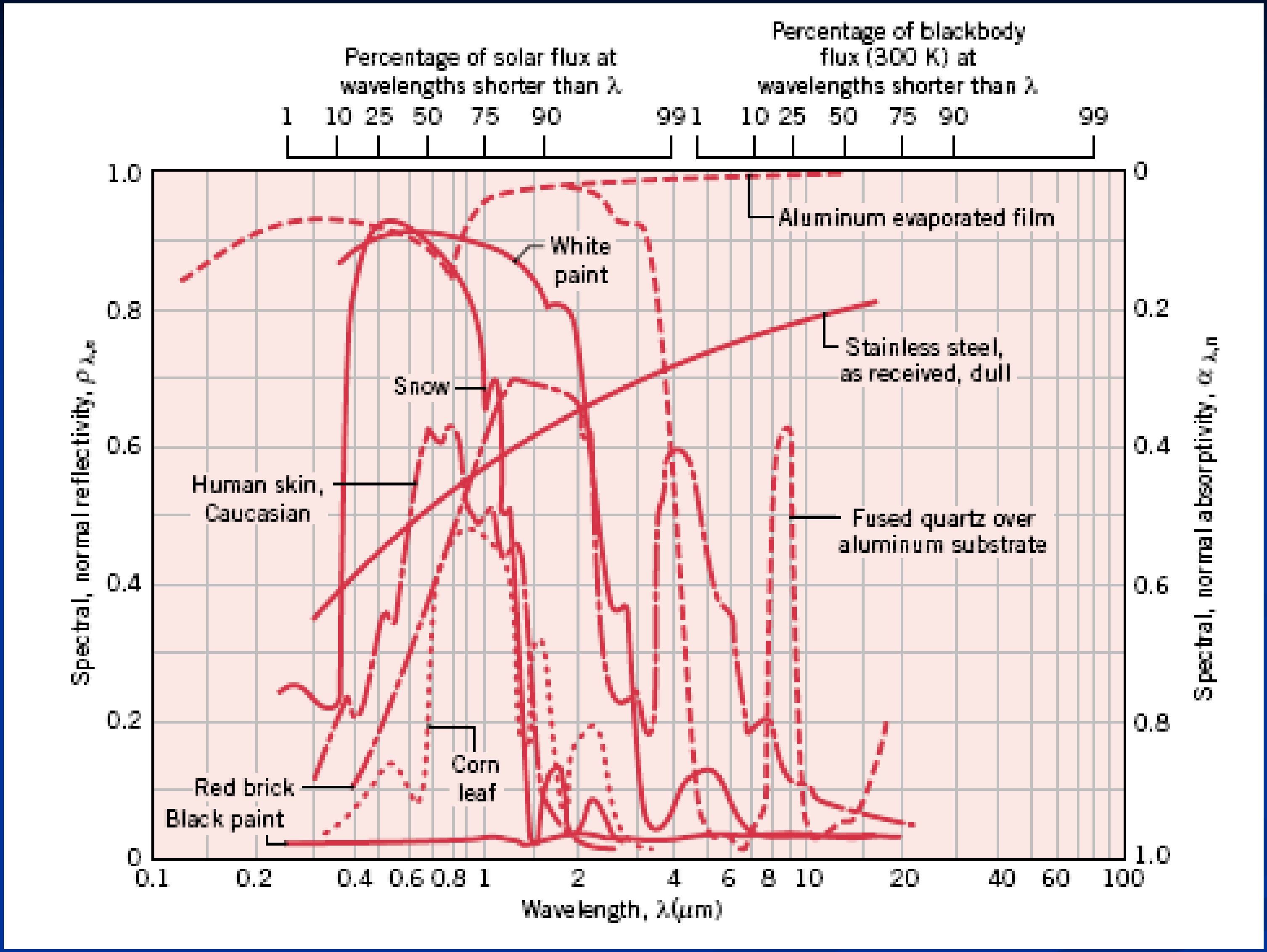

- Note strong dependence of ρ_λ $\left(\text{and } \alpha_\lambda = 1 - \rho_\lambda\right)$ on λ.

Transmissão

A transmissividade espectral hemisférica

$$\tau_\lambda \equiv \frac{G_{\lambda,tr}\lambda}{G_\lambda(\lambda)}$$

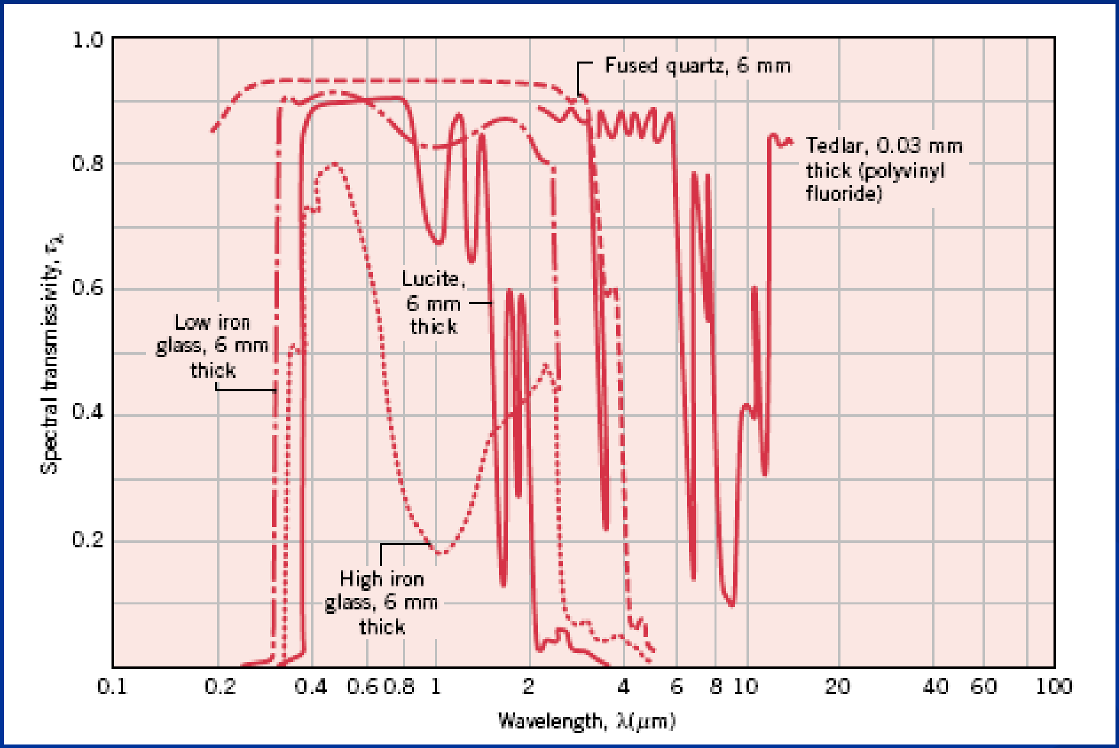

- A transmissividade total hemisférica:

$$\tau \equiv \frac{G_{tr}}{G} = \frac{\int_0^\infty G_{\lambda,tr}(\lambda)\,d\lambda}{\int_0^\infty G_\lambda(\lambda)\,d\lambda}$$

- Para um meio semitransparente,

$$\rho_\lambda + \alpha_\lambda + \tau_\lambda = 1$$
$$\rho + \alpha + \tau + 1$$

Lei de Kirchhoff

•total, hemispherical emissivity = total, hemispherical absorptivity:

$$\varepsilon = \alpha$$

$$\varepsilon_{\lambda,\theta} = \alpha_{\lambda,\theta}$$

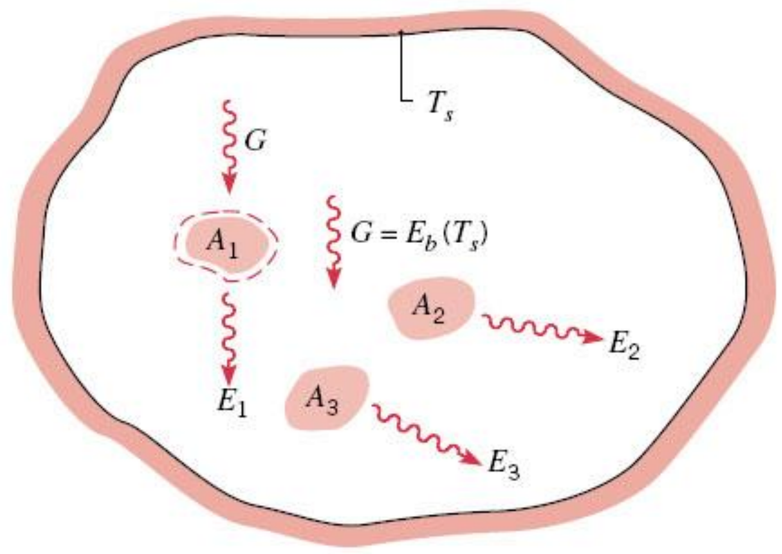

FIGURE 12.24
Radiative exchange in an isothermal enclosure.

Superfícies cinzentas

- $$\varepsilon_\lambda = \frac{\int_0^{2\pi}\int_0^{\pi/2} \varepsilon_{\lambda,\theta} \cos\theta \sin\theta d\theta d\phi}{\int_0^{2\pi}\int_0^{\pi/2} \cos\theta \sin\theta d\theta d\phi}$$

$$\alpha_\lambda = \frac{\int_0^{2\pi}\int_0^{\pi/2} \alpha_{\lambda,\theta} I_{\lambda,i} \cos\theta \sin\theta d\theta d\phi}{\int_0^{2\pi}\int_0^{\pi/2} I_{\lambda,i} \cos\theta \sin\theta d\theta d\phi}$$

- $$\varepsilon = \frac{\int_0^\infty \varepsilon_\lambda E_{\lambda,b}(\lambda) d\lambda}{E_b(T)}$$

$$\alpha = \frac{\int_0^\infty \alpha_\lambda G_\lambda(\lambda) d\lambda}{G}$$

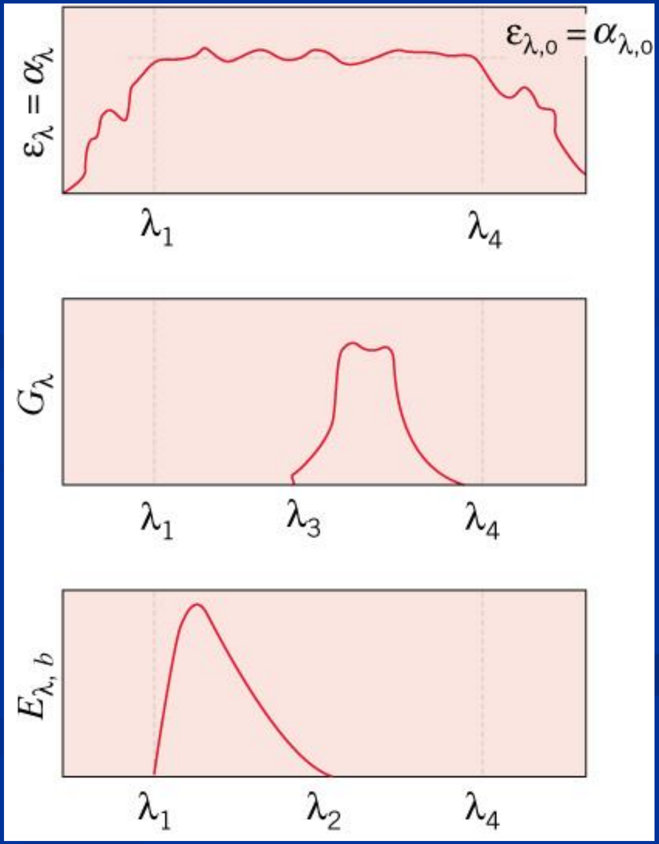

Radiação Solar

- O Sol é uma fonte hermisférica com diâmetro de 1.39 x 10^9 m
- e pode ser aproximado como um corpo negro a 5800 K.

- A distância da Terra ao Sol varia do mínimo de 1.471 x 10^{11} m ao máximo de
- 1.521 x 10^{11} m, com um valor médio de 1.496 x 10^{11} m.

- Devido a grande distância entre o Sol e a Terra pode-se
- assumir que os raios solares chegam a Terra como sendo
- paralelo.

$$q_S'' = f \times S_c$$

$S_c \rightarrow$ the solar constant or heat flux $\left(1353\ \mathrm{W/m^2}\right)$ when the earth is at its mean distance from the sun.

$f \rightarrow$ correction factor accounting for eccentricity of the earth's orbit $\left(0.97 < f < 1.03\right)$

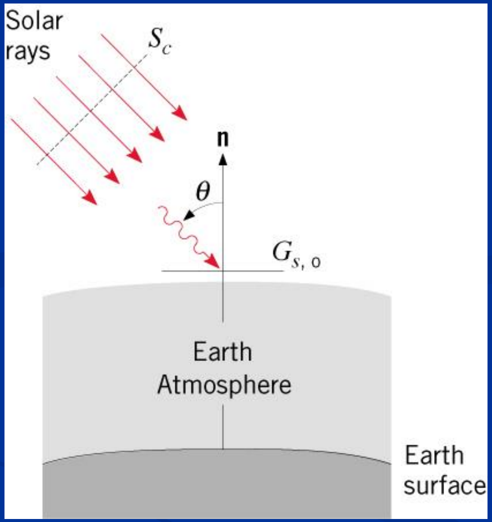

Solar Radiation (cont).

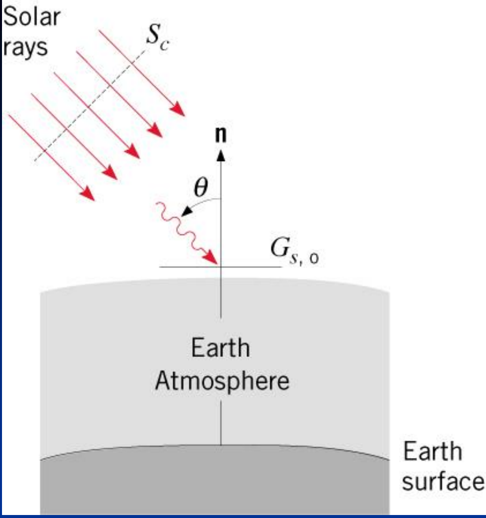

- Irradiação extraterrestre

$$G_{S,o} = f \times S_c \times \cos\theta$$

- Na atmosfera:
  - Absorption by aerosols over the entire spectrum.
  - Absorption by gases (CO_2, H_2O (v), O_3) in discrete wavelength bands.
  - Scattering by gas molecules and aerosols.

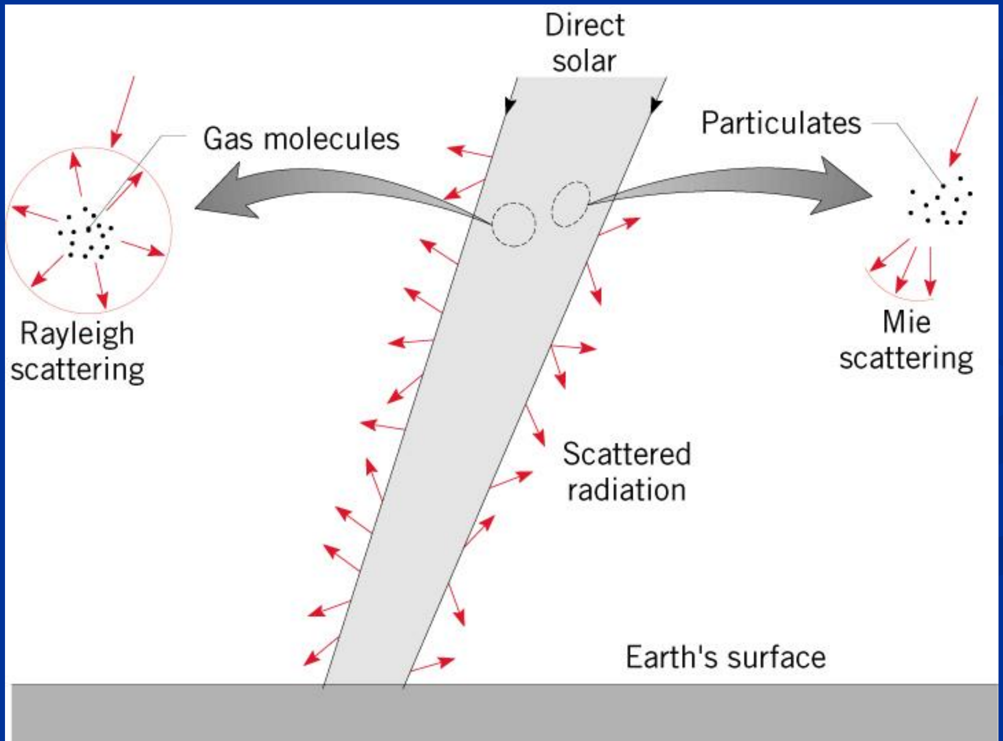

- Efeito da atmosfera:

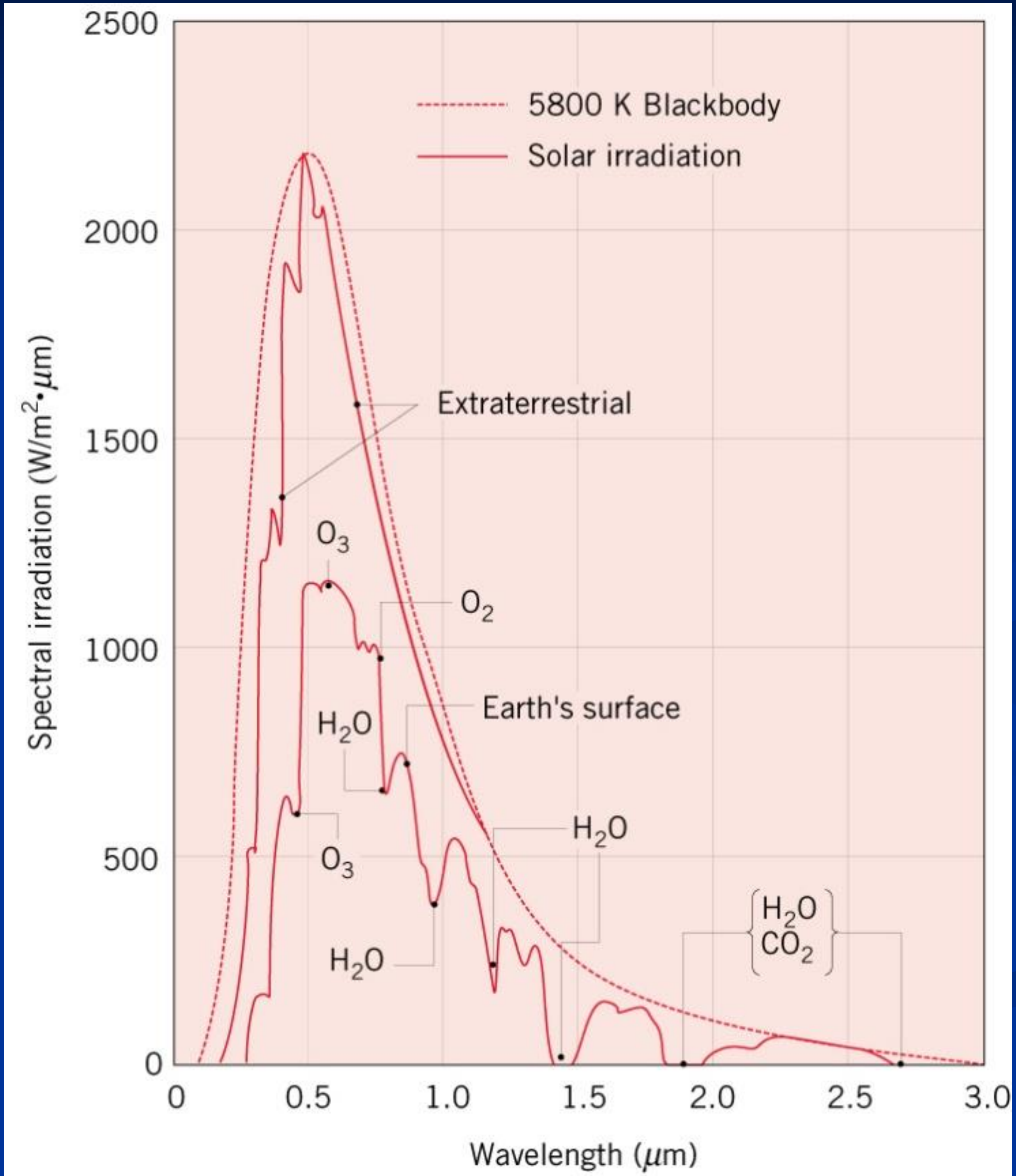

- Effect of Atmosphere on Directional Distribution of Solar Radiation:

  - Rayleigh scattering is approximately uniform in all directions (isotropic scattering), while Mie scattering is primarily in the direction of the sun's rays (forward peaked).

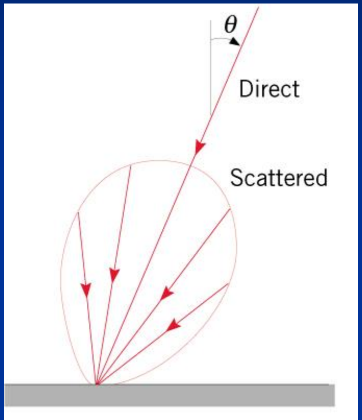

  - Directional distribution of radiation at the earth's surface has two components.
    - Direct radiation: Unscattered and in the direction θ of the sun's rays.
    - Diffuse radiation: Scattered radiation strongly peaked in the forward direction.

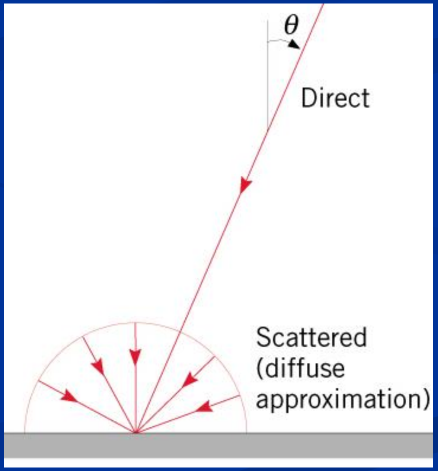

  - Calculation of solar irradiation for a horizontal surface often presumes the scattered component to be isotropic.

$$G_S = G_{S,dir} + G_{S,dif} = q''_{dir}\cos\theta + \pi I_{dif}$$

$$0.1 < \left(G_{S,dif} / G_S\right) < 1.0$$

Clear skies — Completely overcast

Terrestrial Radiation

- Emission by Earth's Surface:

$$E = \varepsilon \sigma T^4$$

  - Emissivities are typically large. For example, from Table A.11:

Sand/Soil:	$\varepsilon > 0.90$
Water/Ice:	$\varepsilon > 0.95$
Vegetation:	$\varepsilon > 0.92$
Snow:	$\varepsilon > 0.82$
Concrete/Asphalt:	$\varepsilon > 0.85$

  - Emission is typically from surfaces with temperatures in the range of $250 < T < 320$ K and hence concentrated in the spectral region $4 < \lambda < 40$ μm, with peak emission at $\lambda \approx 10 \mu$m.

- Atmospheric Emission:
  - Largely due to emission from CO_2 and H_2O (v) and concentrated in the spectral regions $5 < \lambda < 8$ μm and $\lambda > 13 \mu$m.

- Although far from exhibiting the spectral characteristics of blackbody emission, earth irradiation due to atmospheric emission is often approximated by a blackbody emissive power of the form

$$G_{atm} = \sigma T_{sky}^4$$

$T_{sky} \rightarrow$ the effective sky temperature

$$230\text{ K} < T_{sky} < 285\text{ K}$$

Cold, clear sky — Warm, overcast sky

- Can water in the natural environment freeze if the ambient air temperature exceeds 273 K? If so, what environmental conditions (wind and sky) favor ice formation?

Surface Radiative Properties

- Concentration of solar $(0.3 < \lambda < 3\mu m)$ and terrestrial $(4 < \lambda < 40\mu m)$ in different spectral regions often precludes use of the gray surface approximation $(\varepsilon \neq \alpha_S)$.

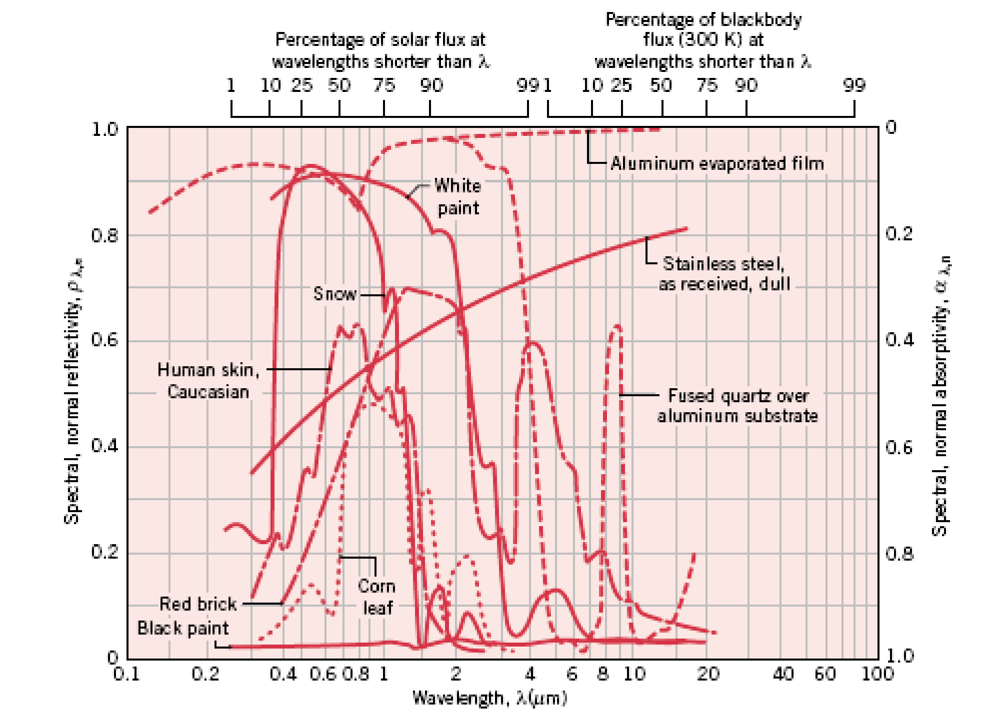

➢ Note significant differences in ρ_λ and α_λ for the two spectral regions: snow, human skin, white paint.

➢ In terms of net radiation transfer to a surface with solar irradiation, the parameter α_S / ε has special significance. Why?

Surface Properties (cont).

Surface	α_S / ε	
Snow	0.29	Rejection
Human skin	0.64	Rejection
White paint	0.22	Rejection
Black paint	1.0	Collection
Evaporated Al film	3.0	Collection

Capítulo 13 – Fator de Forma

The View Factor (also Configuration or Shape Factor)

- The view factor, F_{ij}, is a geometrical quantity corresponding to the fraction of the radiation leaving surface *i* that is intercepted by surface *j*.

$$F_{ij} = \frac{q_{i\to j}}{A_i J_i}$$

- The view factor integral provides a general expression for F_{ij}. Consider exchange between differential areas dA_i *and* dA_j :

$$dq_{i\to j} = I_i \cos\theta_i dA_i d\omega_{j-i} = J_i \frac{\cos\theta_i \cos\theta_j}{\pi R^2} dA_i dA_j$$

$$F_{ij} = \frac{1}{A_i} \int_{A_i} \int_{A_j} \frac{\cos\theta_i \cos\theta_j}{\pi R^2} dA_i dA_j$$

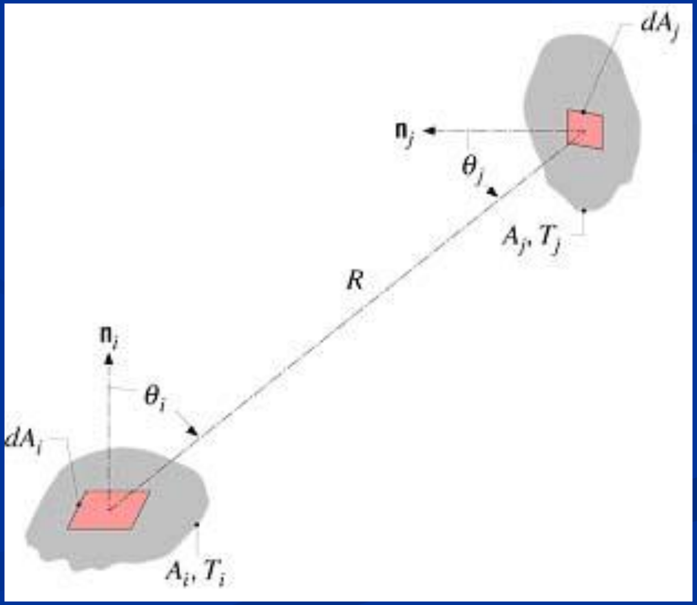

Basic Concepts

- Enclosures consist of two or more surfaces that envelop a region of space (typically gas-filled) and between which there is radiation transfer. Virtual, as well as real, surfaces may be introduced to form an enclosure.

- A nonparticipating medium within the enclosure neither emits, absorbs, nor scatters radiation and hence has no effect on radiation exchange between the surfaces.

- Each surface of the enclosure is assumed to be isothermal, opaque, diffuse and gray, and to be characterized by uniform radiosity and irradiation.

View Factor Relations

- Reciprocity Relation. With

$$F_{ji} = \frac{1}{A_j}\int_{A_i}\int_{A_j}\frac{\cos\theta_i\cos\theta_j}{\pi R^2}dA_i dA_j$$

$$A_i F_{ij} = A_j F_{ji}$$

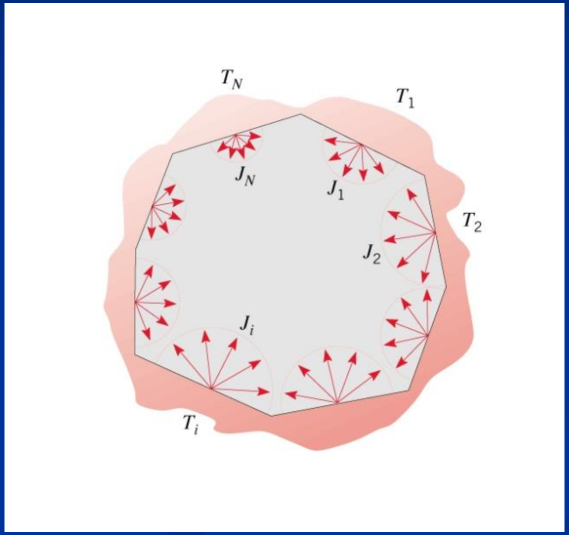

- Summation Rule for Enclosures.

$$\sum_{j=1}^{N} F_{ij} = 1$$

- Two-Dimensional Geometries (Table 13.1) For example,

An Infinite Plane and a Row of Cylinders

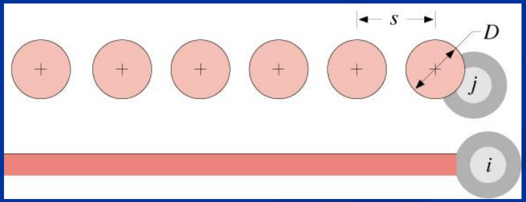

$$F_{ij} = 1 - \left[1 - \left(\frac{D}{s}\right)^2\right]^{1/2} + \left(\frac{D}{s}\right)\tan^{-1}\left[\left(\frac{s^2 - D^2}{D^2}\right)^{1/2}\right]$$

- Three-Dimensional Geometries (Table 13.2). For example,

Coaxial Parallel Disks

$$F_{ij} = \frac{1}{2}\left\{ S - \left[S^2 - 4\left(r_j / r_i \right)^2 \right]^{1/2} \right\}$$

$$S = 1 + \frac{1 + R_j^2}{R_i^2}$$

$$R_i = r_i / L \qquad R_j = r_j / L$$

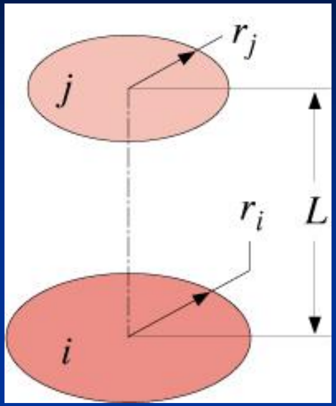

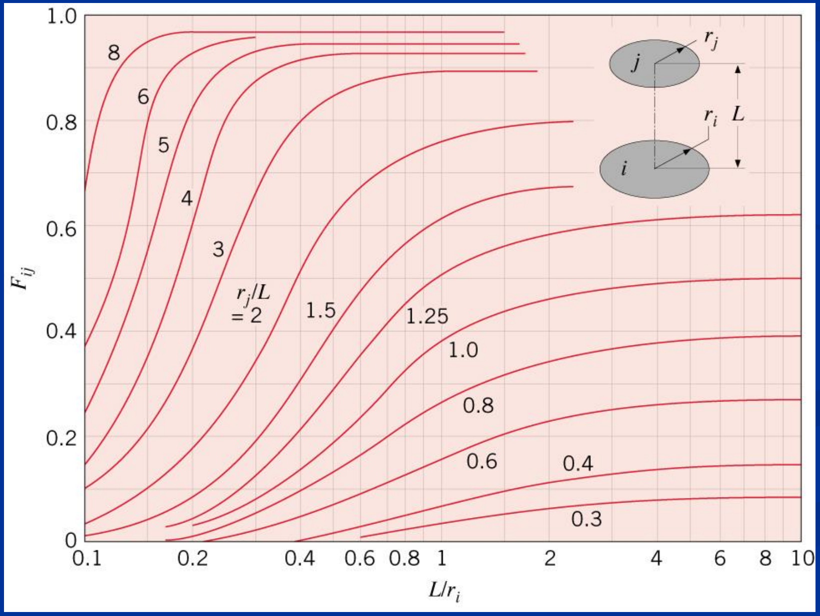

Blackbody Radiation Exchange

- For a blackbody, $J_i = E_{bi}$.

- Net radiative exchange between two surfaces that can be approximated as blackbodies $\longrightarrow$ *net* rate at which radiation leaves surface *i* due to its interaction with *j*

  or net rate at which surface *j* gains radiation due to its interaction with *i*

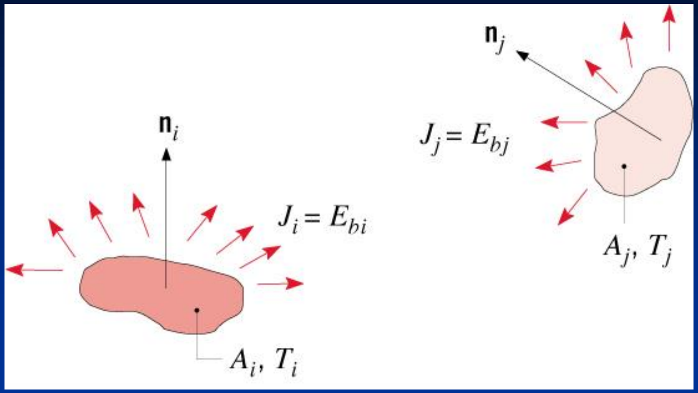

$$q_{ij} = q_{i\to j} - q_{j\to i}$$

$$q_{ij} = A_i F_{ij} E_{bi} - A_j F_{ji} E_{bj}$$

$$q_{ij} = A_i F_{ij} \sigma \left(T_i^4 - T_j^4\right)$$

- Net radiation transfer from surface *i* due to exchange with all (*N*) surfaces of an enclosure:

$$q_i = \sum_{j=1}^{N} A_i F_{ij} \sigma \left(T_i^4 - T_j^4\right)$$

General Radiation Analysis for Exchange between the *N* Opaque, Diffuse, Gray Surfaces of an Enclosure

$(\varepsilon_i = \alpha_i = 1 - \rho_i)$

- Alternative expressions for net radiative transfer from surface *i*:

$$q_i = A_i (J_i - G_i) \rightarrow \text{Fig. (b)} \qquad (1)$$

$$q_i = A_i (E_i - \alpha_i G_i) \rightarrow \text{Fig. (c)} \qquad (2)$$

$$q_i = \frac{E_{bi} - J_i}{(1-\varepsilon_i)/\varepsilon_i A_i} \rightarrow \text{Fig. (d)} \qquad (3)$$

Suggests a surface radiative resistance of the form: $(1-\varepsilon_i)/\varepsilon_i A_i$

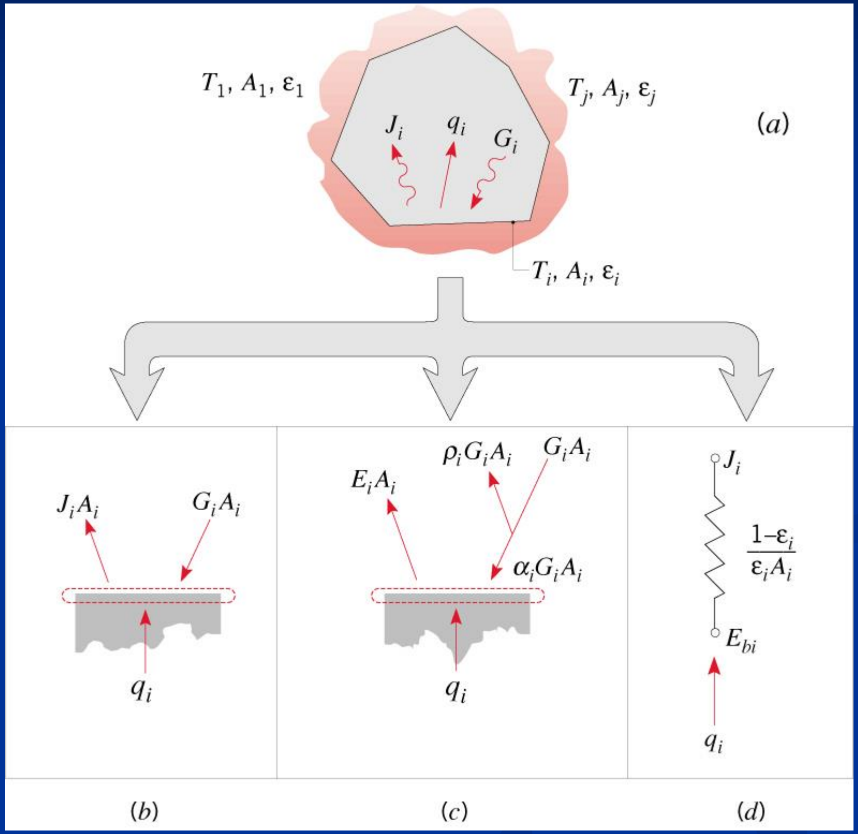

$$q_i = \sum_{j=1}^{N} A_i F_{ij}\left(J_i - J_j\right) = \sum_{j=1}^{N} \frac{J_i - J_j}{\left(A_i F_{ij}\right)^{-1}} \qquad (4)$$

Suggests a space or geometrical resistance of the form: $\left(A_i F_{ij}\right)^{-1}$

- Equating Eqs. (3) and (4) corresponds to a radiation balance on surface *i*:

$$\frac{E_{bi} - J_i}{\left(1-\varepsilon_i\right)/\varepsilon_i A_i} = \sum_{j=1}^{N} \frac{J_i - J_j}{\left(A_i F_{ij}\right)^{-1}} \qquad (5)$$

which may be represented by a radiation network of the form

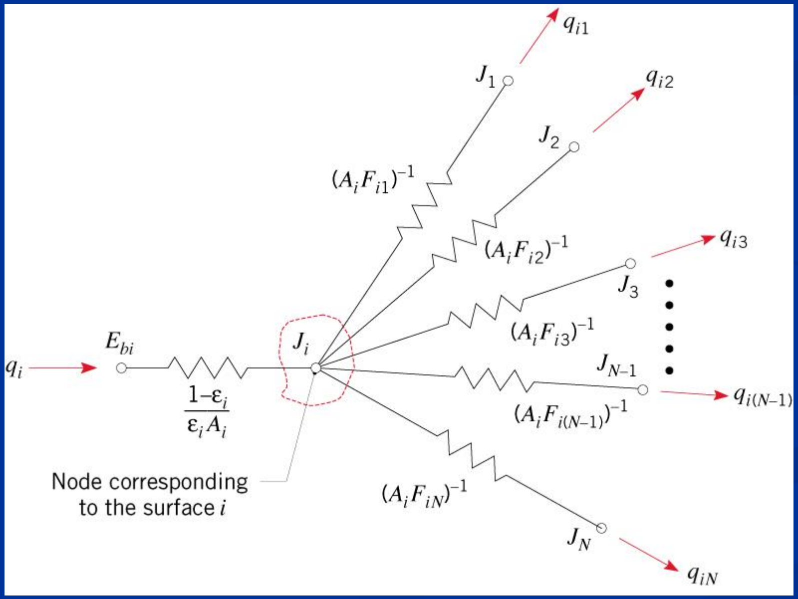

Two-Surface Enclosures

- Simplest enclosure for which radiation exchange is exclusively between two surfaces and a single expression for the rate of radiation transfer may be inferred from a network representation of the exchange.

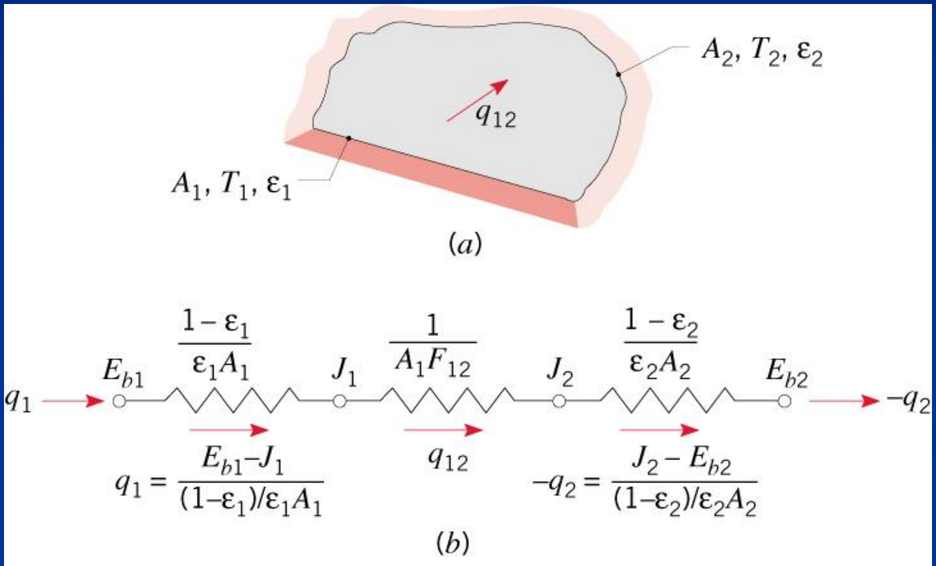

$$q_1 = -q_2 = q_{12} = \frac{\sigma\left(T_1^4 - T_2^4\right)}{\frac{1-\varepsilon_1}{\varepsilon_1 A_1} + \frac{1}{A_1 F_{12}} + \frac{1-\varepsilon_2}{\varepsilon_2 A_2}}$$

- Special cases are presented in Table 13.3. For example,
  - ➢ Large (Infinite) Parallel Plates

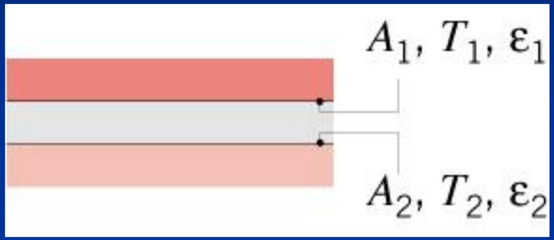

$$A_1 = A_2 \equiv A$$

$$F_{12} = 1$$

$$q_{12} = \frac{A_1 \sigma \left(T_1^4 - T_2^4\right)}{\frac{1}{\varepsilon_1} + \frac{1}{\varepsilon_2} - 1}$$

  - ➢ Note result for *Small Convex Object in a Large Cavity.*

Radiation Shields

- High reflectivity (low $\alpha = \varepsilon$) surface(s) inserted between two surfaces for which a reduction in radiation exchange is desired.

- Consider use of a single shield in a two-surface enclosure, such as that associated with large parallel plates:

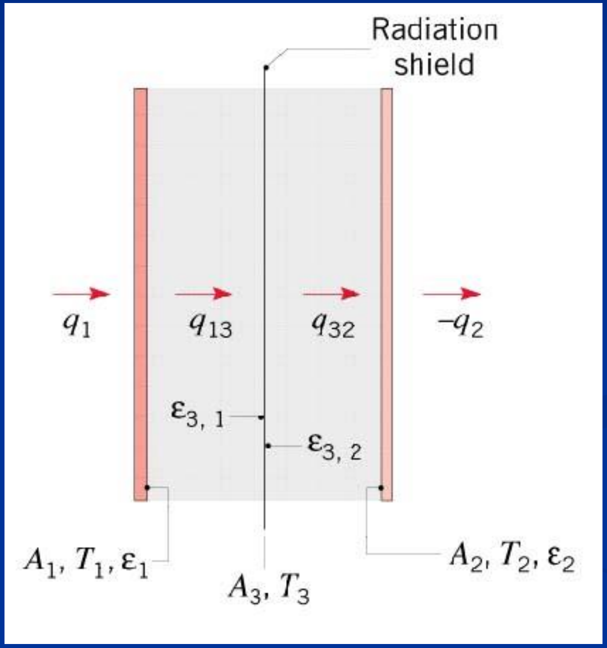

Note that, although rarely the case, emissivities may differ for opposite surfaces of the shield.

- Radiation Network:

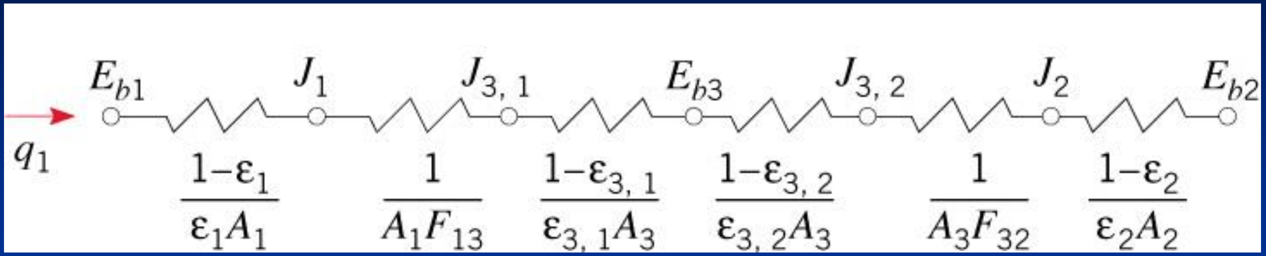

$$q_{12} = q_1 = -q_2 = \frac{\sigma\left(T_1^4 - T_2^4\right)}{\frac{1-\varepsilon_1}{\varepsilon_1 A_1} + \frac{1}{A_1 F_{13}} + \frac{1-\varepsilon_{3,1}}{\varepsilon_{3,1} A_3} + \frac{1-\varepsilon_{3,2}}{\varepsilon_{3,2} A_3} + \frac{1}{A_3 F_{32}} + \frac{1-\varepsilon_2}{\varepsilon_2 A_2}}$$

- The foregoing result may be readily extended to account for multiple shields and may be applied to long, concentric cylinders and concentric spheres, as well as large parallel plates.

The Reradiating Surface

- An idealization for which $G_R = J_R$. Hence, $q_R = 0$ and $J_R = E_{bR}$.

- Approximated by surfaces that are well insulated on one side and for which convection is negligible on the opposite (radiating) side.

- Three-Surface Enclosure with a Reradiating Surface:

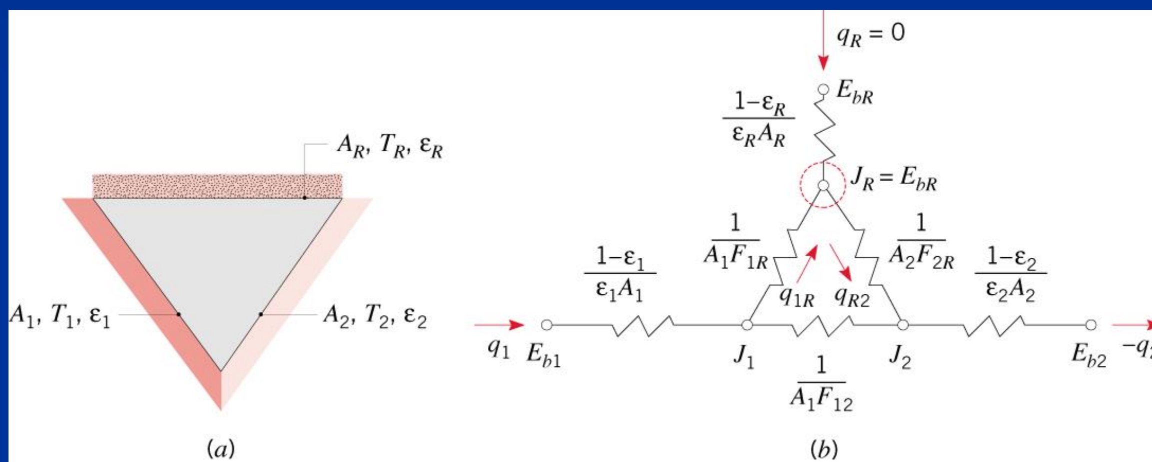

$$q_1 = -q_2 = \frac{\sigma\left(T_1^4 - T_2^4\right)}{\frac{1-\varepsilon_1}{\varepsilon_1 A_1} + \frac{1}{A_1 F_{12} + \left[\left(1/A_1 F_{1R}\right) + \left(1/A_2 F_{2R}\right)\right]^{-1}} + \frac{1-\varepsilon_2}{\varepsilon_2 A_2}}$$

Reradiating Surfaces (cont)

- Temperature of reradiating surface T_R may be determined from knowledge of its radiosity J_R. With $q_R = 0$, a radiation balance on the surface yields

$$\frac{J_1 - J_R}{(1/A_1F_{1R})} = \frac{J_R - J_2}{(1/A_2F_{2R})}$$

$$T_R = \left(\frac{J_R}{\sigma}\right)^{1/4}$$

Radiation Exchange between Surfaces: Participating Media

General Considerations

- The medium separating surfaces of an enclosure may affect radiation at each surface through its ability to absorb, emit and/or scatter (redirect) radiation.
- Participating media may involve semitransparent solids and liquids, as well as polar gases such as CO_2, $H_2O(v)$, CH_4, and O_3.
- Radiation transport in participating media is a volumetric phenomenon, and for polar gases is confined to discrete wavelength bands.
- Beer's law: A simple relation for predicting the exponential decay of radiation propagating through an absorbing medium.

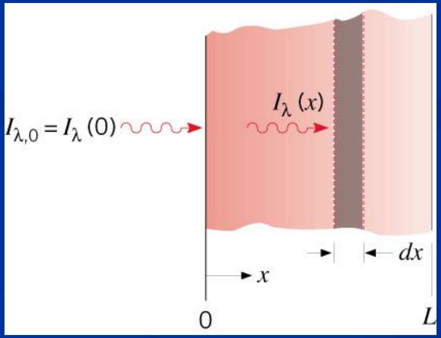

$$\frac{I_{\lambda,x}}{I_{\lambda,0}} = \exp(-\kappa_\lambda x)$$

$\kappa_\lambda \rightarrow$ spectral absorption coefficient (1/m)

- ➢ Transmissivity and absorptivity of medium of thickness L:

$$\tau_\lambda = \left(I_{\lambda,L} / I_{\lambda,0}\right) = \exp\left(-\kappa_\lambda L\right) \qquad \alpha_\lambda = 1 - \tau_\lambda = 1 - \exp\left(-\kappa_\lambda L\right)$$

- ➢ Emissivity of medium. Assuming applicability of Kirchhoff's law:

$$\varepsilon_\lambda = \alpha_\lambda$$

Radiant Heat Flux from an Emitting/Absorbing Gas to an Adjoining Surface

- An approximate procedure involves use of a mean beam length, L_e, to apply emissivity data obtained for a hemispherical gas mass to other gas geometries.

$L_e \rightarrow$ radius of a hemispherical gas mass whose emissivity, ε_g, is equivalent to that for the geometry of interest.

- Emissivity data have been obtained for a hemispherical gas mass with radiating species of H_2O (v) $\rightarrow$ w and/or CO_2 $\rightarrow$ c in a mixture with other nonradiating gases. Results depend on

T_g – the gas temperature

p_w, p_c – the partial pressures of H_2O (v) and CO_2

p – the total pressure of the mixture

L – the radius of the hemisphere

Mudança de Índice de refração

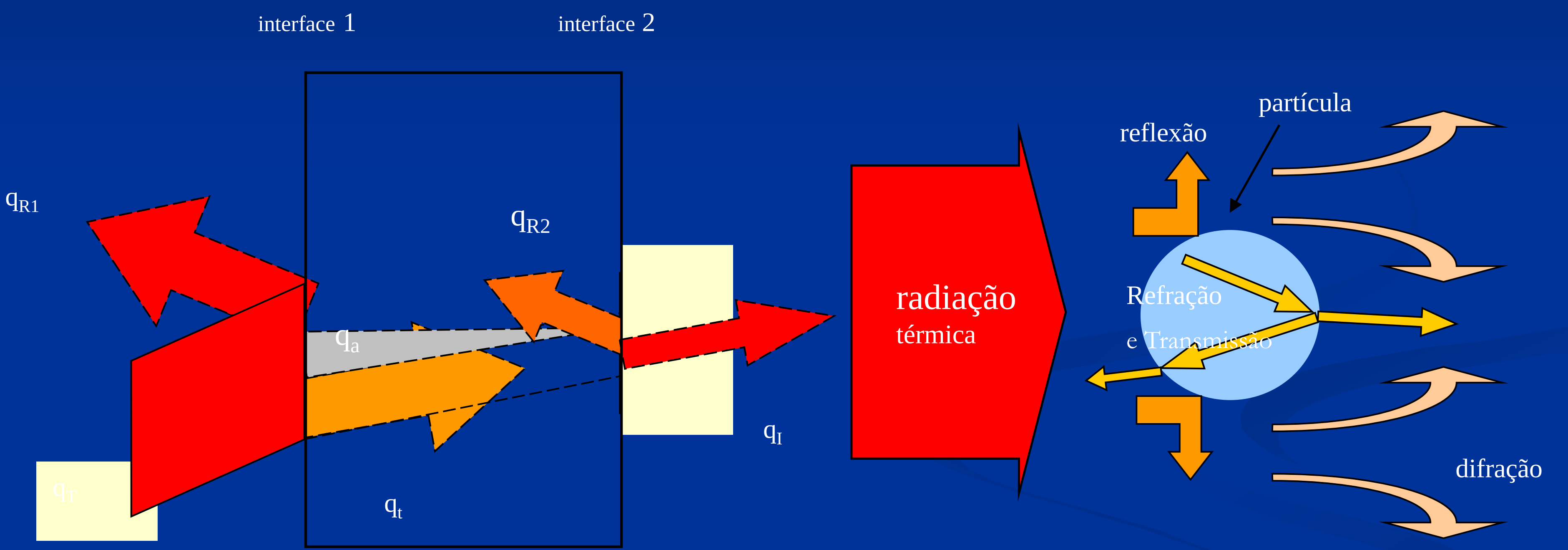

q_T: Fluxo de calor incidente
q_{R1}: Fluxo de calor refletido na interface 1
q_a: Fluxo de calor absorvido pelo meio
q_{R2}: Fluxo de calor refletido na interface 2
q_I: Fluxo de calor resultante noutro lado da parede
q_t: Fluxo de calor transmitido

Exemplos de materiais difusores

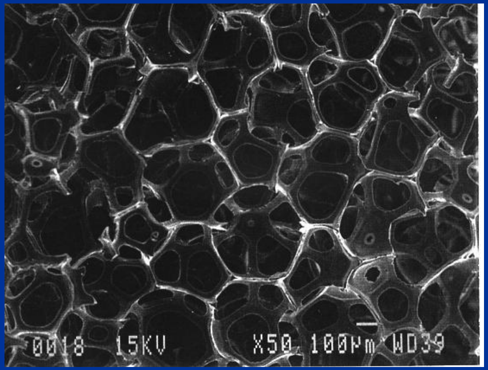

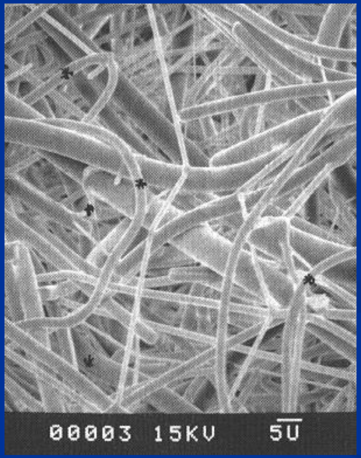

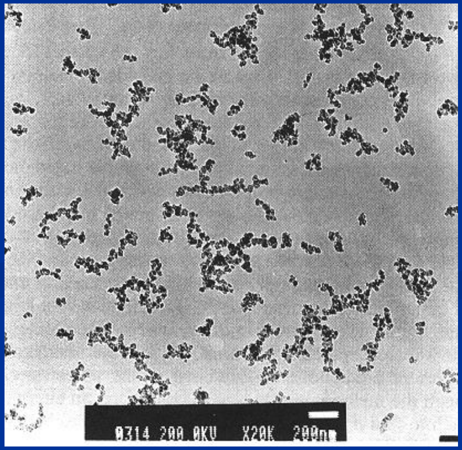

Espuma de Carbono

Lã de vidro (isolante térmico)

Cinzas em suspensão

Exemplos de materiais difusores

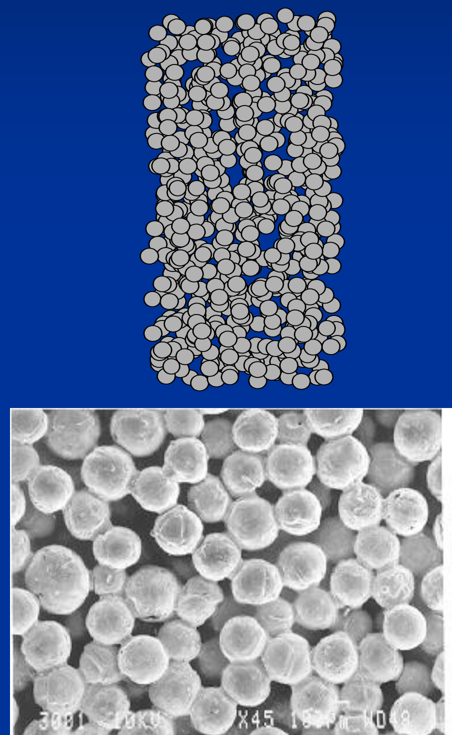

Partículas metálicas aquecidas a temperatura elevadas

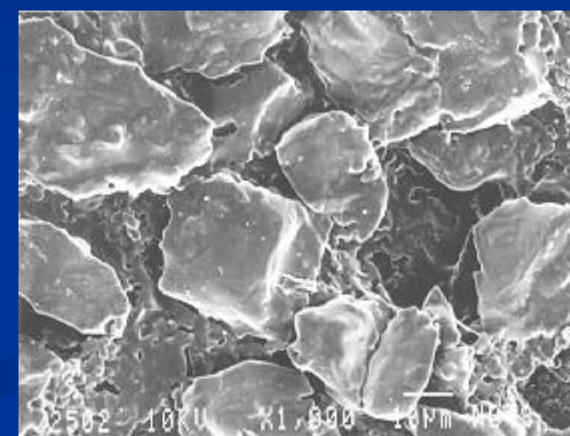

Partículas de alumina (isolante térmico e utilizado em paredes de fornos)

Exemplos de meios semitransparentes dispersos, SACADURA, 2006

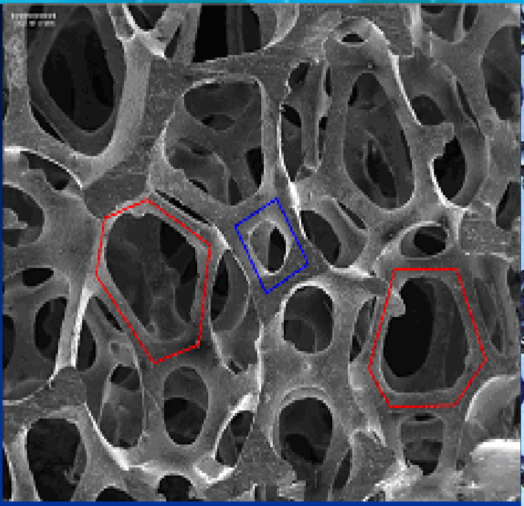

Espuma poros abertos

Vidro com bolhas

Chama

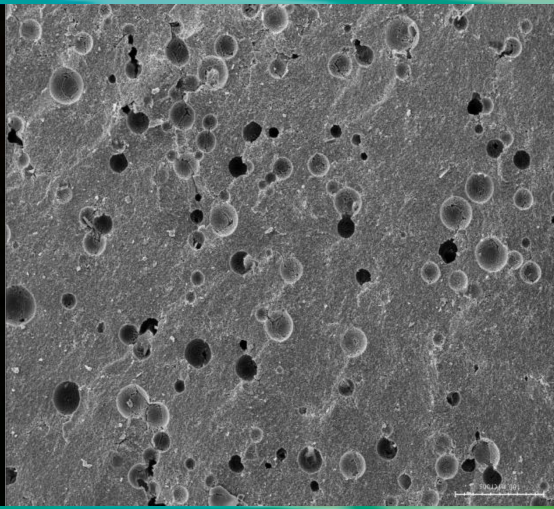

Cerâmica porosa

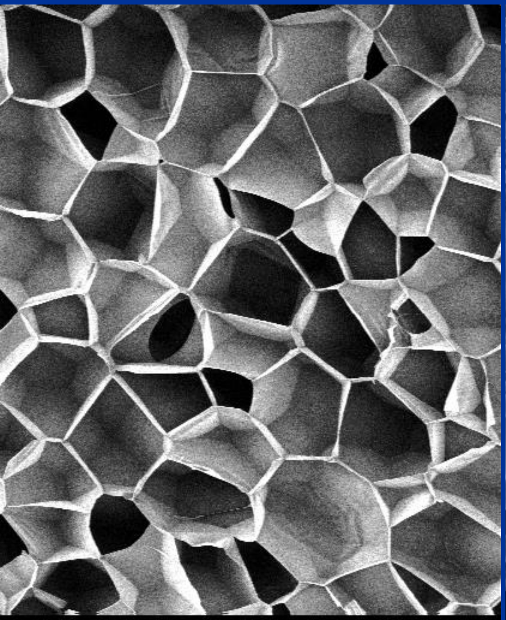

Espuma poros fechados
(corte)

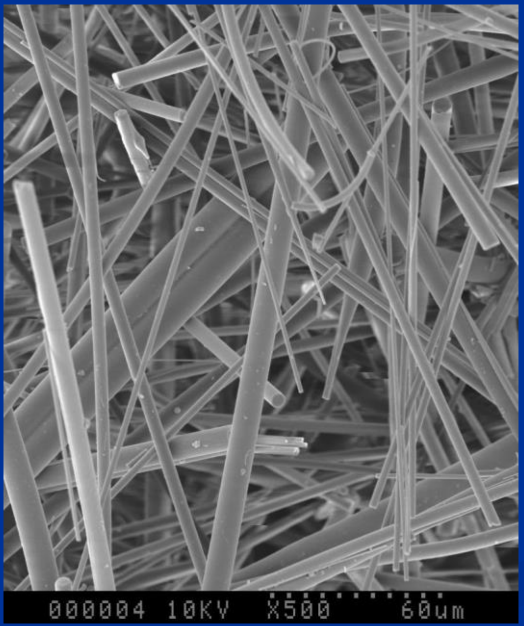

Fibra de vidro

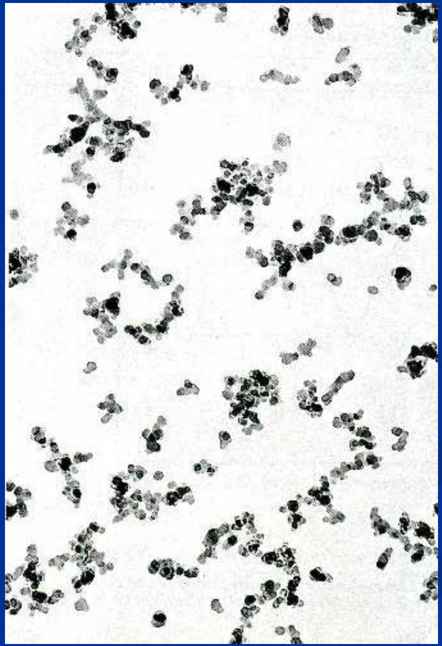

Fuligem

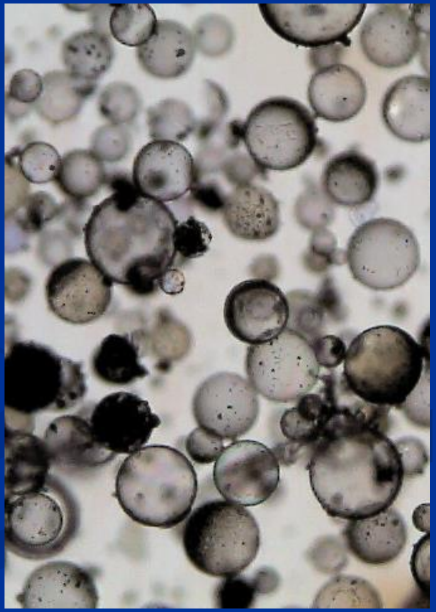

Polímero contendo
esféras ôcas

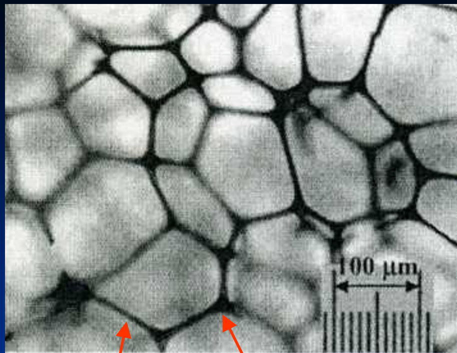

Strut Juncture

Poros abertos :

Melamina

Alumínio

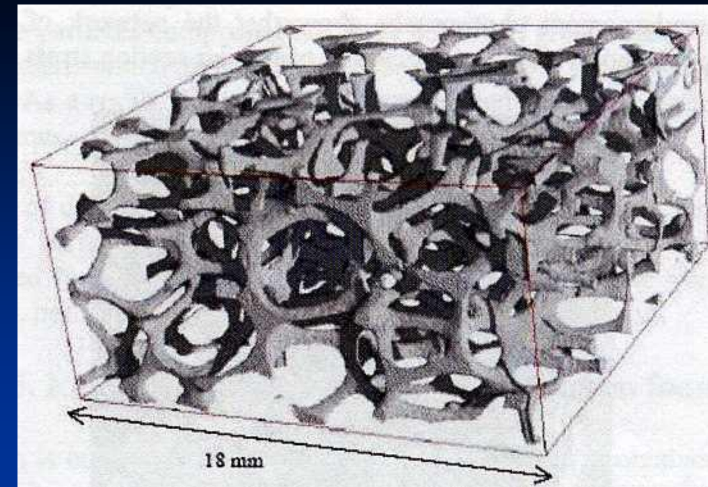

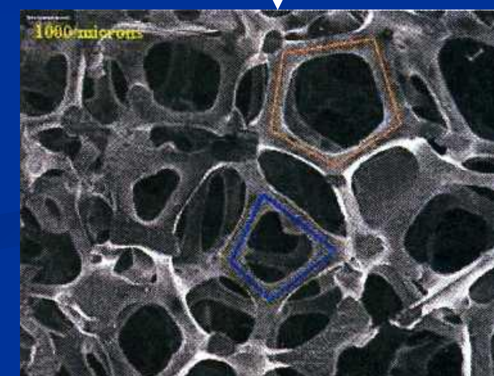

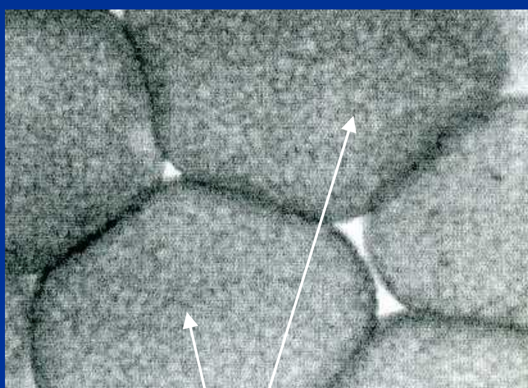

Poros fechados :

Poliestireno expandido (EPS)

dupla escala celular

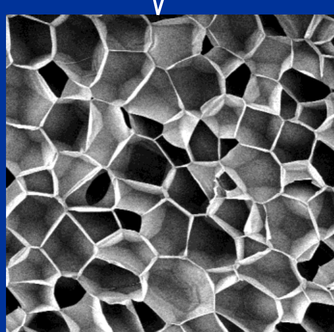

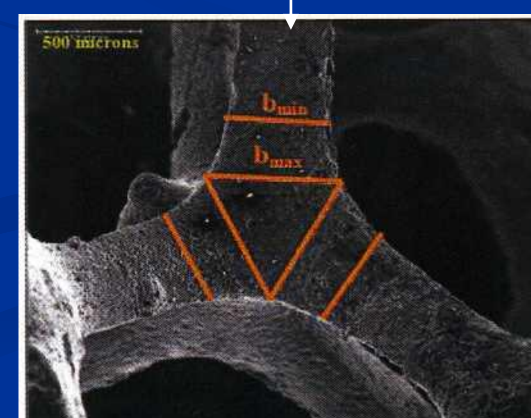

Sacadura, 2006

Exemplos de função de fase de uma partícula esférica para diversos valores de $\pi D/\lambda$ e do índice de refração do material $m_\lambda = n_\lambda - i\, k_\lambda$

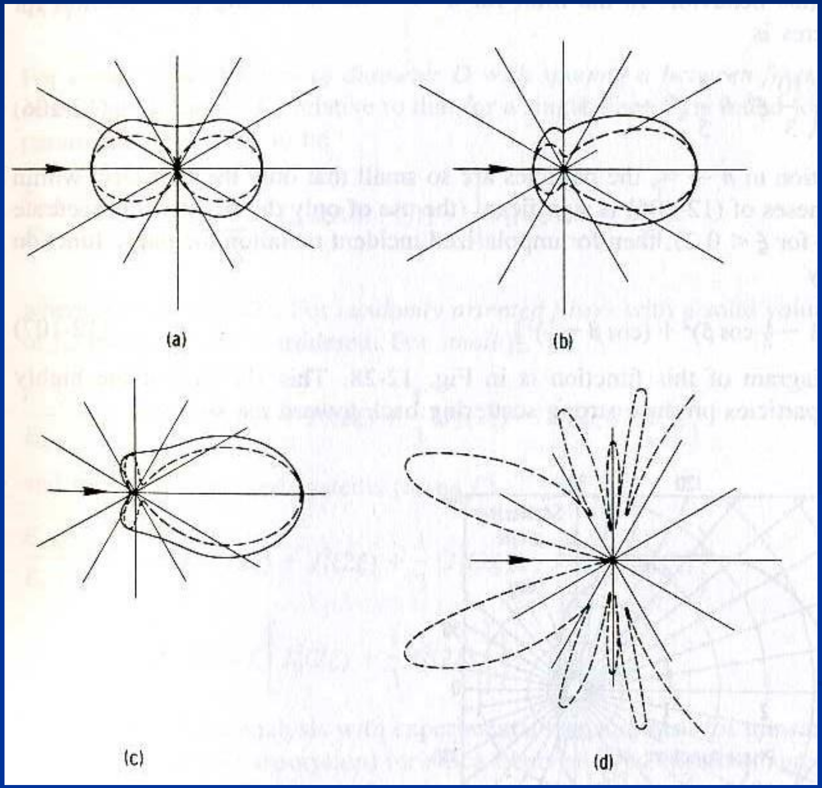

SACADURA, 2006

a) $\pi D/\lambda \rightarrow 0$, m = 0.57 - 4.29i (metal) b) $\pi D/\lambda$ = 9.15, m = 0.57-4.29i

c) $\pi D/\lambda$ = 10.3, m = 0.57-4.29i d) $\pi D/\lambda$ = 8 , n = 1.25 (dieléletrico)

(fonte: livros de Van de Hulst, Kerker e Siegel & Howell)

Outros exemplos de função de fase, SACADURA 2006

Isotrópica

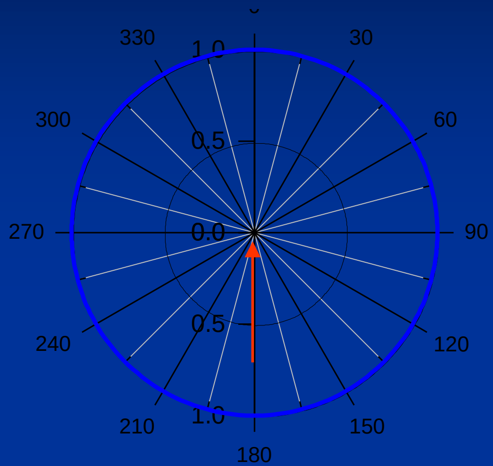

$P(\theta_0)=1$

Esfera ópaca com reflexão difusa

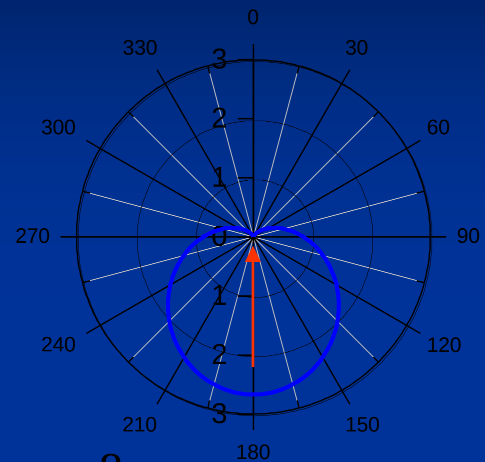

$$P=\frac{8}{3\pi}\left(\sin\theta_0-\theta_0\cos\theta_0\right)$$

Henyey-Greenstein g=0.9

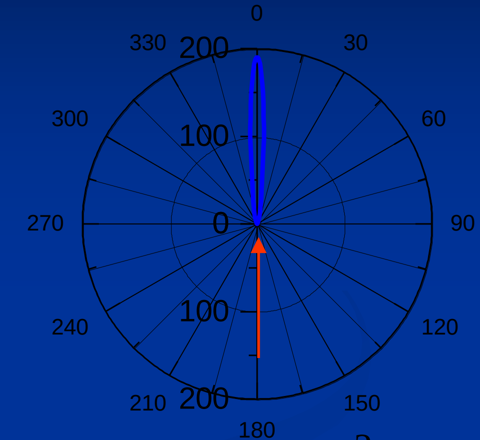

$$P=\frac{1-g_\lambda^2}{\left(1+g_\lambda^2+2g_\lambda\cos(\theta_0)\right)^{3/2}}$$

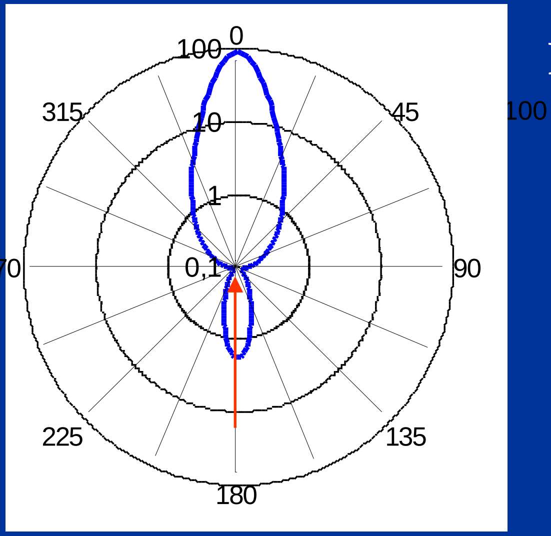

g1=0.86, g2=0.8, f_1=0.96, f_2=0.96

Função de fase composta (Nicolau 1994)

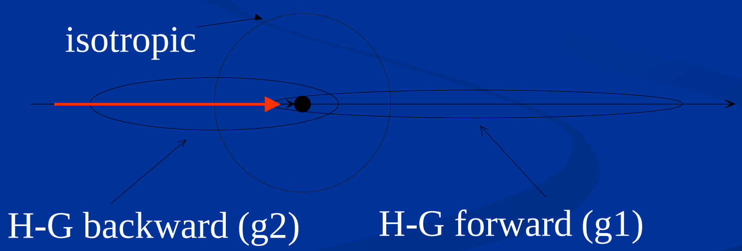

$$P=f_1 f_2 p_{HG,g1}(\theta_0)+(1-f_1)f_2 p_{HG,g2}(\theta_0)+(1-f_2)$$